2D and 3D Imaging by Nuclear Resonance Absorption/Fluorescence Using Extremely Brilliant Compton Sources

Trevor Reutershan and Prof. CPJ Barty

Medical Scientist Training Program (MD/PhD)
Department of Physics and Astronomy
Barty Research Group

Nuclear Photonics 2023 : Durham, North Carolina : September 11th, 2023

Nuclear Resonance Absorption and Fluorescence

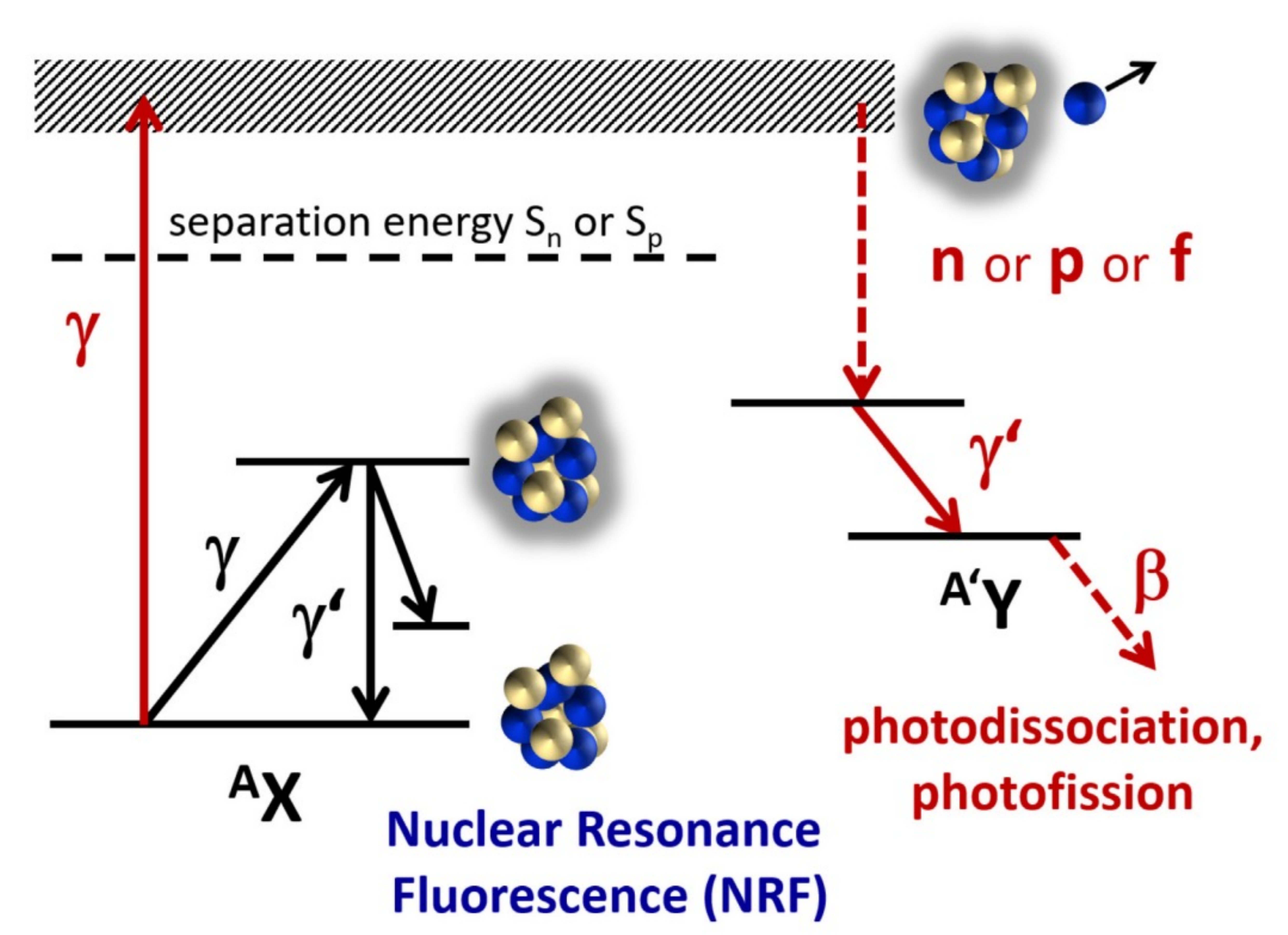

Other interactions include:

- **Nuclear Thomson/Compton Scattering**

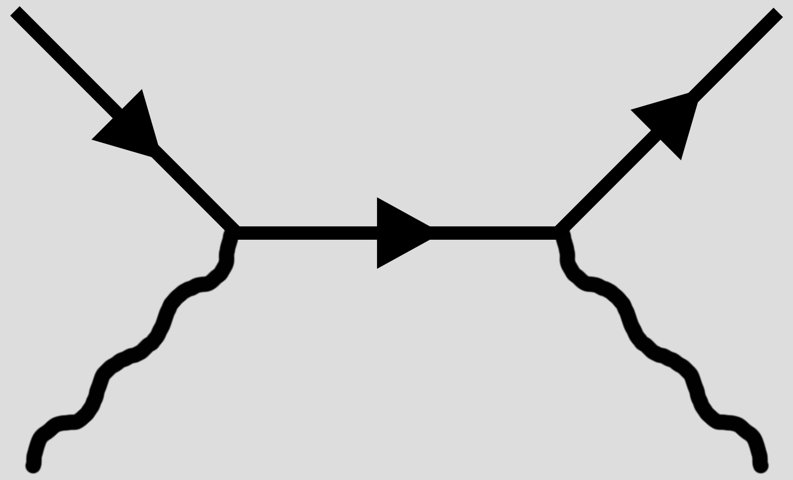

- **Delbrück Scattering**

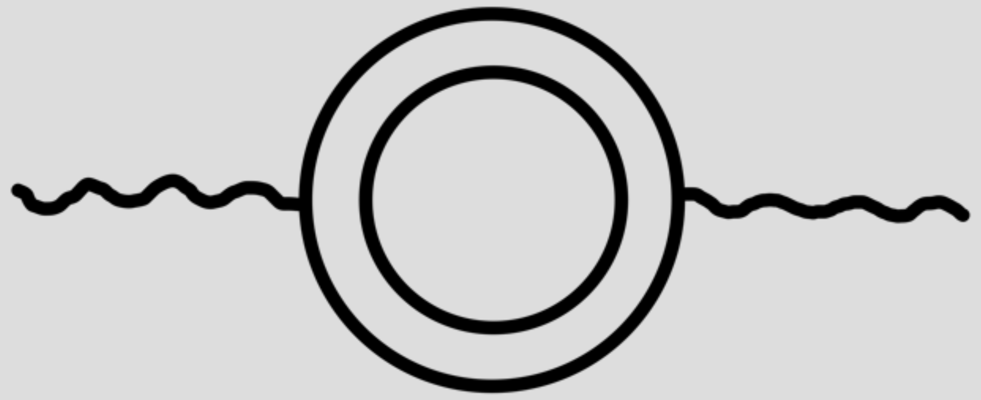

Photon scattering processes with the nucleus

Zilges A, Balabanski DL, Isaak J, Pietralla N. Progress in Particle and Nuclear Physics 122 (2022) 103903

Energy Levels Are Unique to the Isotope

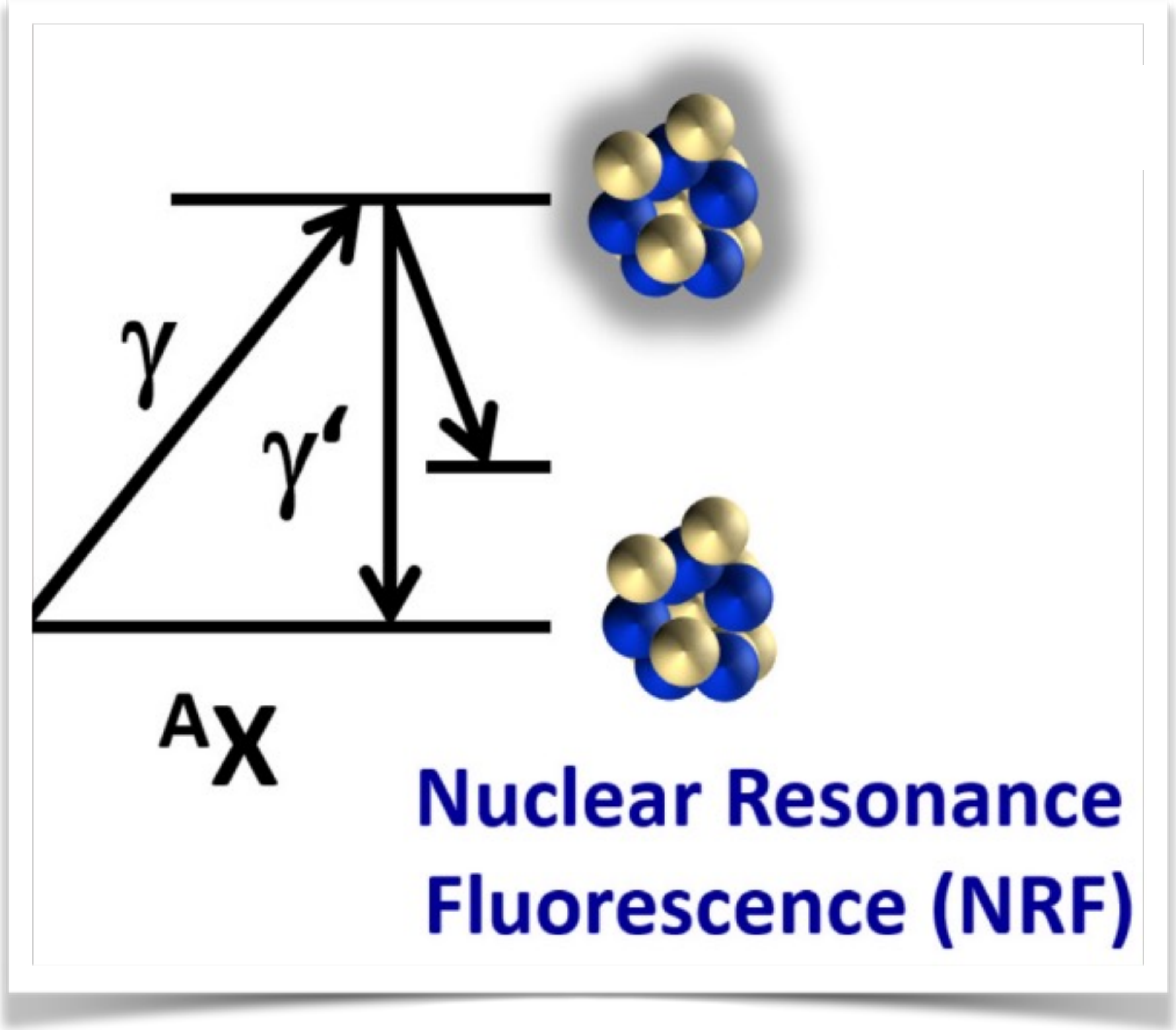

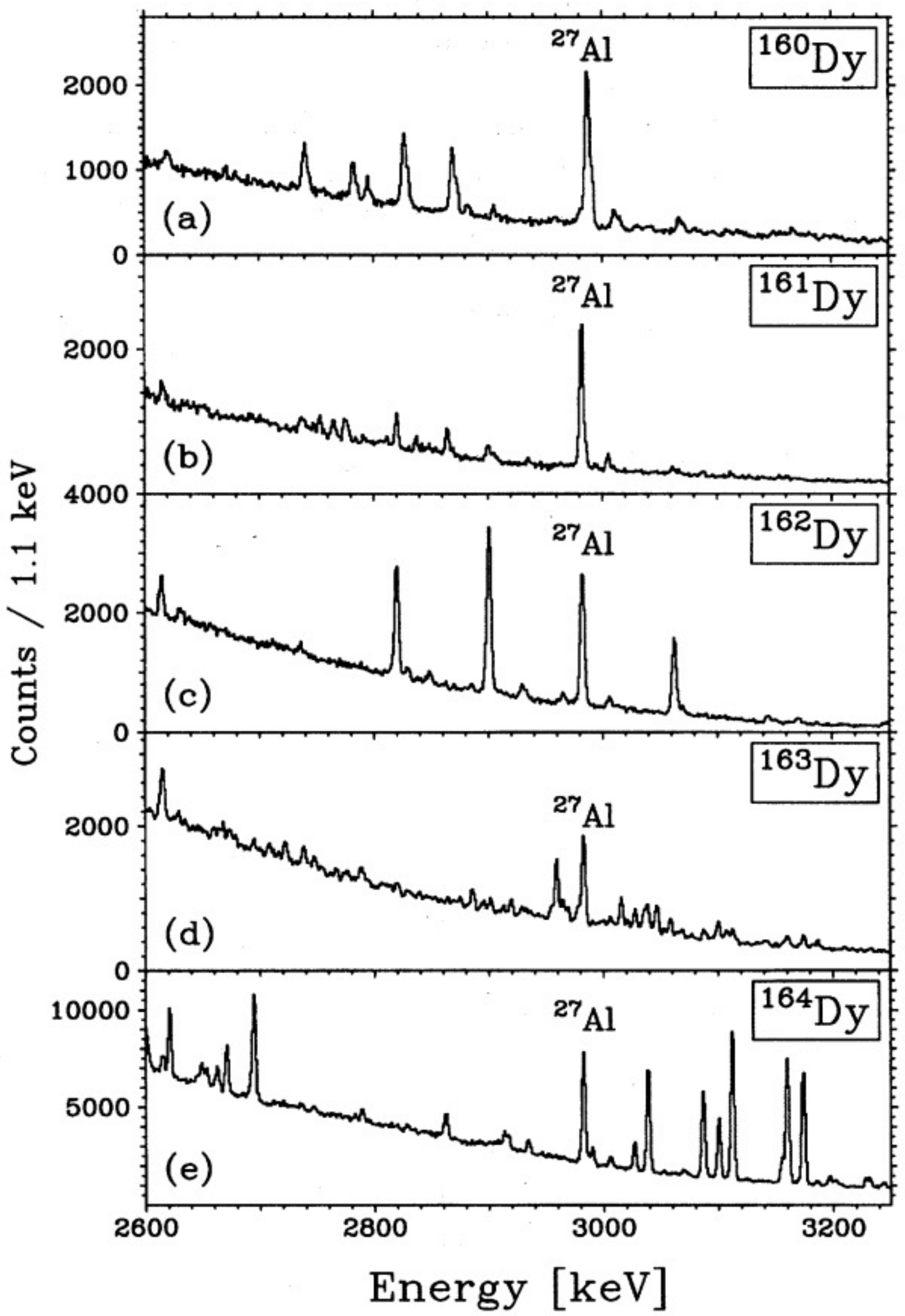

Margraf J, Eckert T, Rittner M, Bauske I, Beck O, Kneissl U, Maser H, Pitz HH, Schiller A, von Brentano P, Fischer R, Herzbert RD, Pietralla N, Zilges A, Friedrichs H. Physical Review C. (1995) 52(5) 2429
Zilges A, Balabanski DL, Isaak J, Pietralla N. Progress in Particle and Nuclear Physics 122 (2022) 103903

A Narrow Phenomenon…

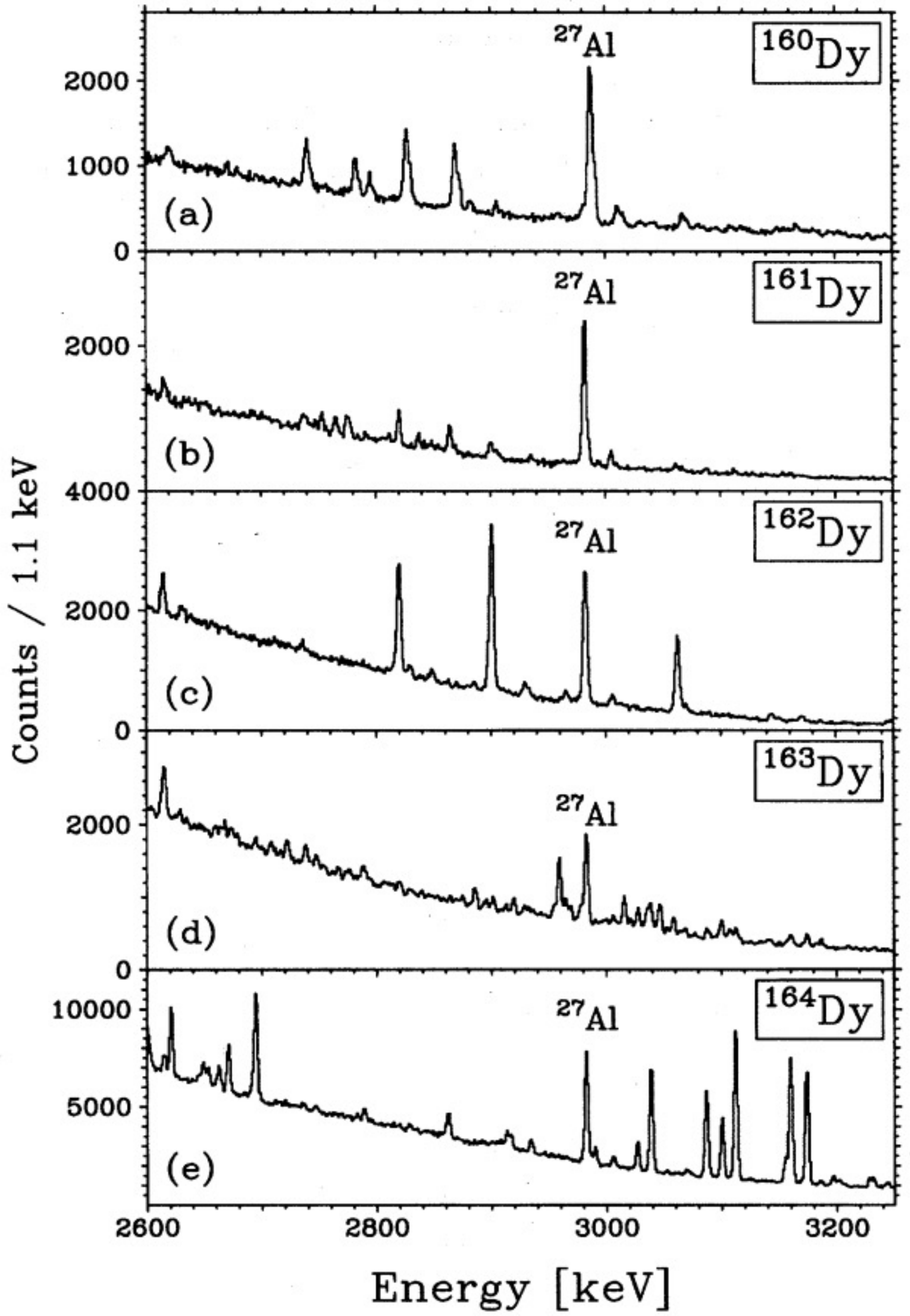

$$\frac{\Delta E}{E}\left({}^{7}Li\right) = 4.69\times10^{-6}$$

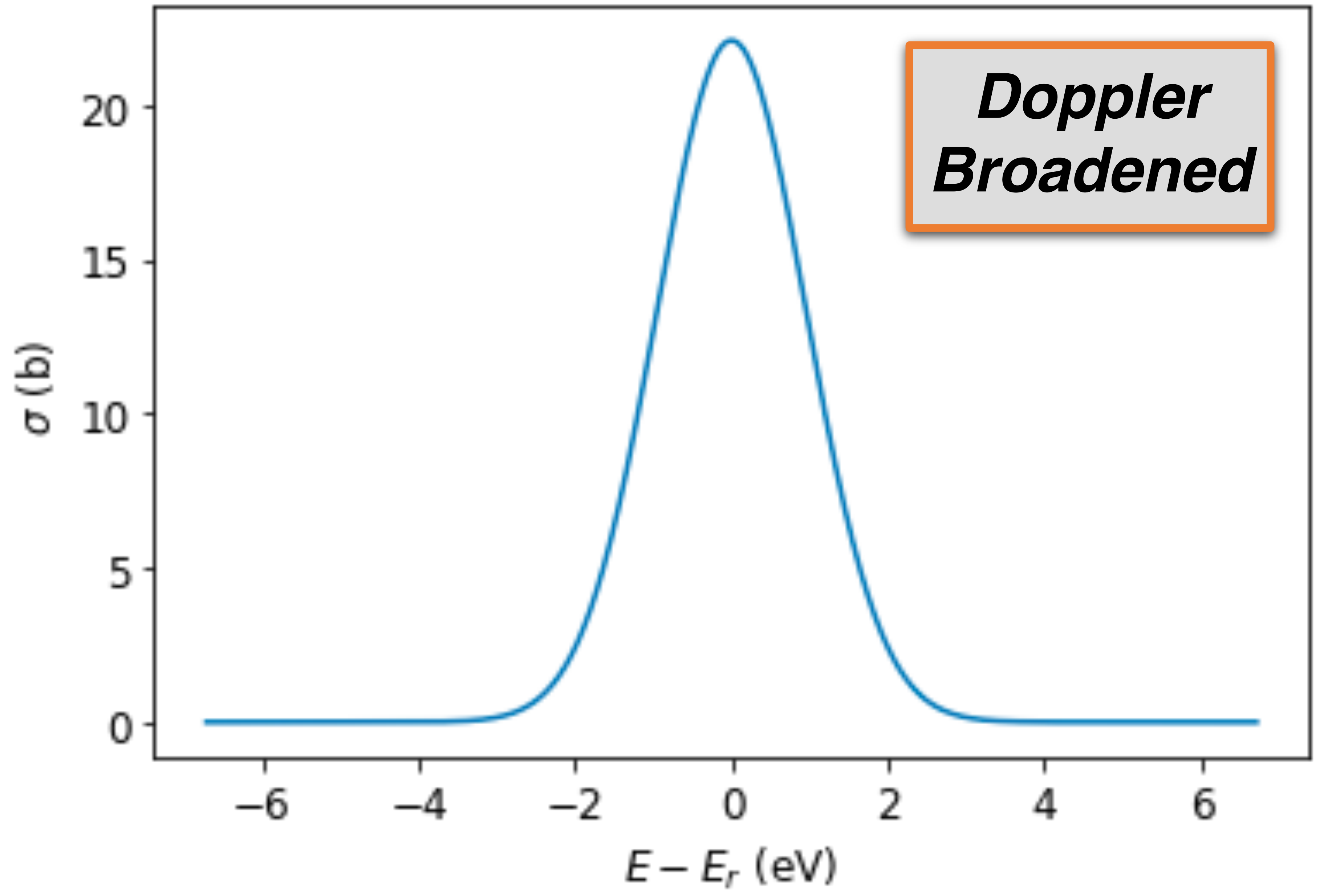

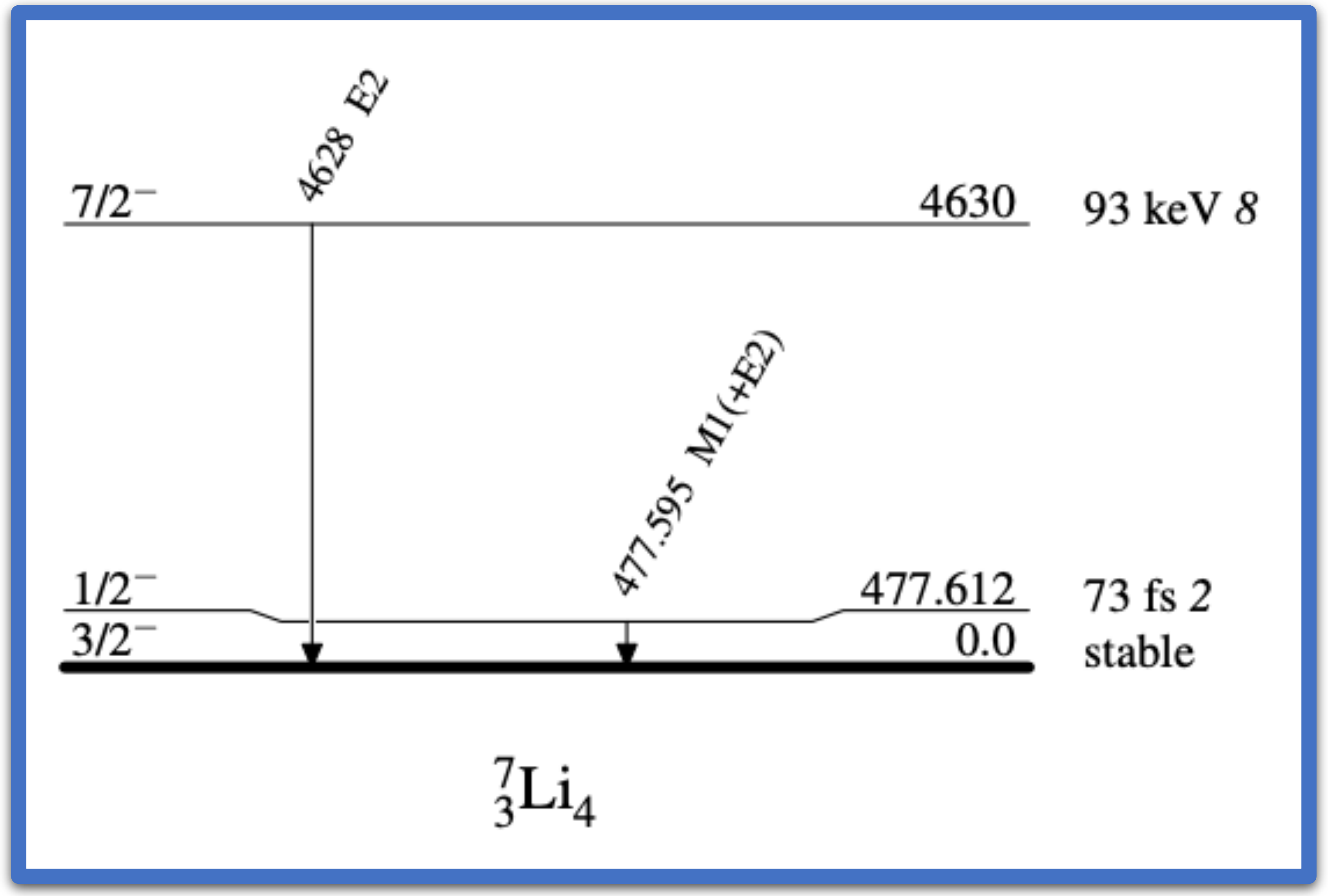

Line widths can be as low as 10^{-6} $\Delta E/E$

Margraf J, Eckert T, Rittner M, Bauske I, Beck O, Kneissl U, Maser H, Pitz HH, Schiller A, von Brentano P, Fischer R, Herzbert RD, Pietralla N, Zilges A, Friedrichs H. Physical Review C. (1995) 52(5) 2429
National Nuclear Data Center, Brookhaven National Lab, Evaluated Nuclear Structure Data File

How NRF Experiments are Typically Done

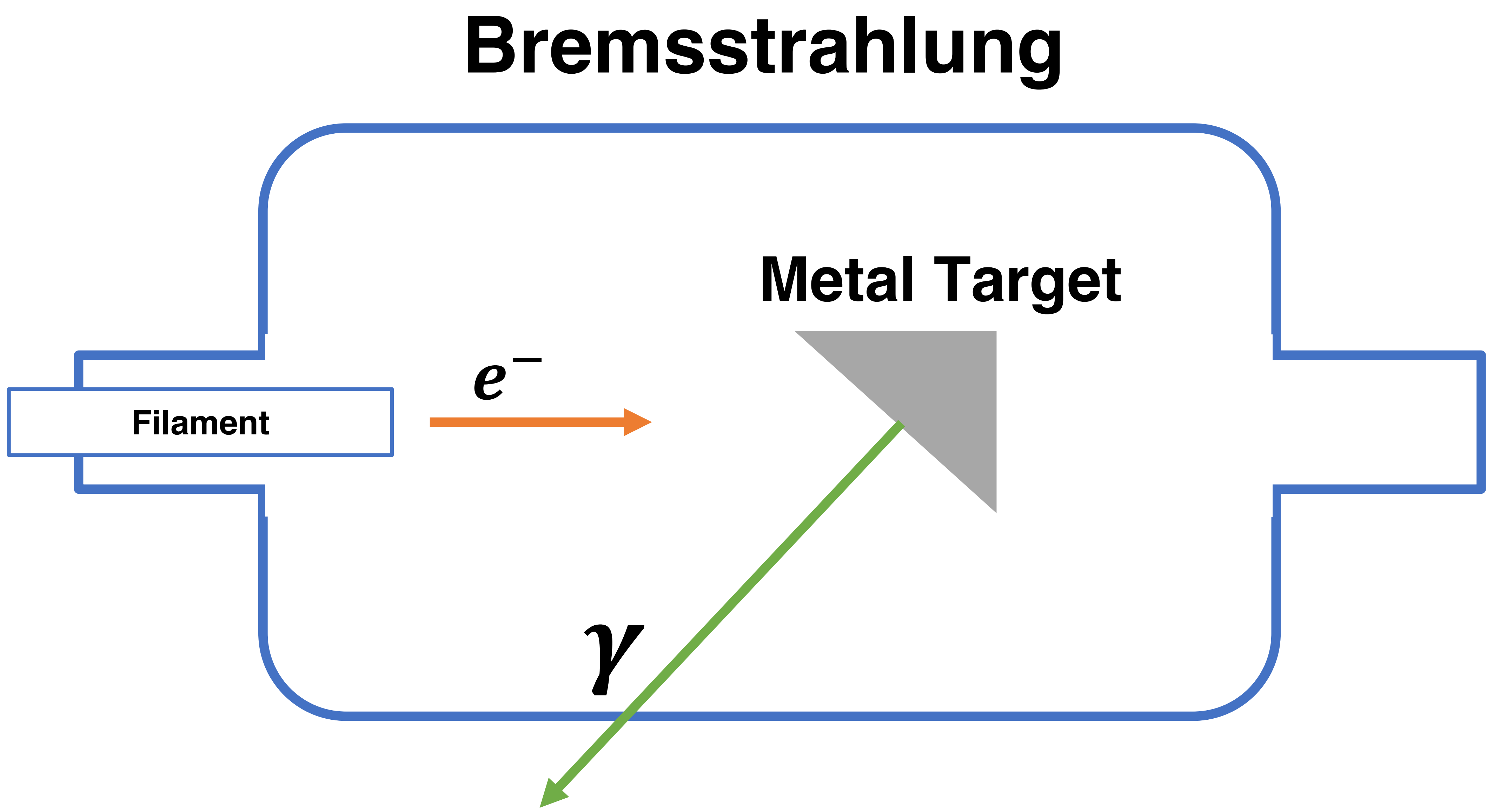

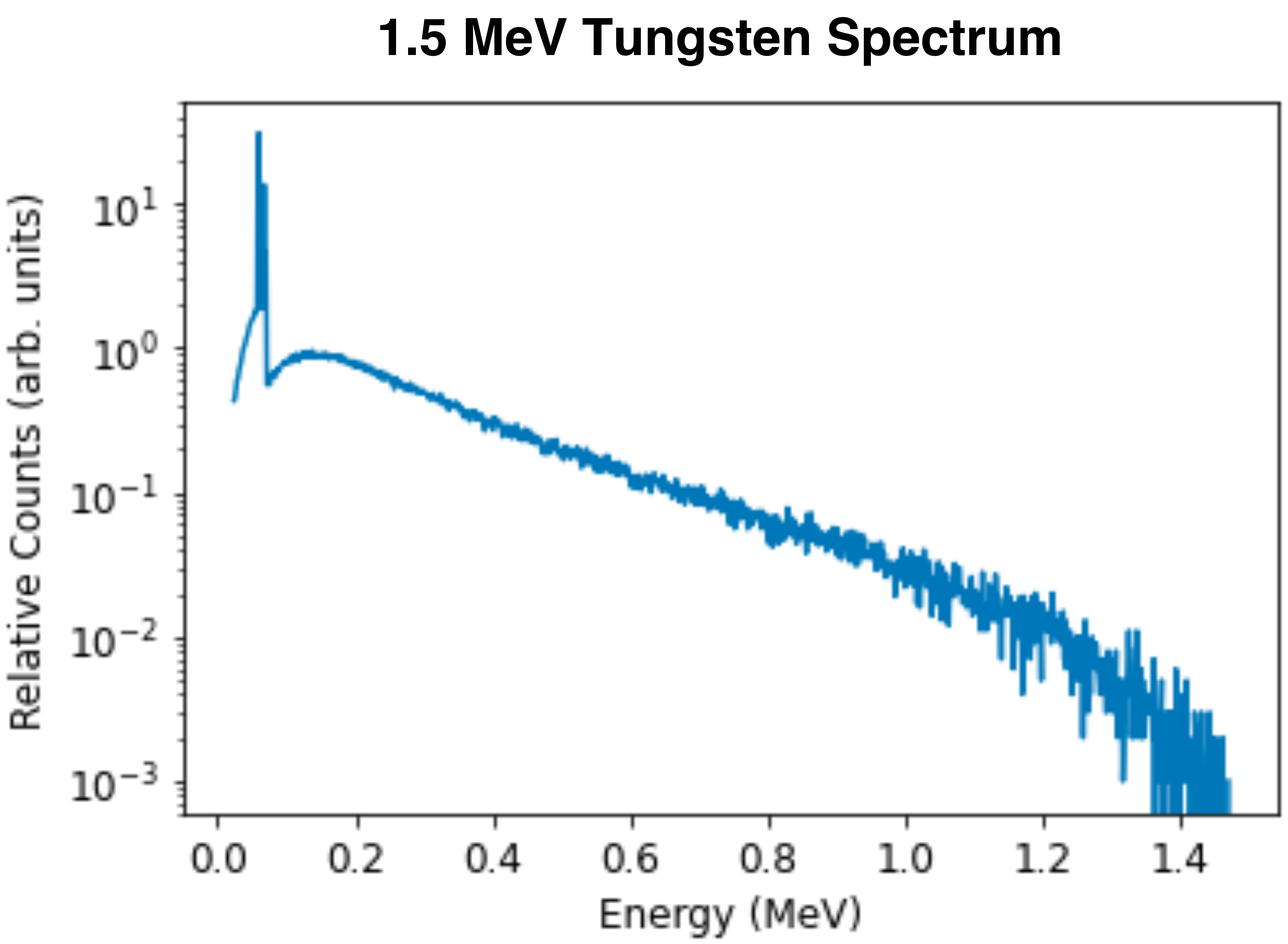

UCI

How NRF Experiments are Typically Done

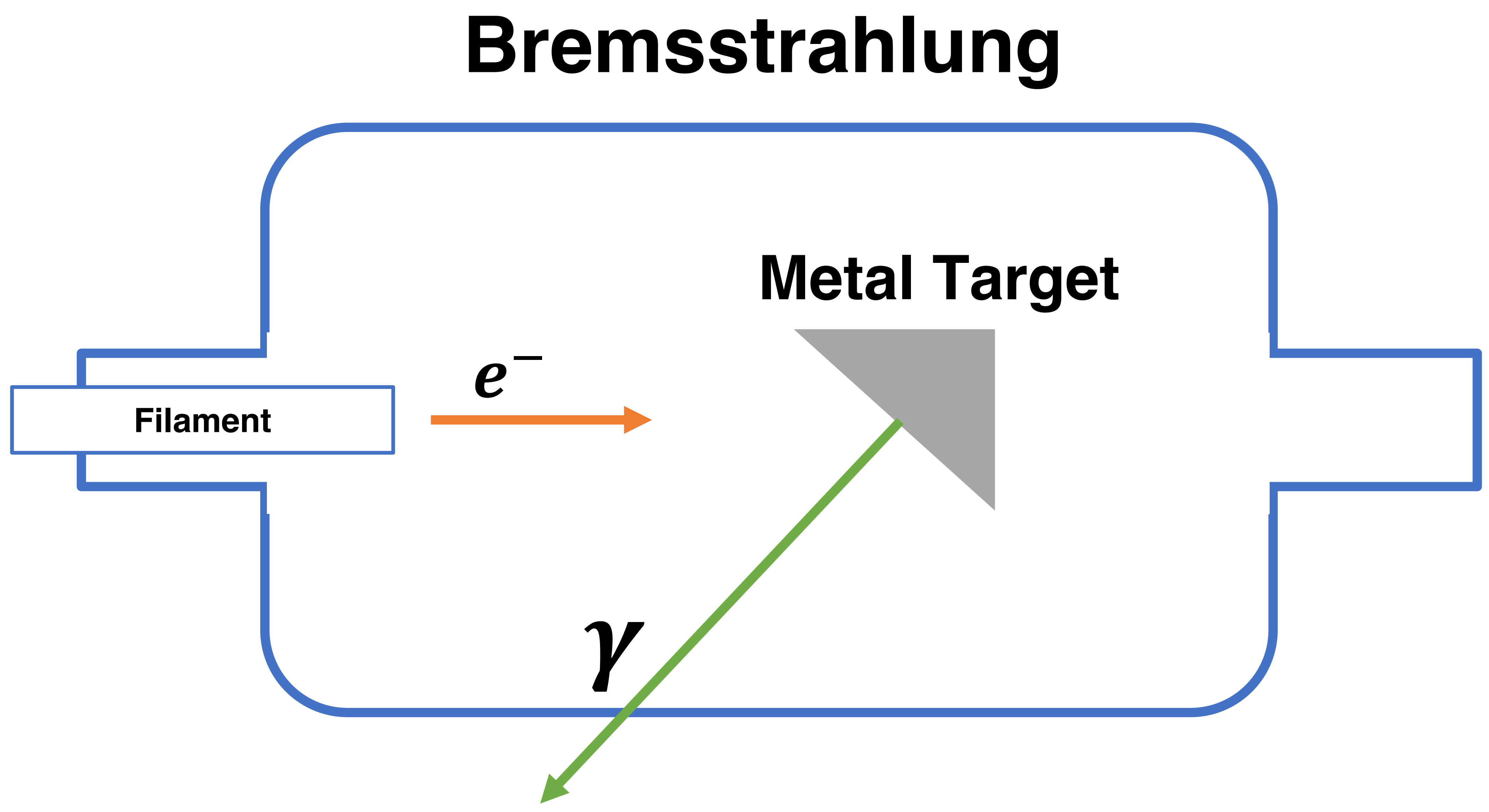

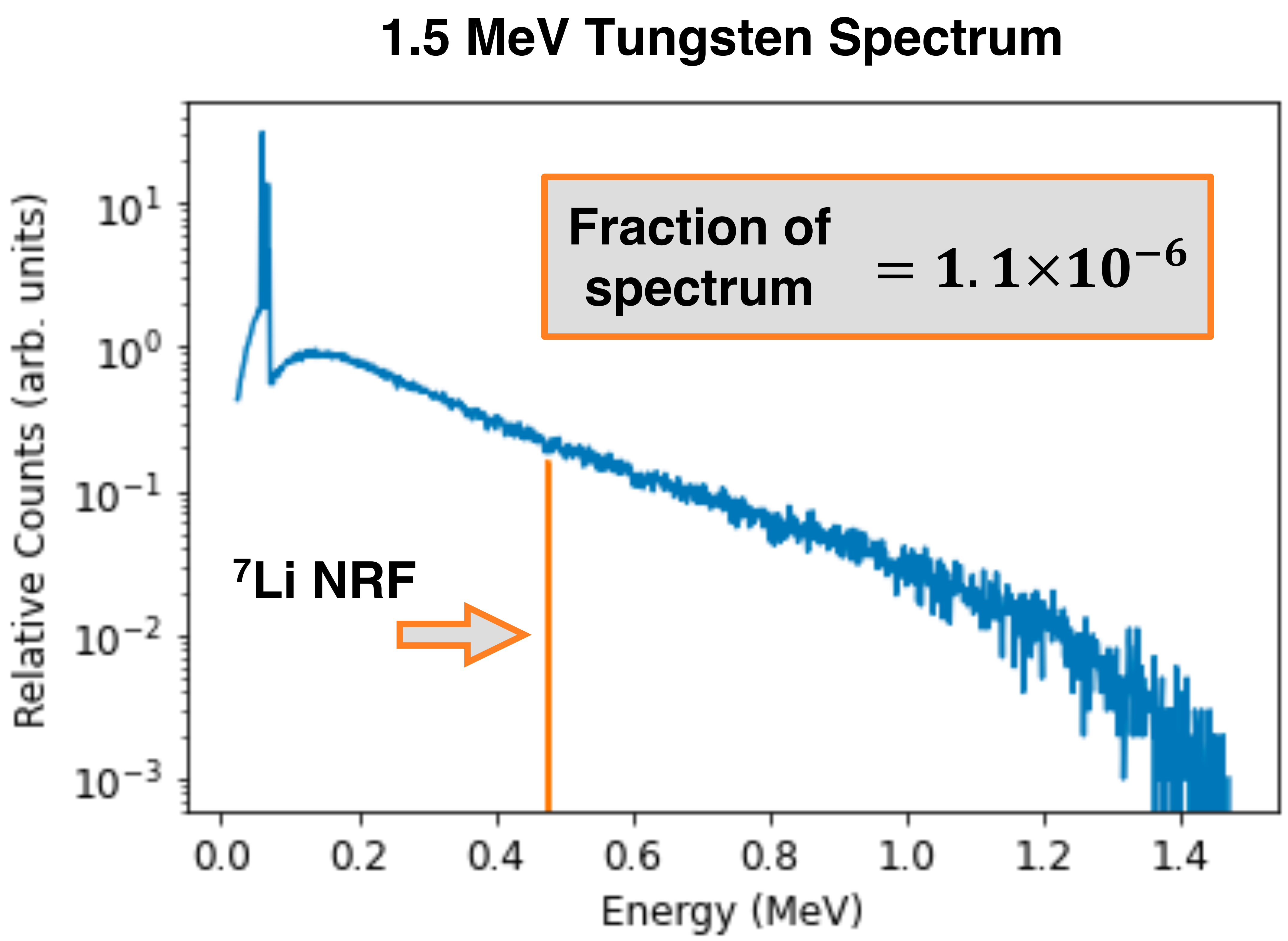

Not an ideal source for single resonance line measurements

Laser-Compton Scattering has the Edge

Bremsstrahlung

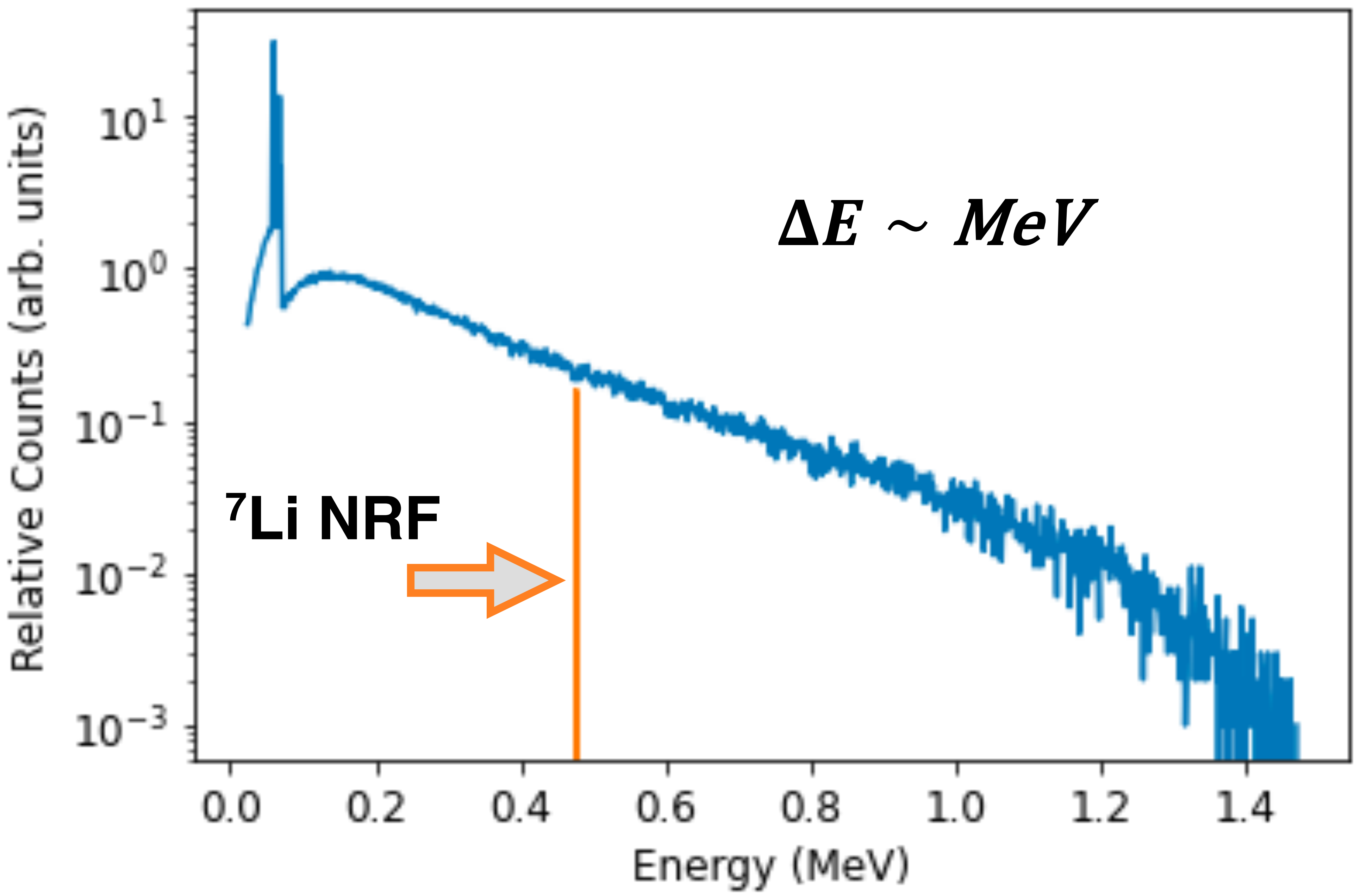

Fraction of spectrum $= 1.1\times10^{-6}$

LCS

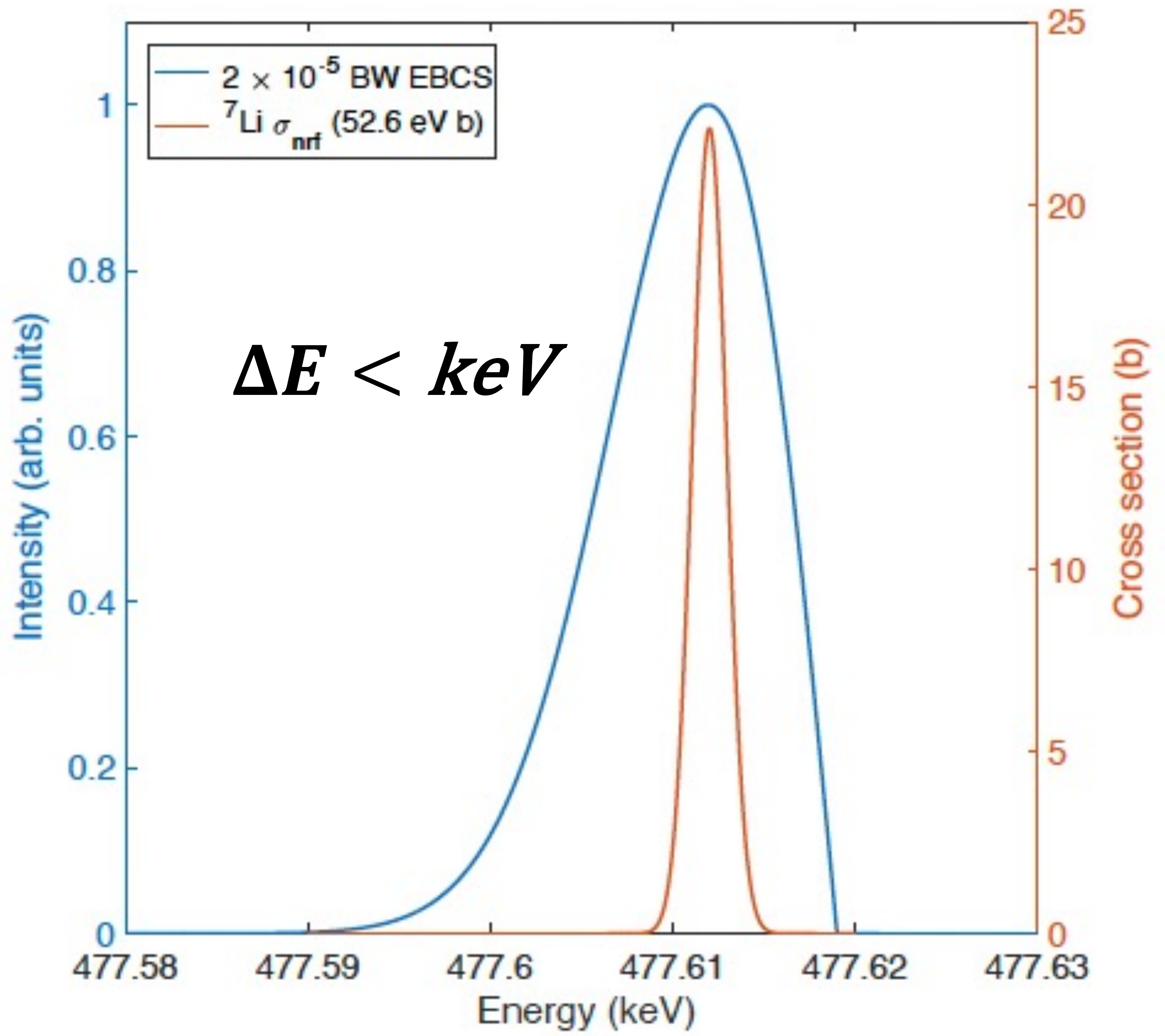

Fraction of spectrum $= 0.21$

LCS has narrow bandwidths that make probing these lines much better

Laser-Compton Source

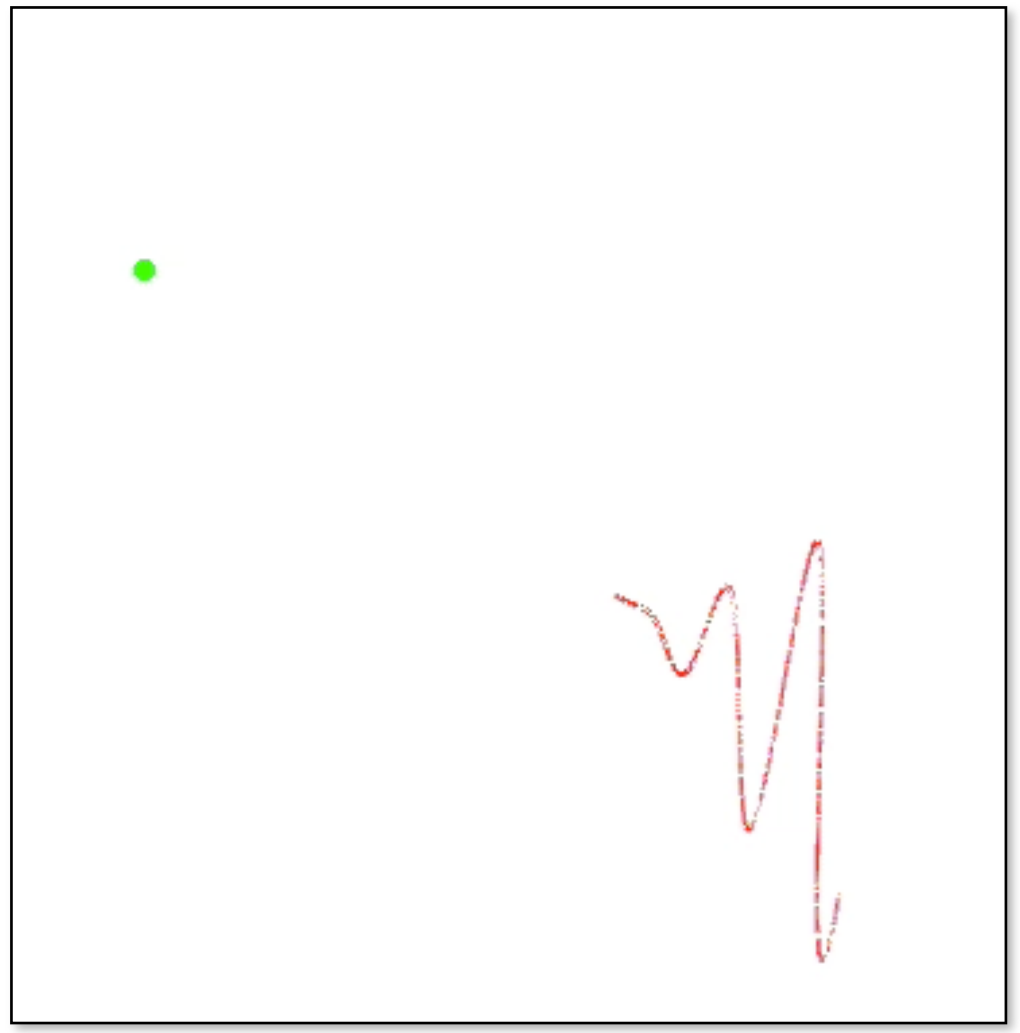

$$E_\gamma = \frac{4\gamma^2}{1 + \gamma^2\theta^2 + 4\gamma k_0 \bar{\lambda}_c} E_L$$

Reutershan T, Effarah HH, Lagzda A, Barty CPJ. Applied Optics (2022) 61(6):C162:178

Laser-Compton Source

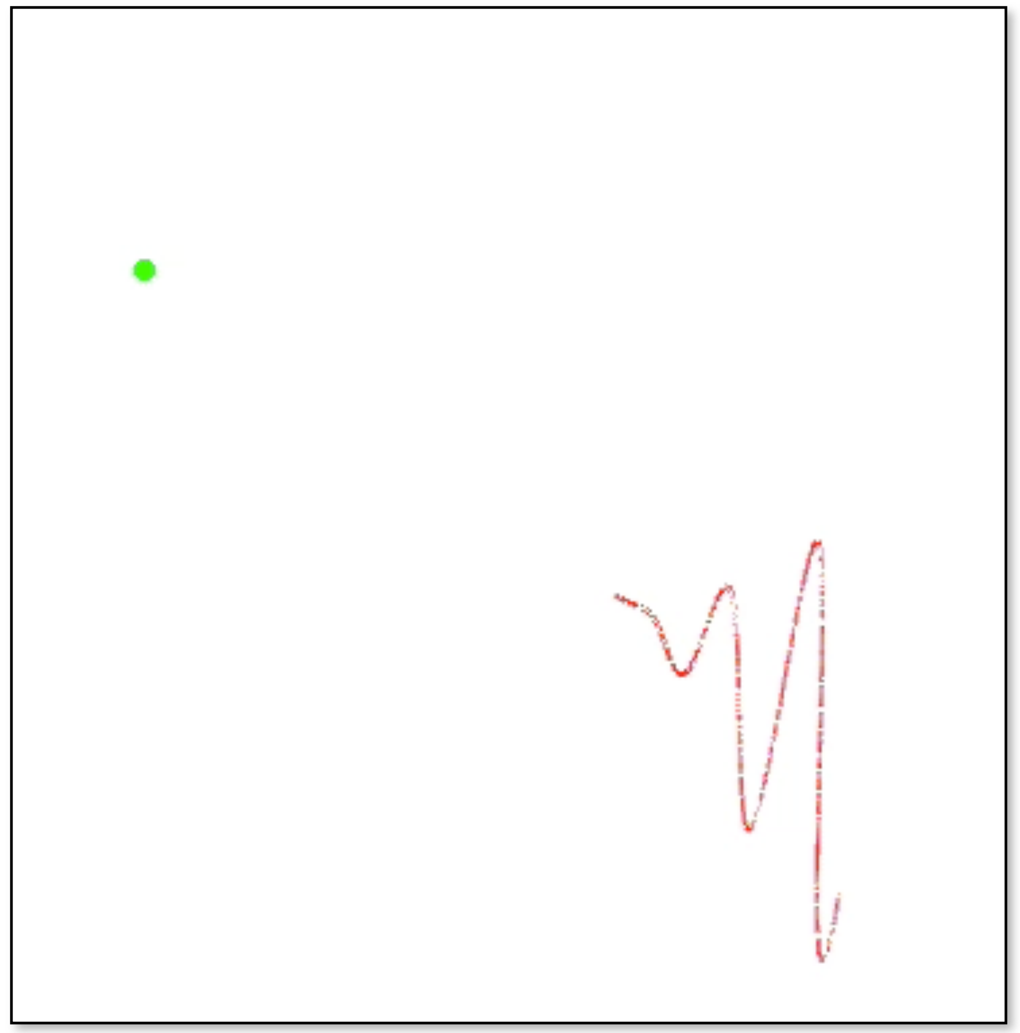

Double Doppler upshift

$$E_\gamma = \frac{4\gamma^2}{1 + \gamma^2\theta^2 + 4\gamma \bar{k}_0 \lambda_c} E_L$$

Laser-Compton Source

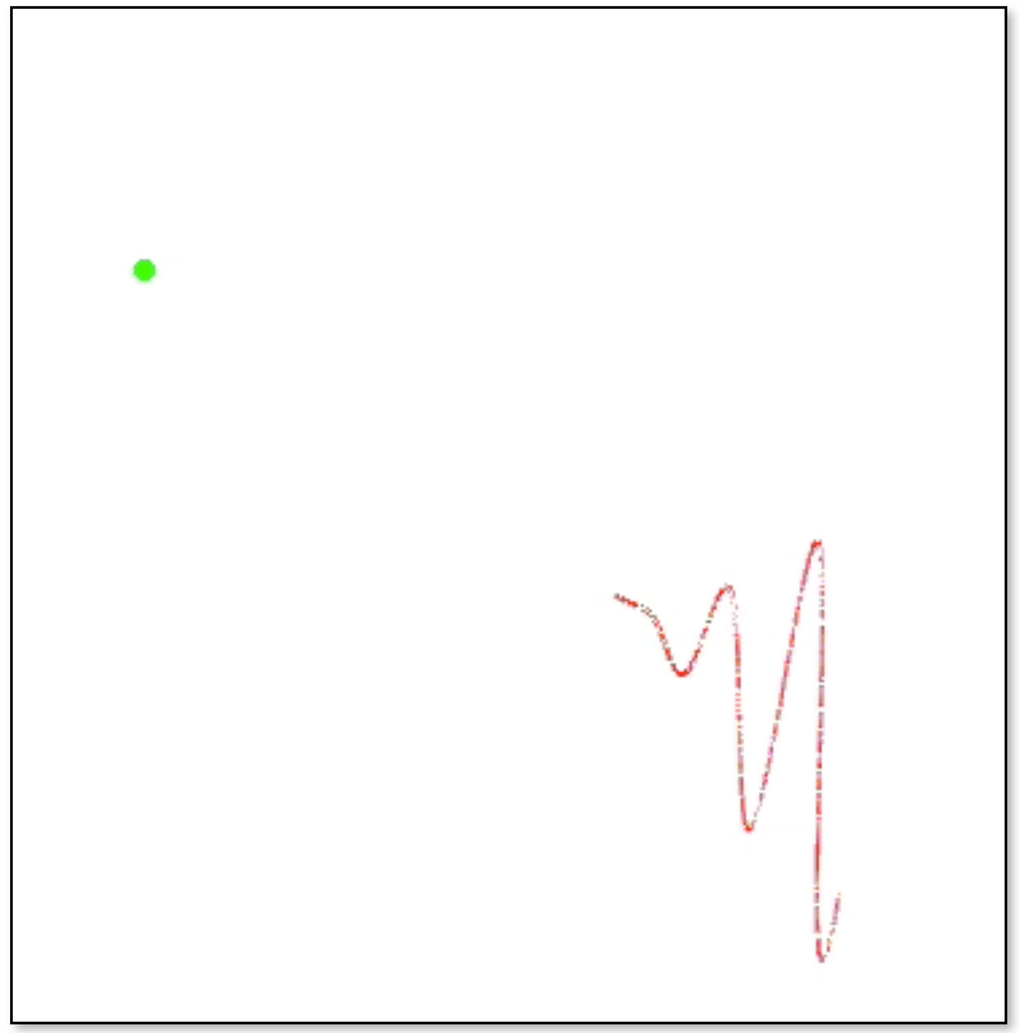

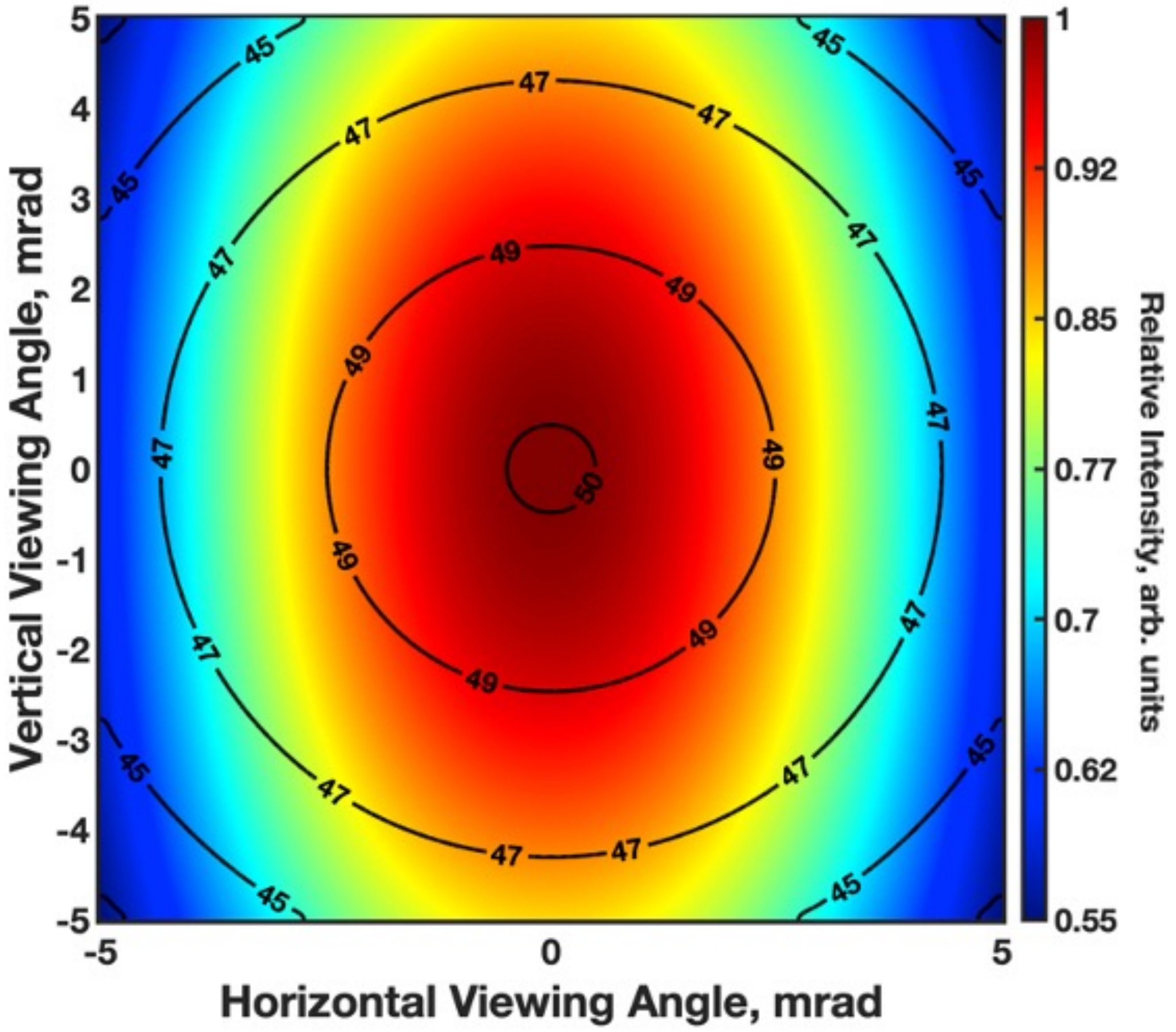

Double Doppler upshift

$$E_\gamma = \frac{4\gamma^2}{1 + \gamma^2\theta^2 + 4\gamma k_0^{-}\lambda_c} E_L$$

Angle correlated spectrum

Reutershan T, Effarah HH, Lagzda A, Barty CPJ. Applied Optics (2022) 61(6):C162:178

Laser-Compton Source

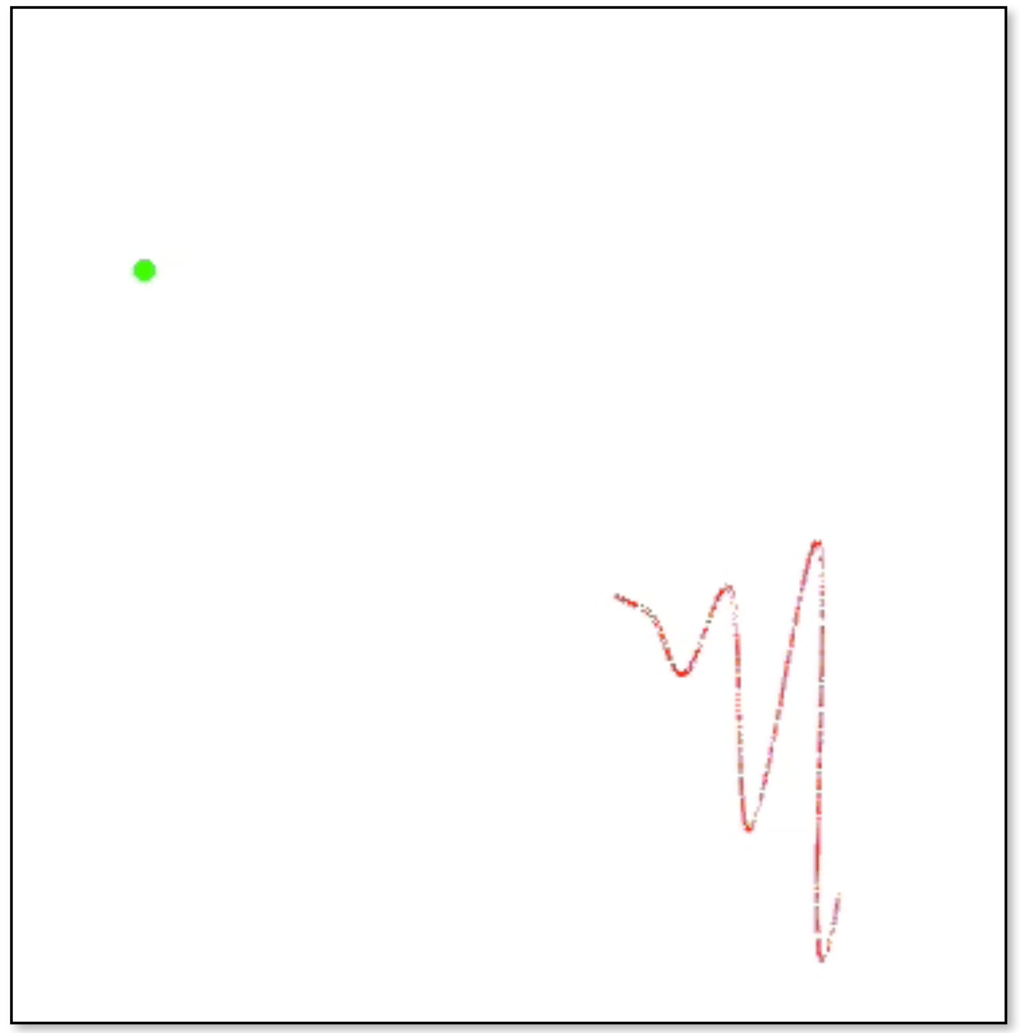

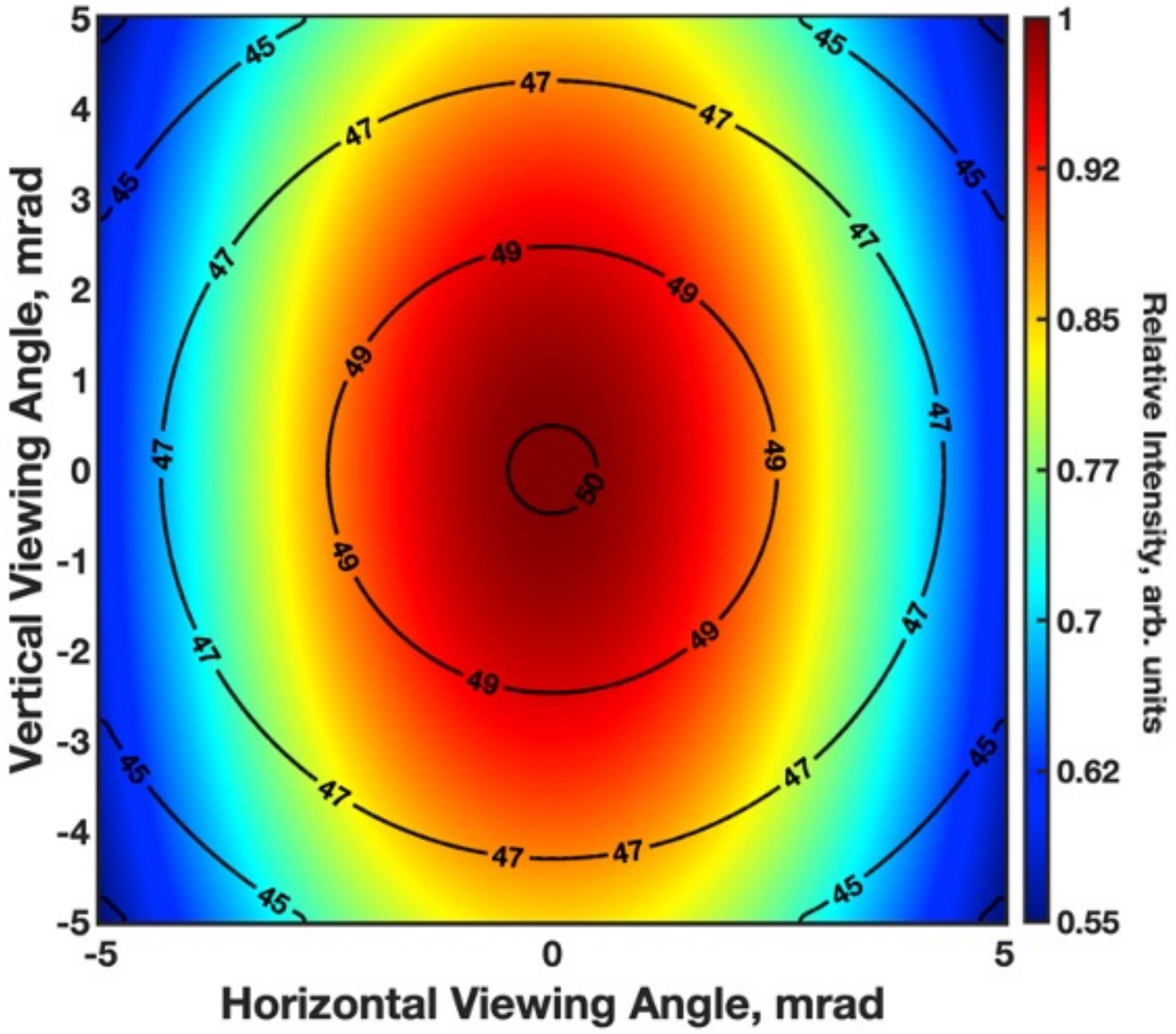

Double Doppler upshift

$$E_\gamma = \frac{4\gamma^2}{1 + \gamma^2\theta^2 + 4\gamma k_0^- \lambda_c} E_L$$

Angle correlated spectrum

$$\frac{dN}{d\Omega d\omega} = \int \frac{d\sigma}{d\Omega} \delta\left(\omega - \omega_l \frac{\kappa_l}{\kappa}\right)(1 + \beta_0) n_l(x_\mu) n_e(x_\mu) d^4 x_\mu$$

Reutershan T, Effarah HH, Lagzda A, Barty CPJ. Applied Optics (2022) 61(6):C162:178

Laser-Compton Source

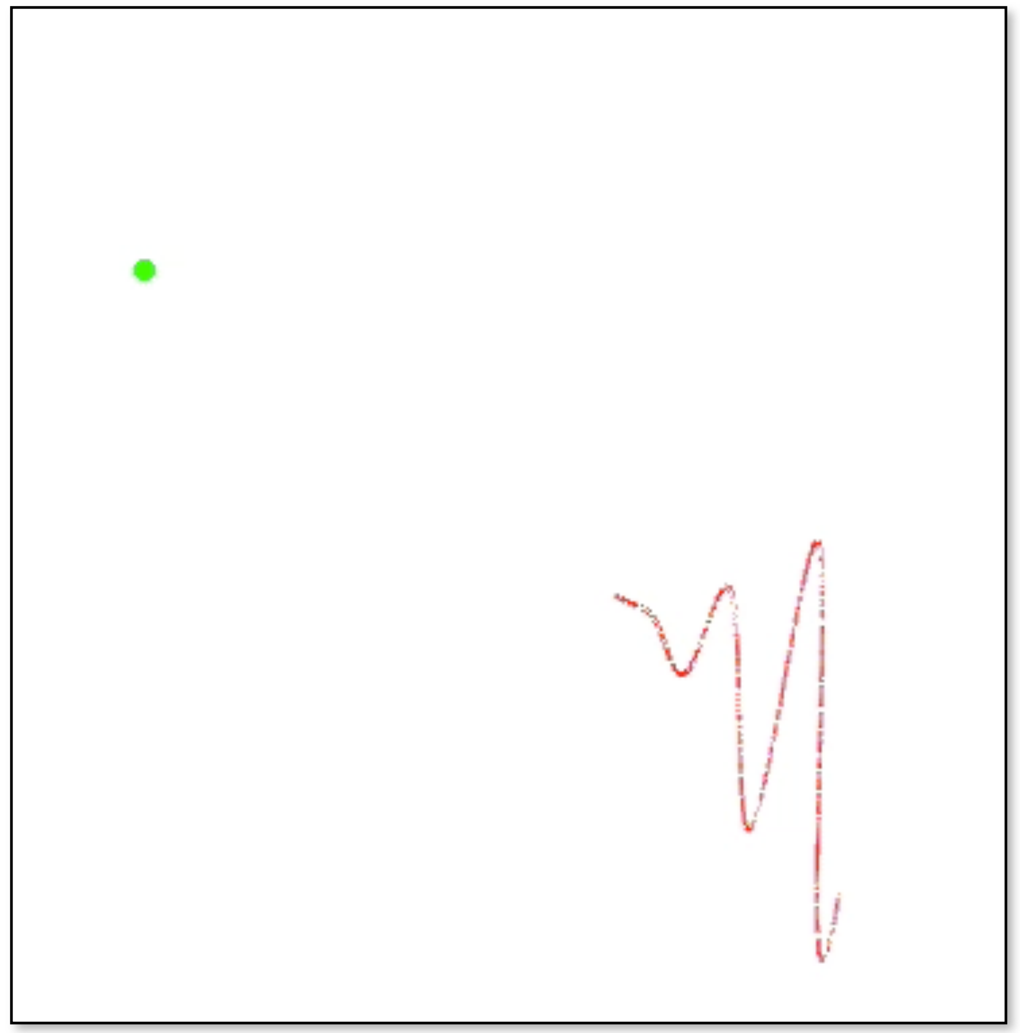

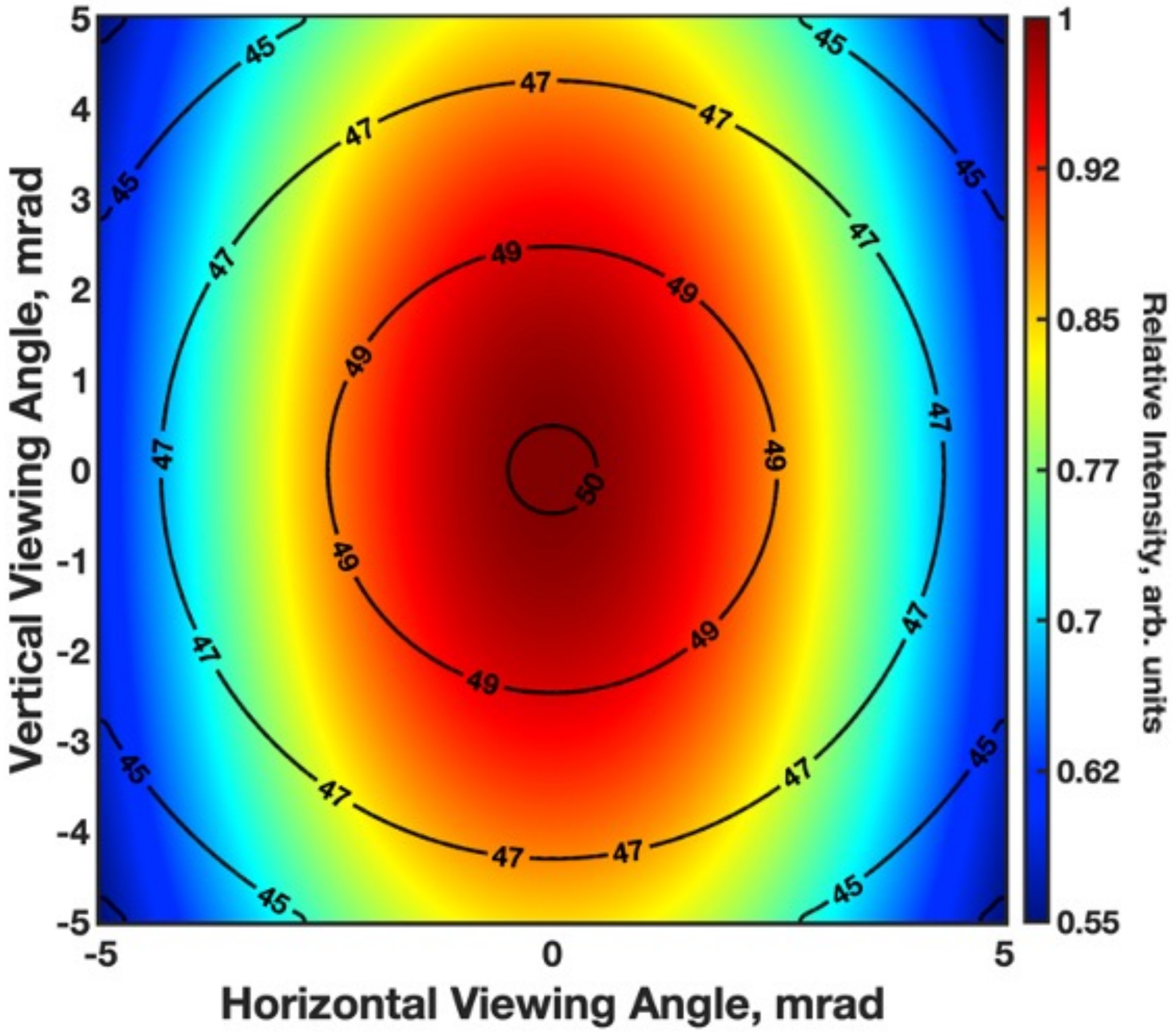

Double Doppler upshift

$$E_\gamma = \frac{4\gamma^2}{1 + \gamma^2\theta^2 + 4\gamma k_0^{-}\lambda_c} E_L$$

Angle correlated spectrum

$$\frac{dN}{d\Omega d\omega} = \int \frac{d\sigma}{d\Omega}\delta\left(\omega - \omega_l\frac{\kappa_l}{\kappa}\right)(1+\beta_0)n_l(x_\mu)n_e(x_\mu)d^4x_\mu$$

Laser beam properties

Reutershan T, Effarah HH, Lagzda A, Barty CPJ. Applied Optics (2022) 61(6):C162:178

UCI

Laser-Compton Source

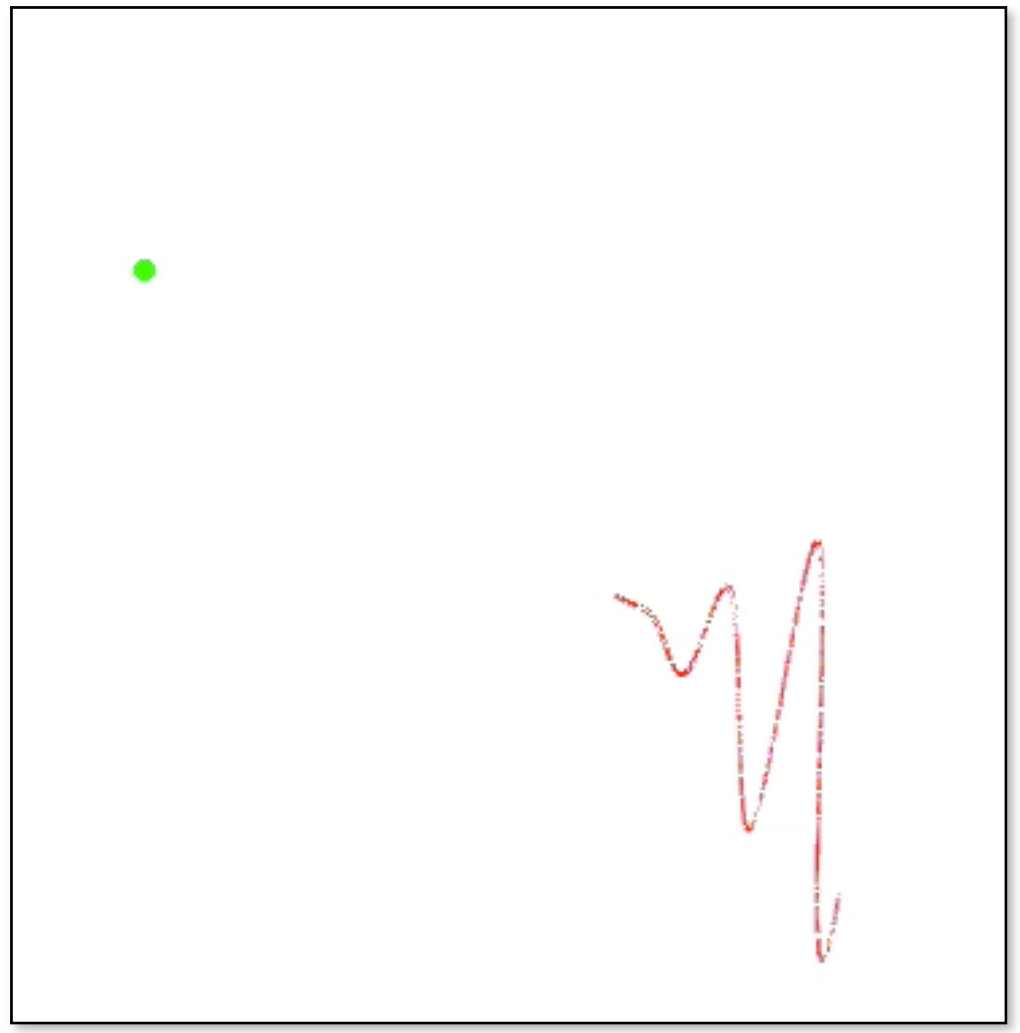

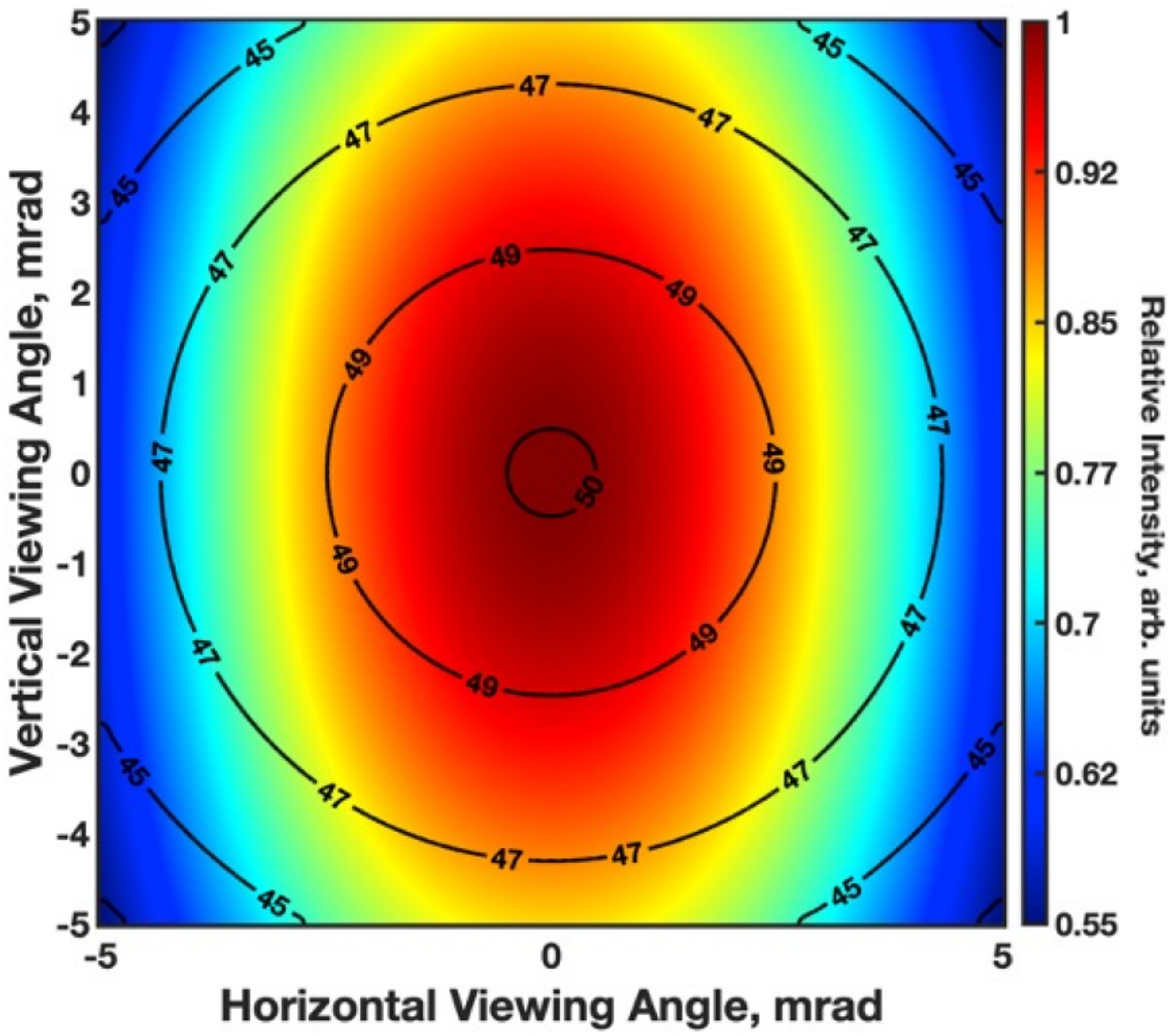

Double Doppler upshift

$$E_\gamma = \frac{4\gamma^2}{1 + \gamma^2\theta^2 + 4\gamma k_0^{-}\lambda_c} E_L$$

Angle correlated spectrum

$$\frac{dN}{d\Omega d\omega} = \int \frac{d\sigma}{d\Omega}\delta\left(\omega - \omega_l \frac{\kappa_l}{\kappa}\right)(1+\beta_0) n_l(x_\mu) n_e(x_\mu) d^4 x_\mu$$

Laser beam properties

Electron beam properties

Reutershan T, Effarah HH, Lagzda A, Barty CPJ. Applied Optics (2022) 61(6):C162:178

UCI

Laser-Compton Source

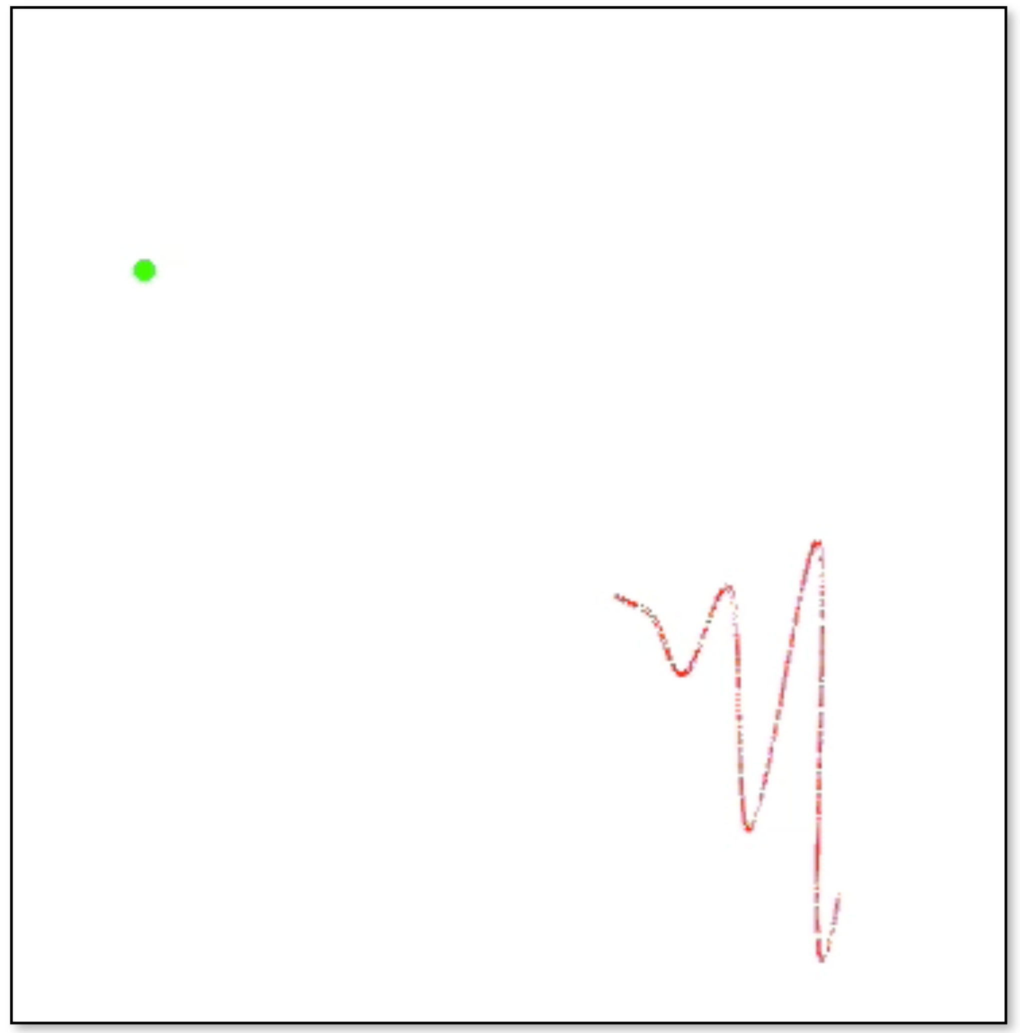

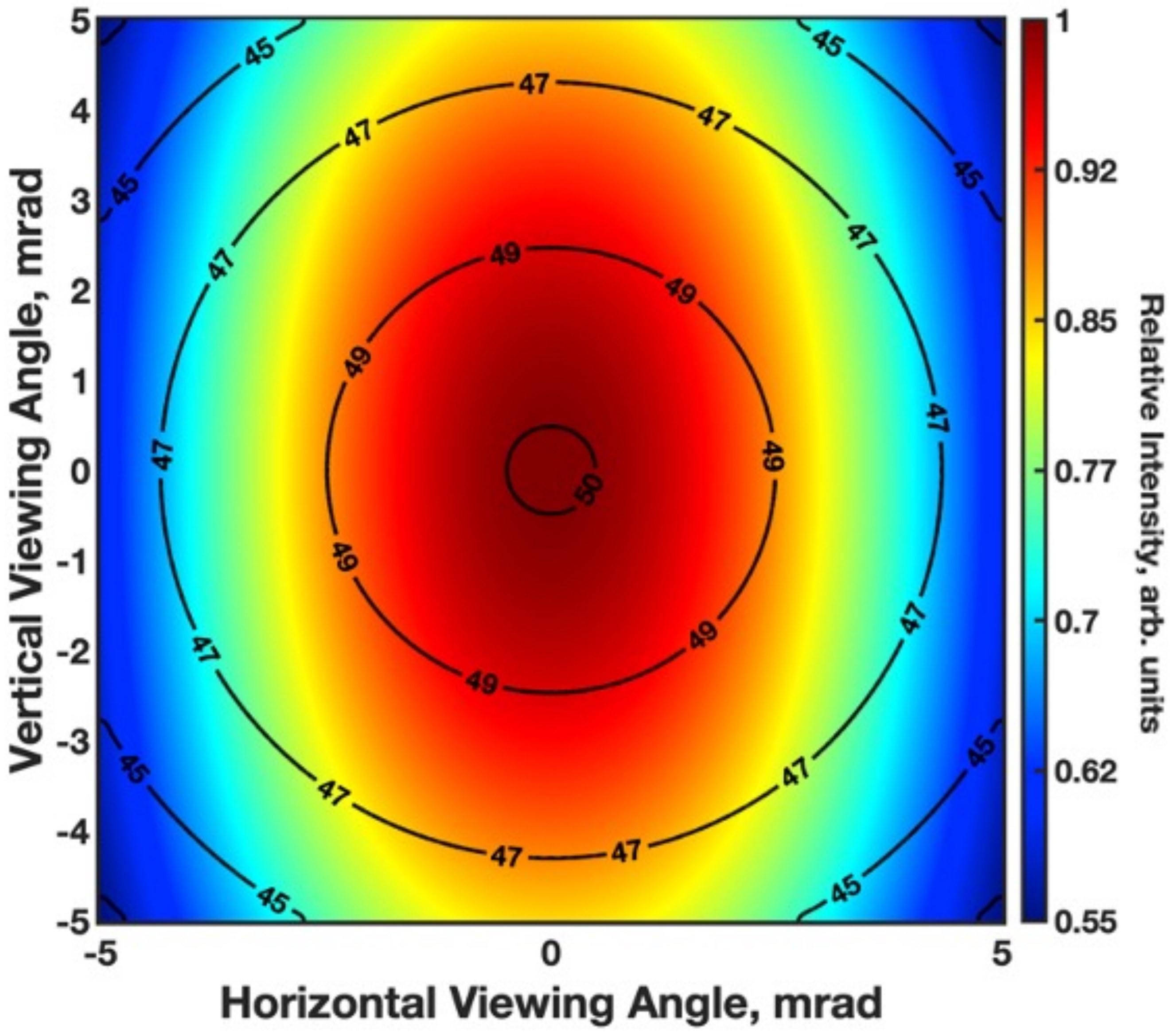

Double Doppler upshift

$$E_\gamma = \frac{4\gamma^2}{1 + \gamma^2\theta^2 + 4\gamma k_0^{-}\lambda_c} E_L$$

Angle correlated spectrum

$$\frac{dN}{d\Omega d\omega} = \int \frac{d\sigma}{d\Omega}\delta\left(\omega - \omega_l \frac{\kappa_l}{\kappa}\right)(1 + \beta_0) n_l(x_\mu) n_e(x_\mu) d^4 x_\mu$$

Klein-Nishina

Laser beam properties

Electron beam properties

UCI

Reutershan T, Effarah HH, Lagzda A, Barty CPJ. Applied Optics (2022) 61(6):C162:178

Laser-Compton Source

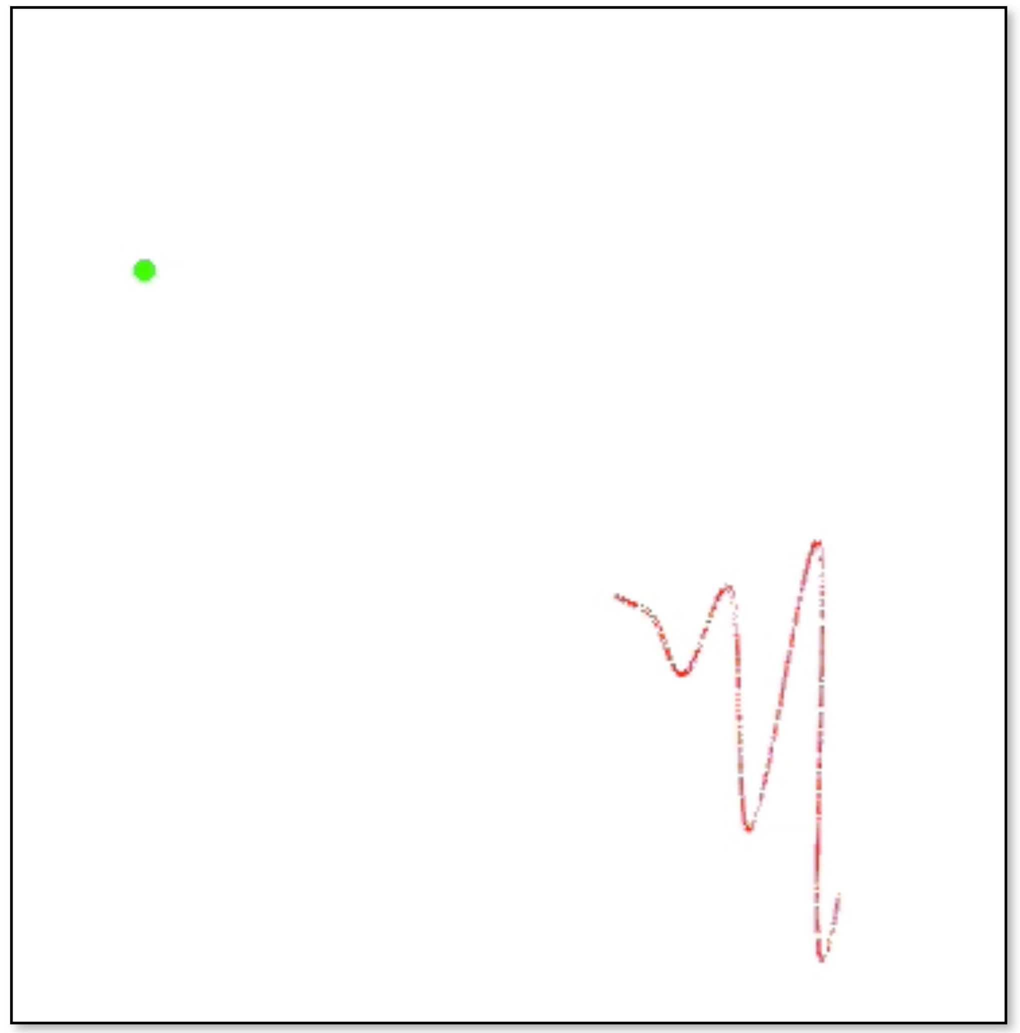

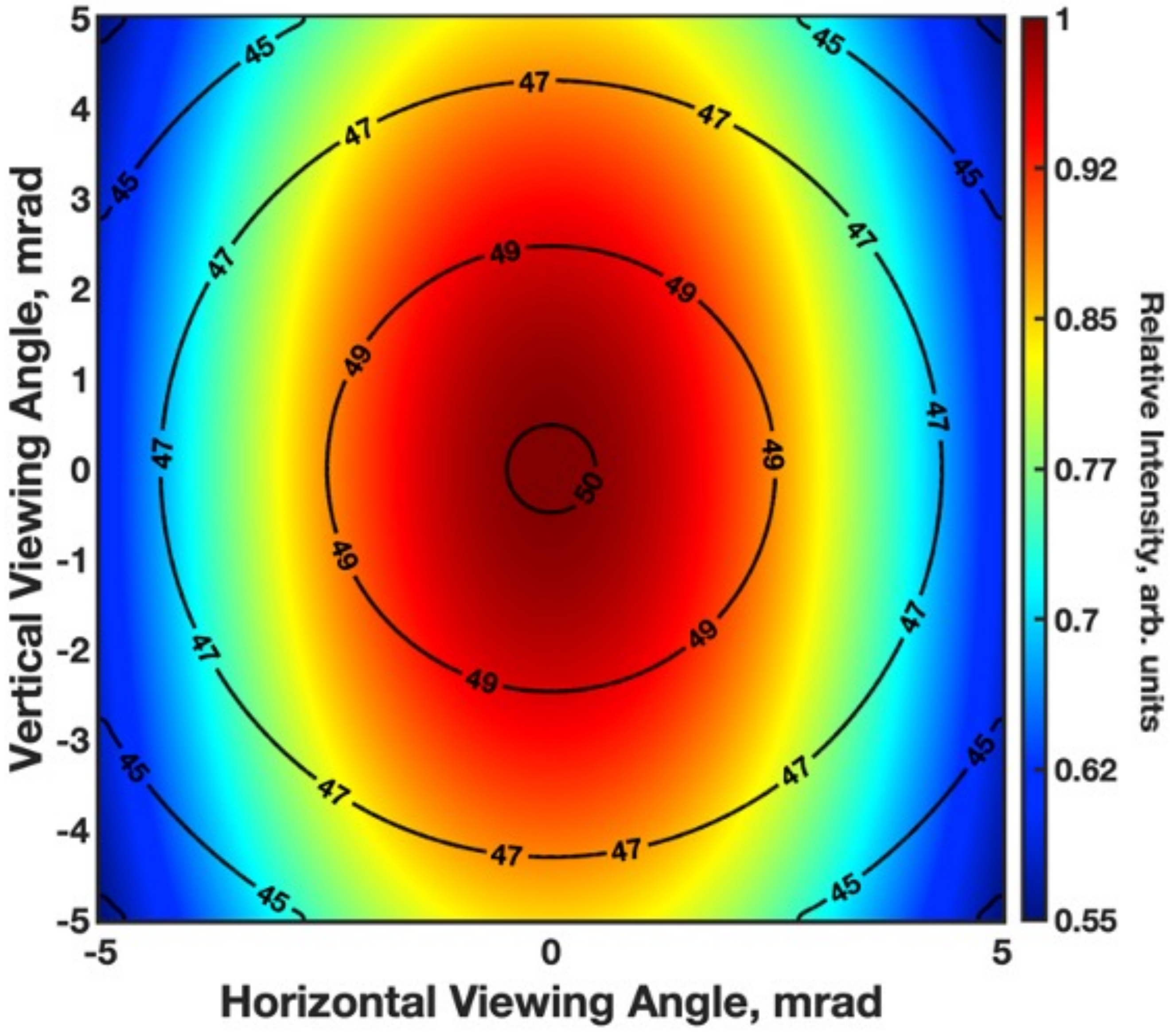

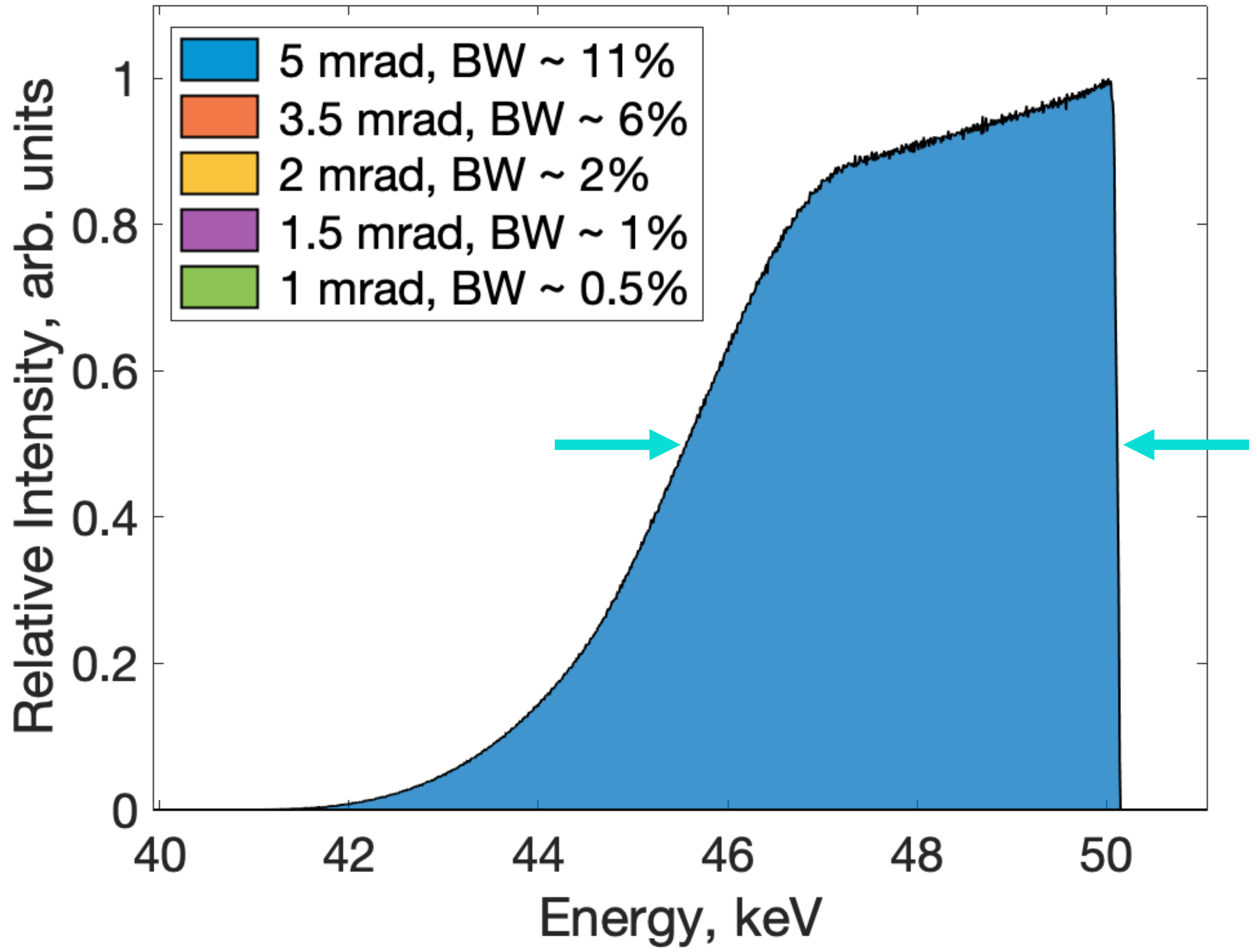

Double Doppler upshift

$$E_\gamma = \frac{4\gamma^2}{1+\gamma^2\theta^2+4\gamma \bar{k}_0\lambda_c} E_L$$

Angle correlated spectrum

$$\frac{dN}{d\Omega d\omega} = \int \frac{d\sigma}{d\Omega}\delta\left(\omega - \omega_l\frac{\kappa_l}{\kappa}\right)(1+\beta_0)n_l(x_\mu)n_e(x_\mu)d^4x_\mu$$

Klein-Nishina

Laser beam properties

Electron beam properties

Reutershan T, Effarah HH, Lagzda A, Barty CPJ. Applied Optics (2022) 61(6):C162:178

Laser-Compton Source

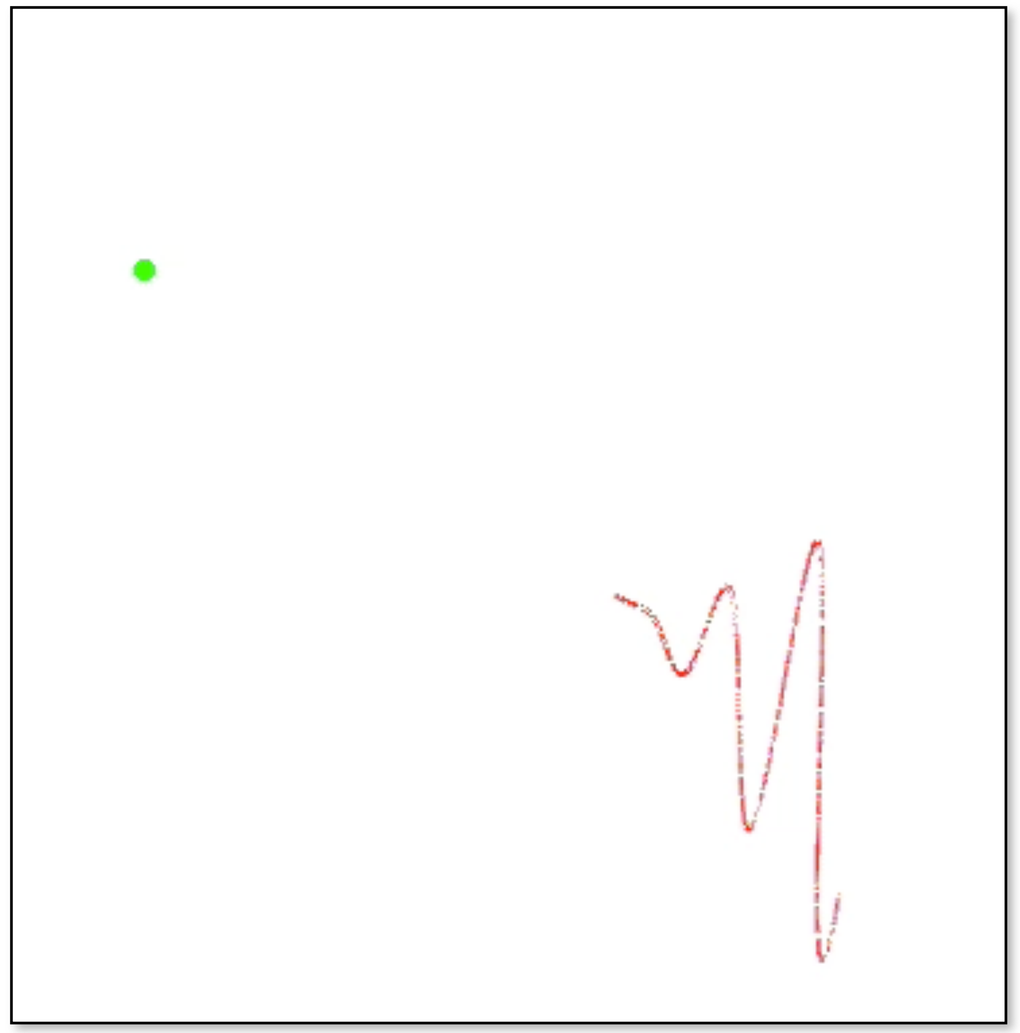

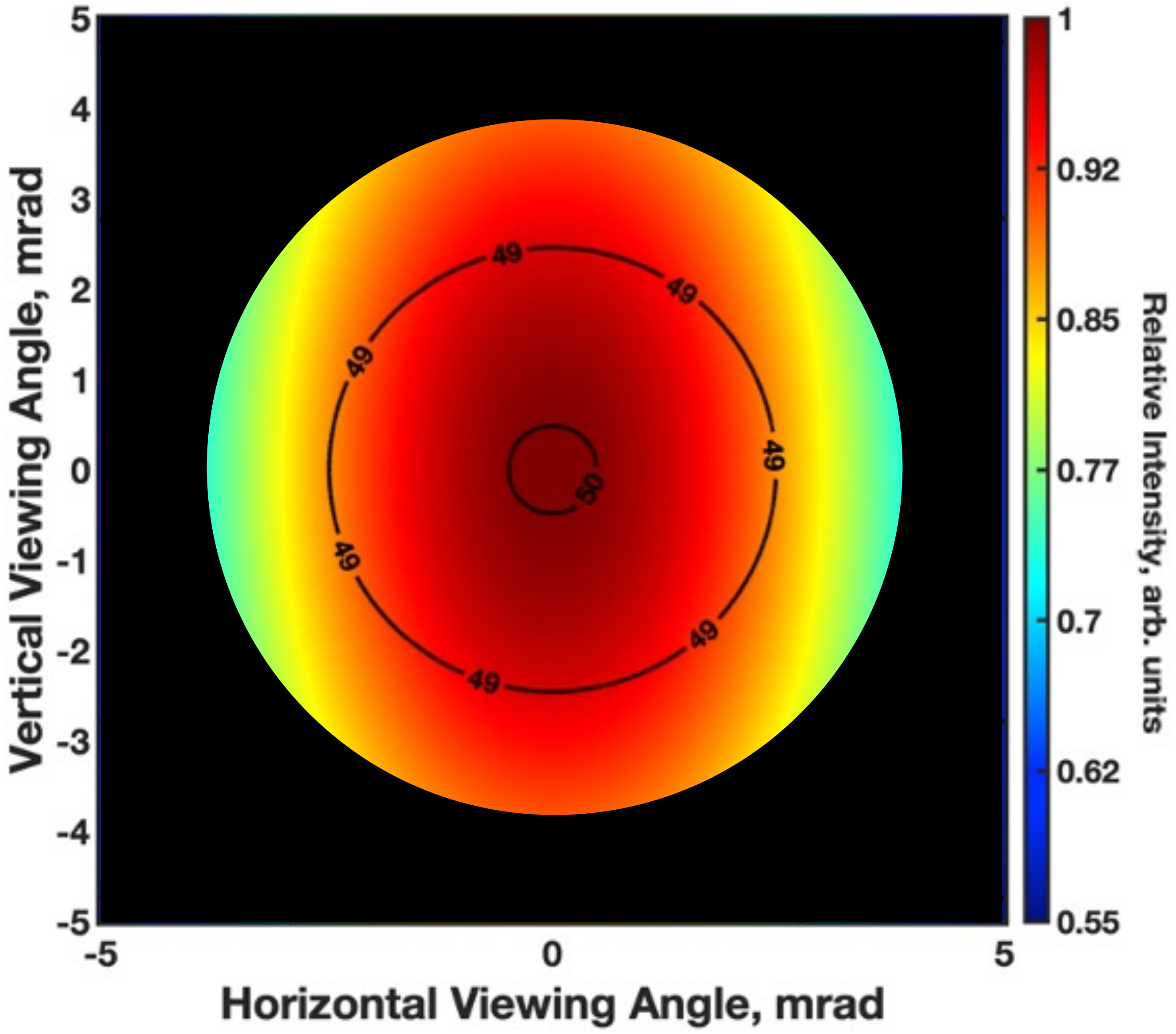

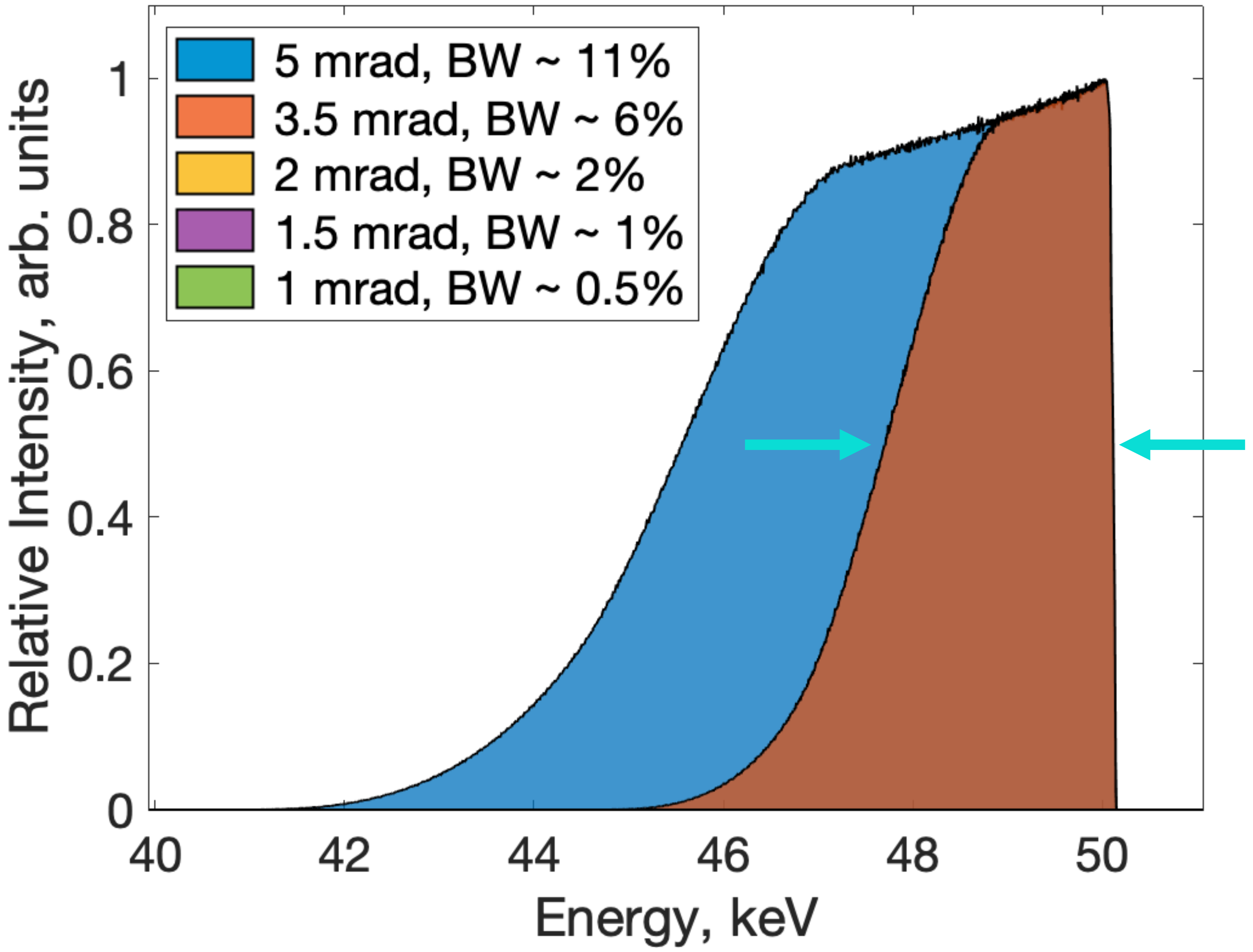

Double Doppler upshift

$$E_\gamma = \frac{4\gamma^2}{1 + \gamma^2\theta^2 + 4\gamma k_0^{-}\lambda_c} E_L$$

Angle correlated spectrum

$$\frac{dN}{d\Omega d\omega} = \int \frac{d\sigma}{d\Omega}\,\delta\left(\omega - \omega_l \frac{\kappa_l}{\kappa}\right)(1+\beta_0)\,n_l(x_\mu)\,n_e(x_\mu)\,d^4x_\mu$$

Klein-Nishina

Laser beam properties

Electron beam properties

Reutershan T, Effarah HH, Lagzda A, Barty CPJ. Applied Optics (2022) 61(6):C162:178

UCI

Laser-Compton Source

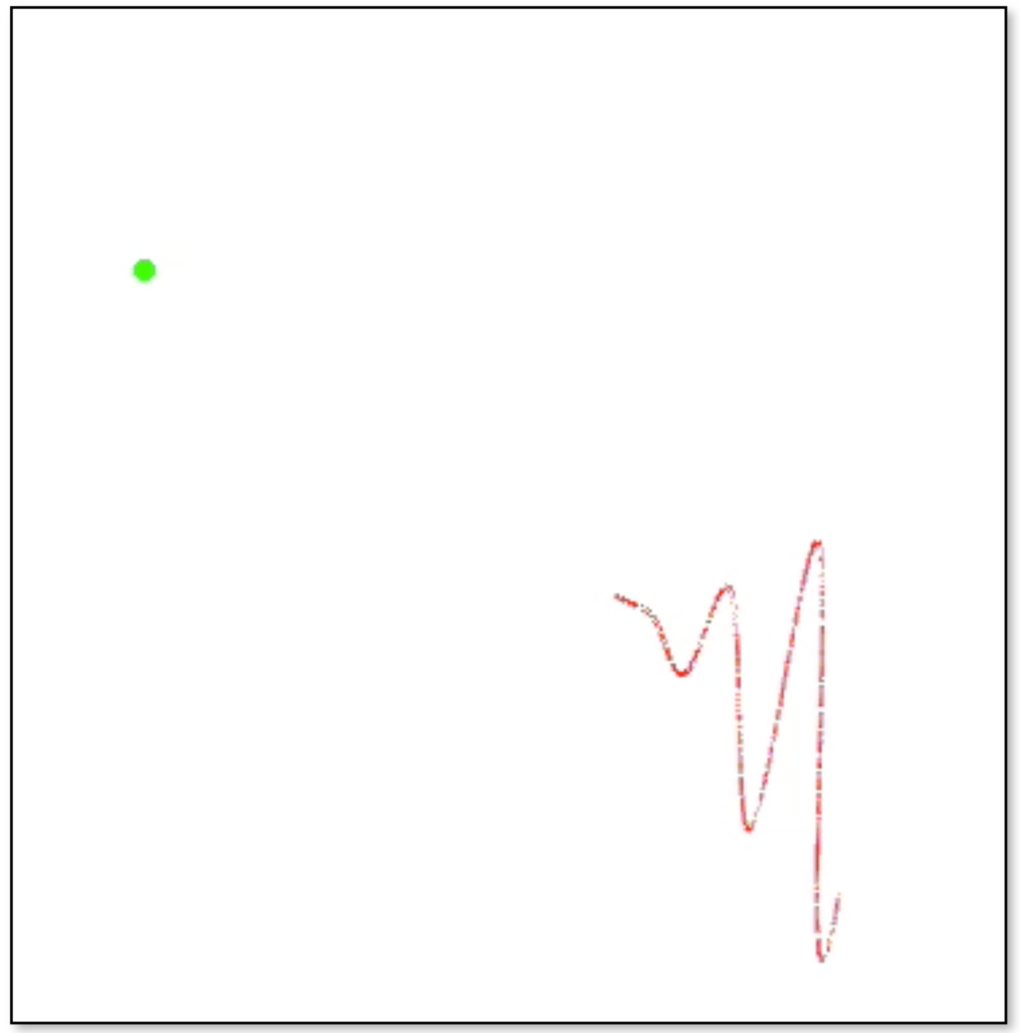

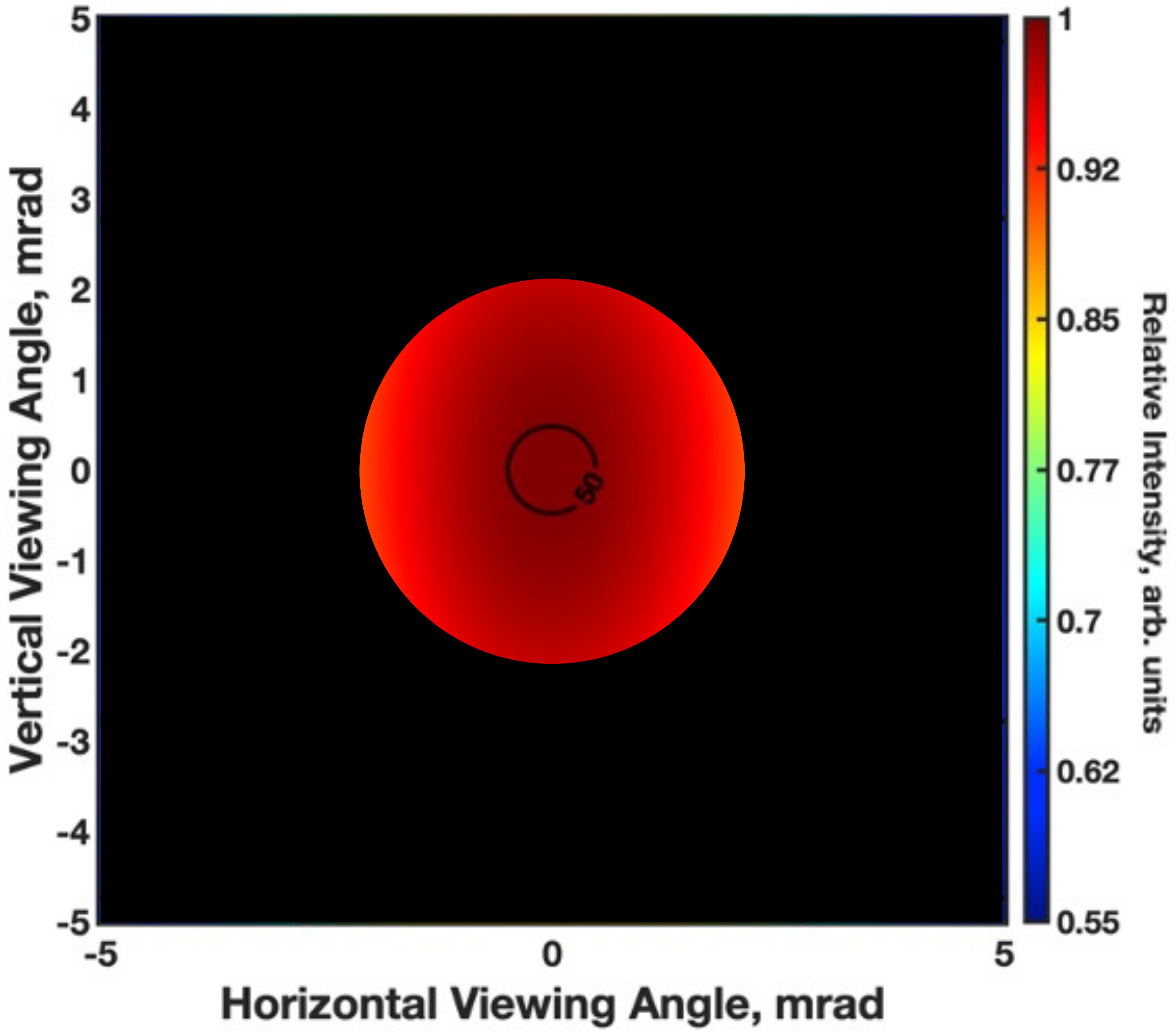

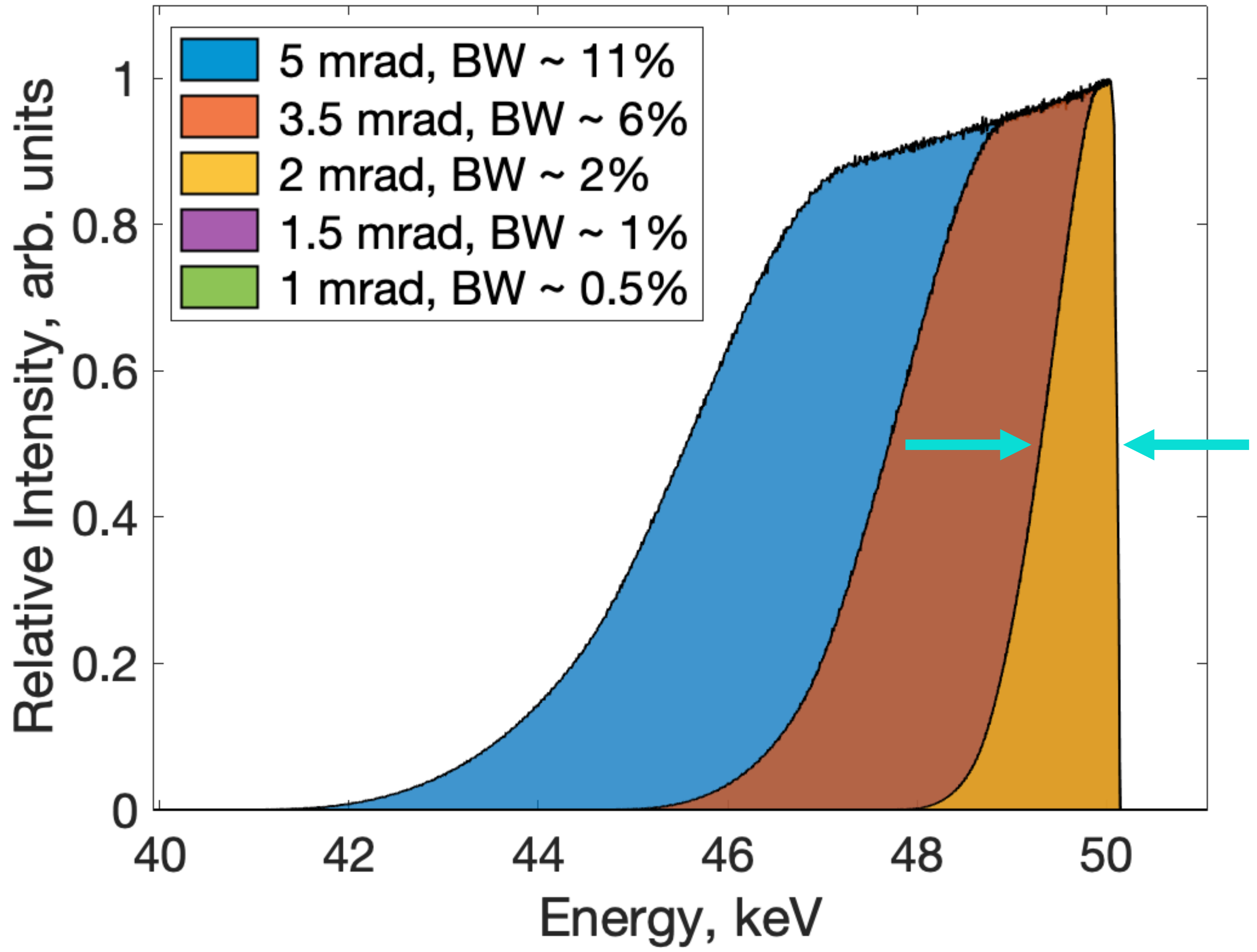

Double Doppler upshift

$$E_\gamma = \frac{4\gamma^2}{1+\gamma^2\theta^2+4\gamma \bar{k_0}\lambda_c} E_L$$

Angle correlated spectrum

$$\frac{dN}{d\Omega d\omega} = \int \frac{d\sigma}{d\Omega}\,\delta\left(\omega - \omega_l \frac{\kappa_l}{\kappa}\right)(1+\beta_0)\,n_l(x_\mu)\,n_e(x_\mu)\,d^4x_\mu$$

Klein-Nishina

Laser beam properties

Electron beam properties

Reutershan T, Effarah HH, Lagzda A, Barty CPJ. Applied Optics (2022) 61(6):C162:178

Laser-Compton Source

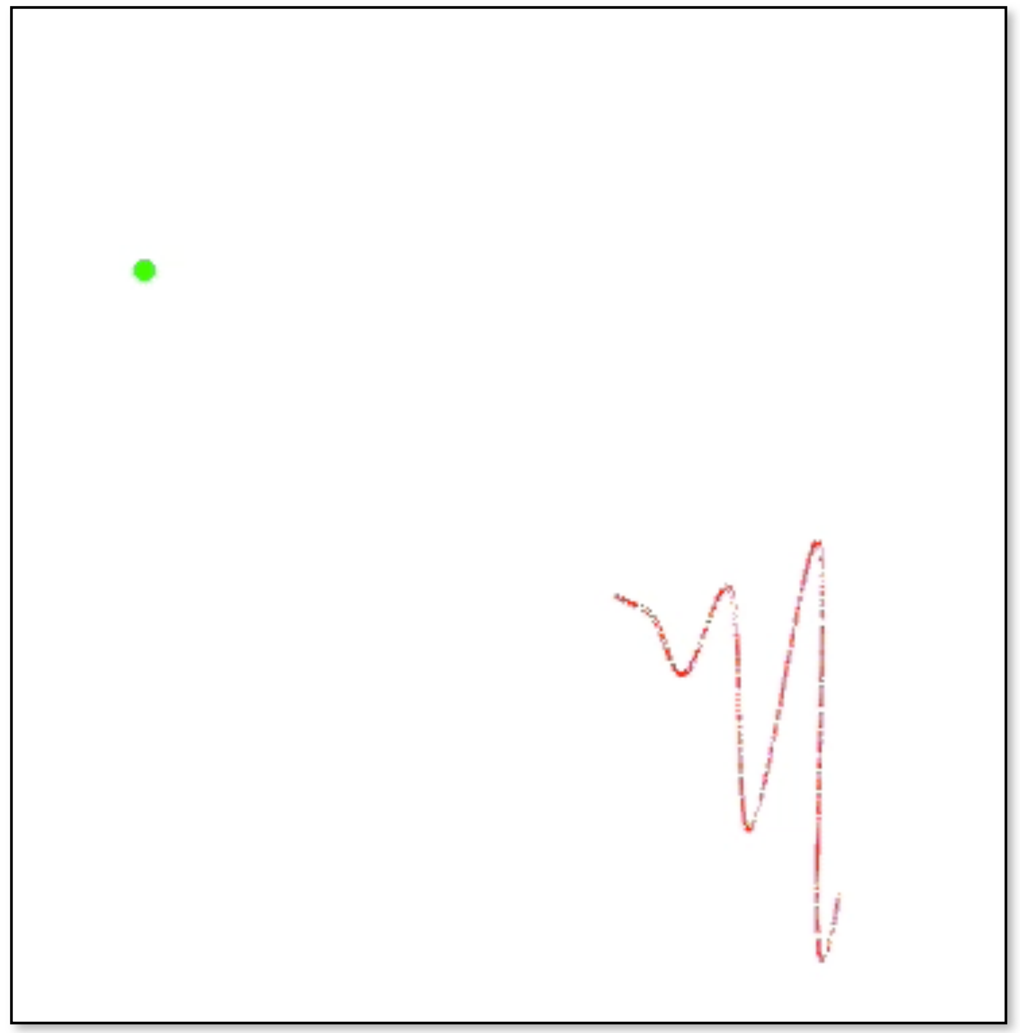

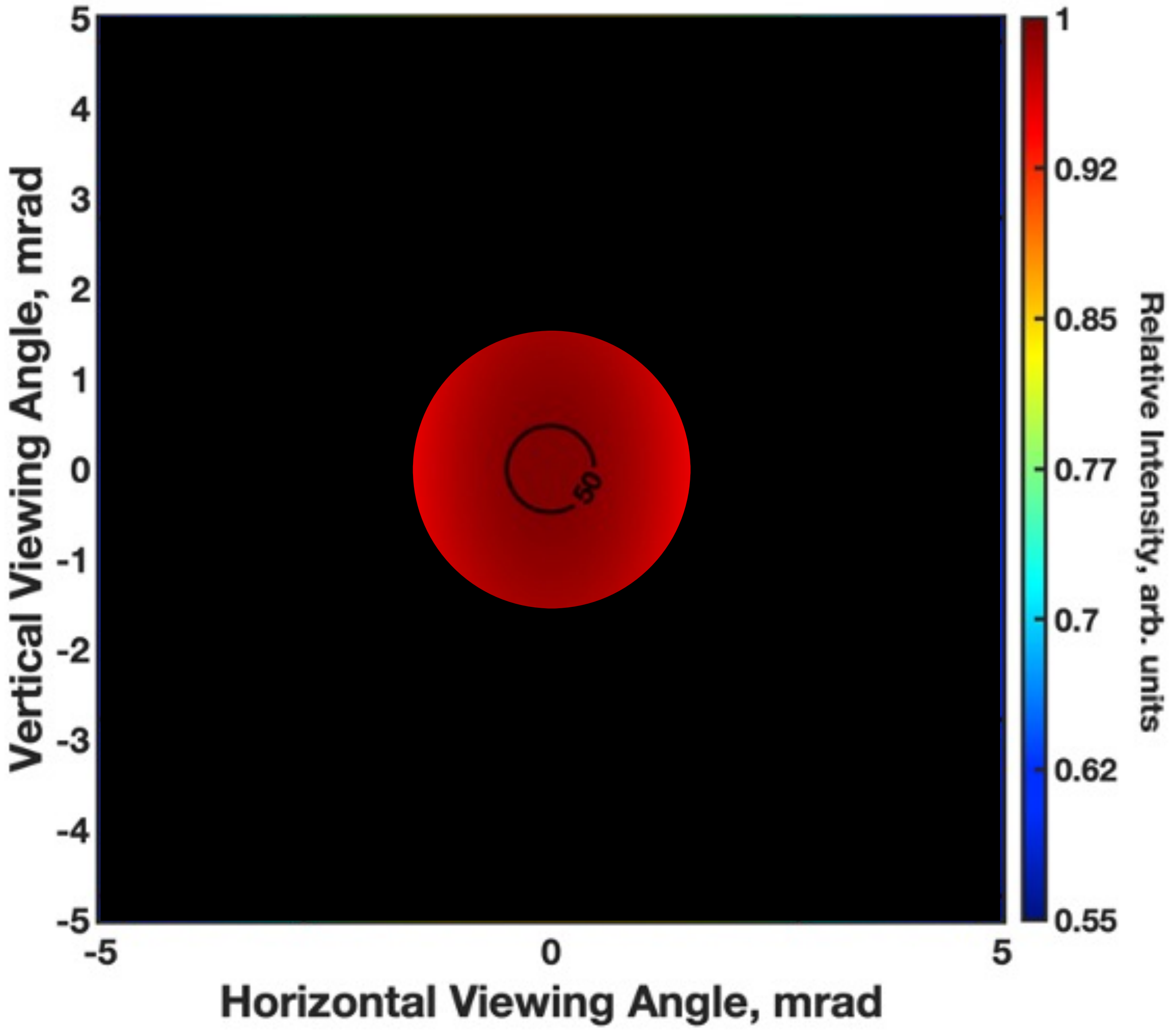

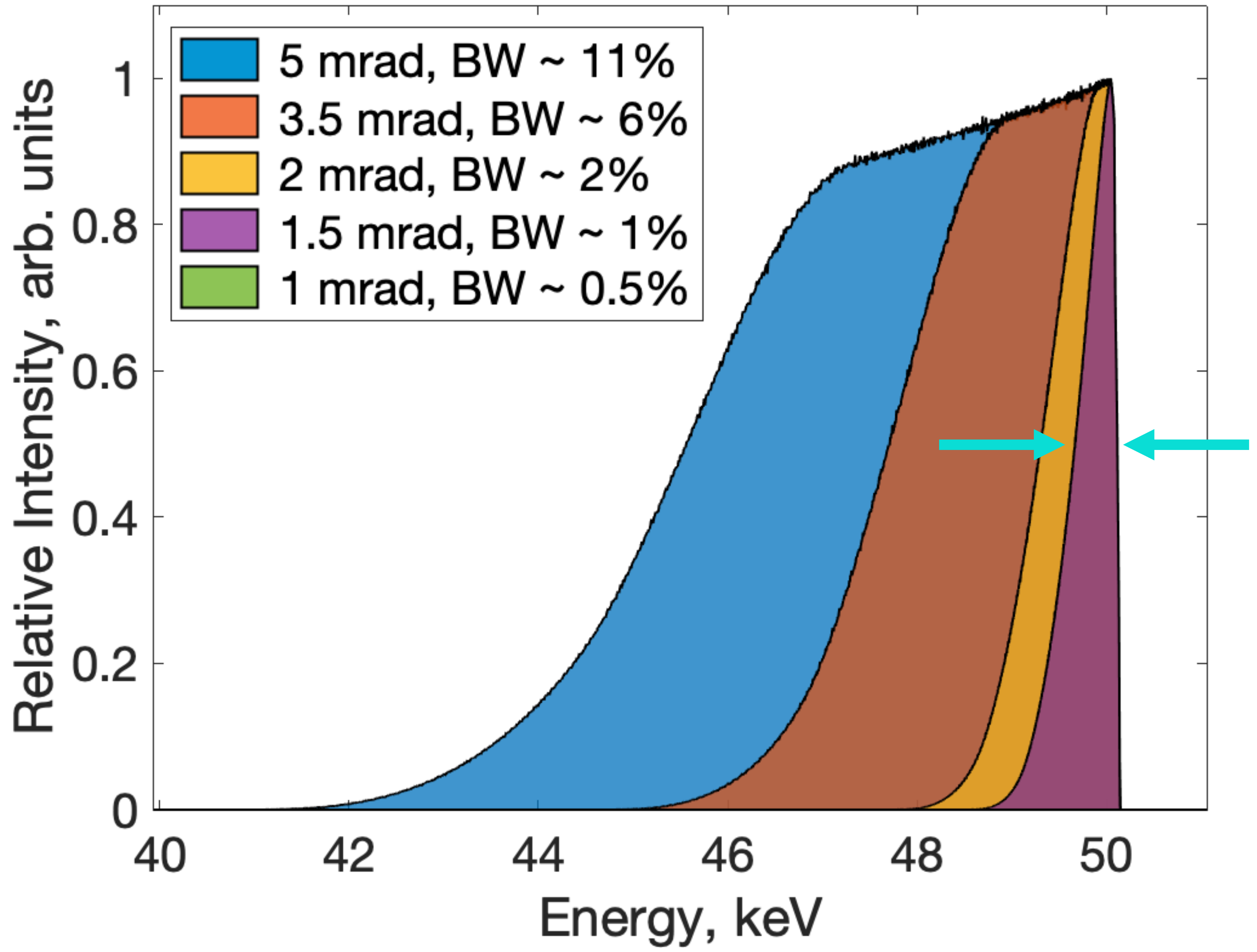

Double Doppler upshift

$$E_\gamma = \frac{4\gamma^2}{1 + \gamma^2\theta^2 + 4\gamma k_0^{-}\lambda_c} E_L$$

Angle correlated spectrum

$$\frac{dN}{d\Omega d\omega} = \int \frac{d\sigma}{d\Omega}\delta\left(\omega - \omega_l \frac{\kappa_l}{\kappa}\right)(1+\beta_0)n_l(x_\mu)n_e(x_\mu)d^4x_\mu$$

Klein-Nishina

Laser beam properties

Electron beam properties

Reutershan T, Effarah HH, Lagzda A, Barty CPJ. Applied Optics (2022) 61(6):C162:178

Laser-Compton Source

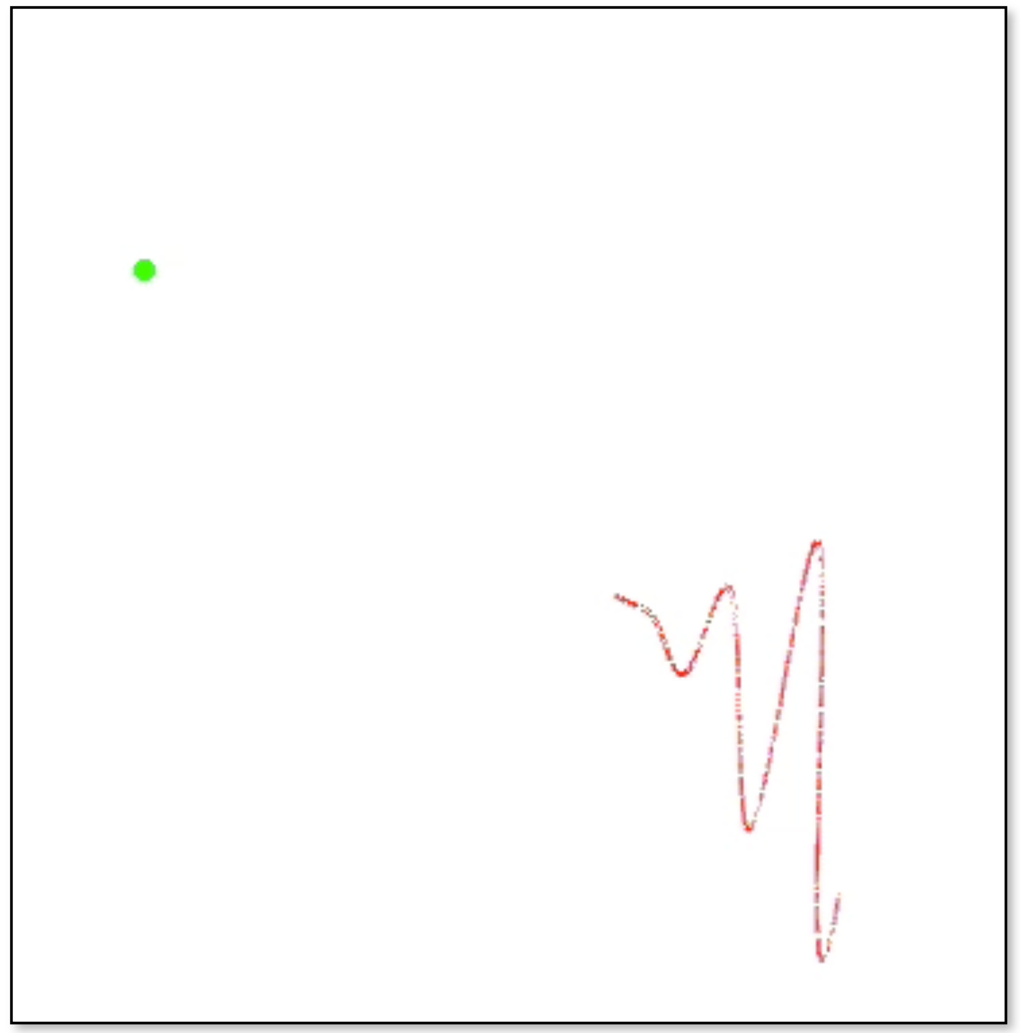

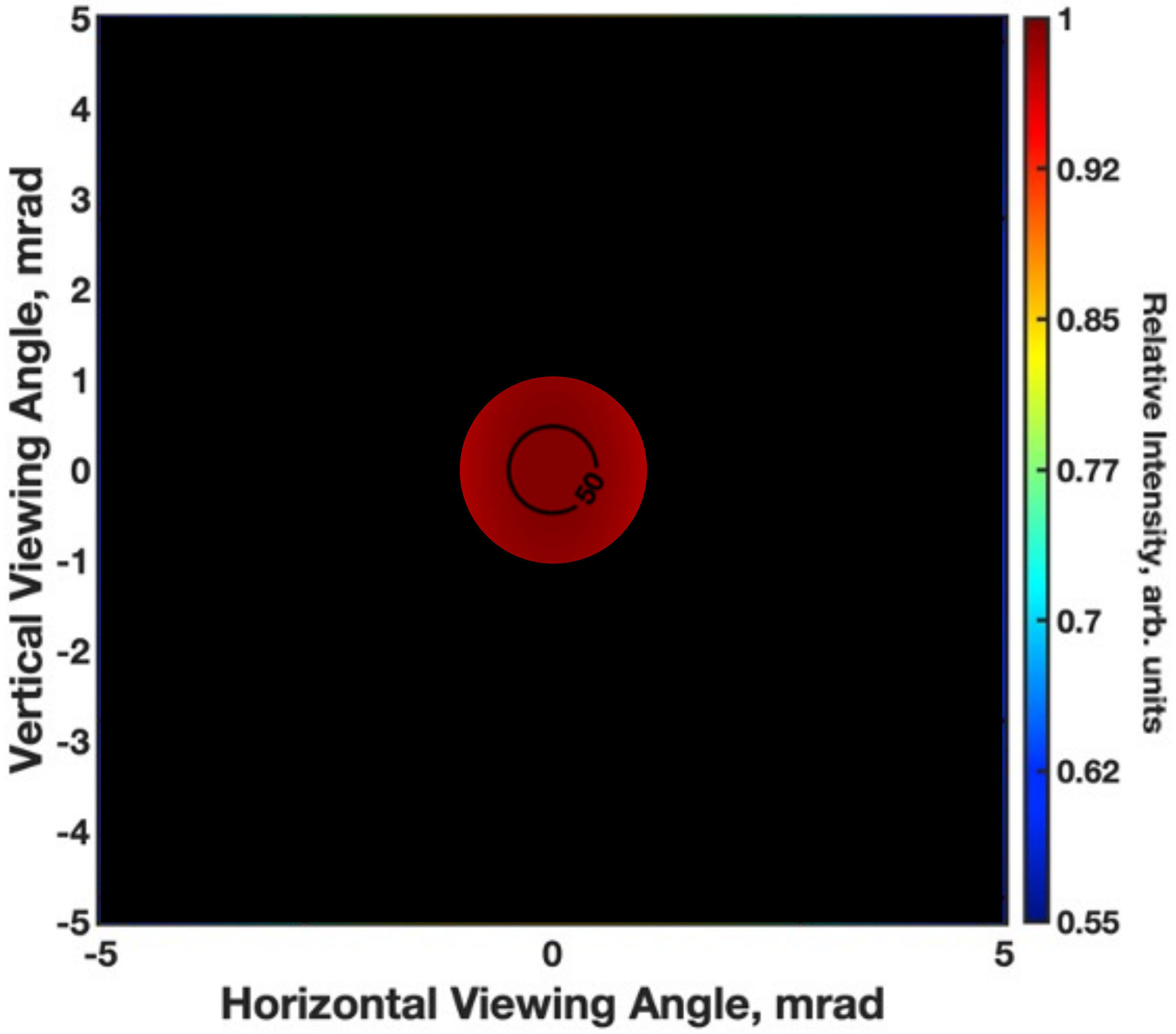

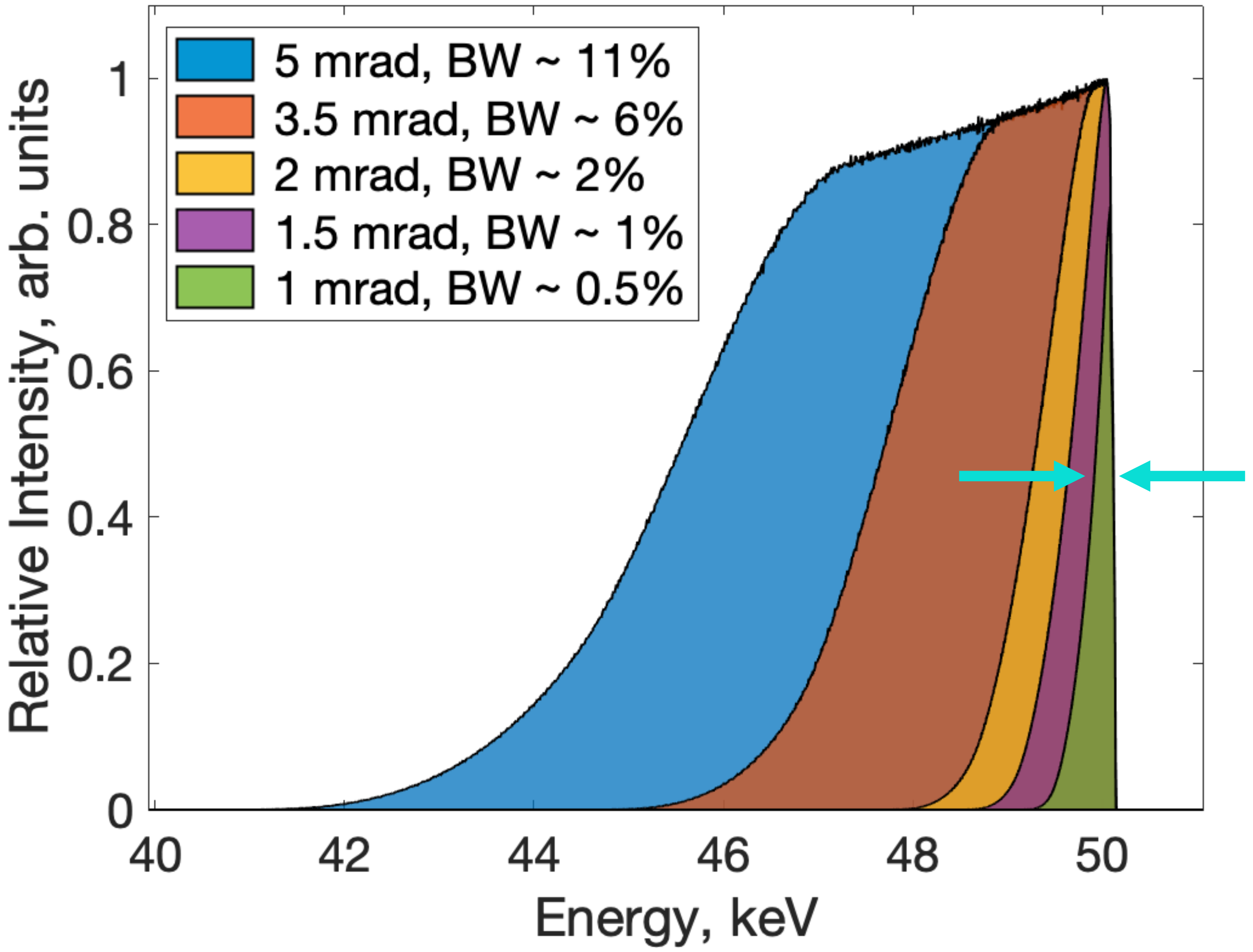

Double Doppler upshift

$$E_\gamma = \frac{4\gamma^2}{1 + \gamma^2\theta^2 + 4\gamma k_0^{-}\lambda_c} E_L$$

Angle correlated spectrum

$$\frac{dN}{d\Omega d\omega} = \int \frac{d\sigma}{d\Omega} \delta\left(\omega - \omega_l \frac{\kappa_l}{\kappa}\right) (1 + \beta_0) n_l(x_\mu) n_e(x_\mu) d^4 x_\mu$$

Klein-Nishina

Laser beam properties

Electron beam properties

UCI

Reutershan T, Effarah HH, Lagzda A, Barty CPJ. Applied Optics (2022) 61(6):C162:178

1D Imaging has been Demonstrated

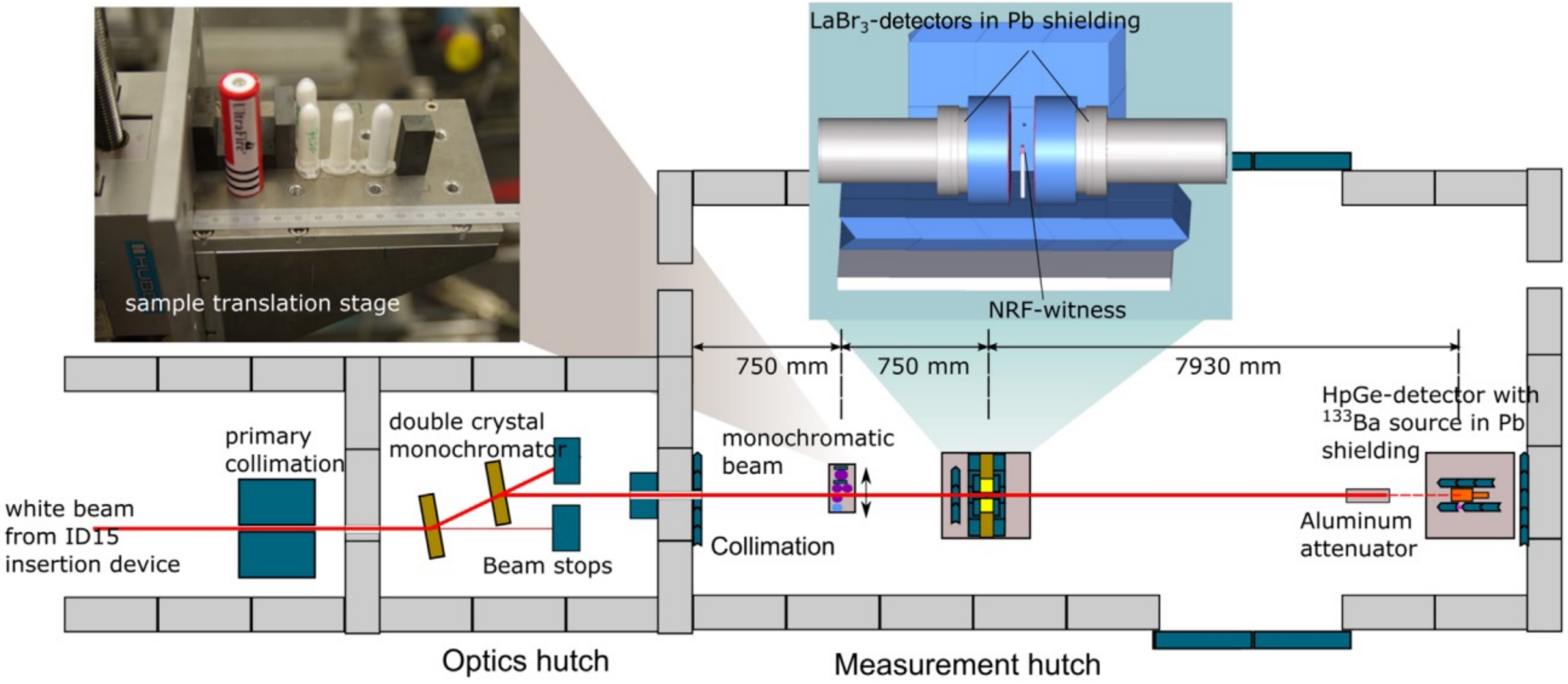

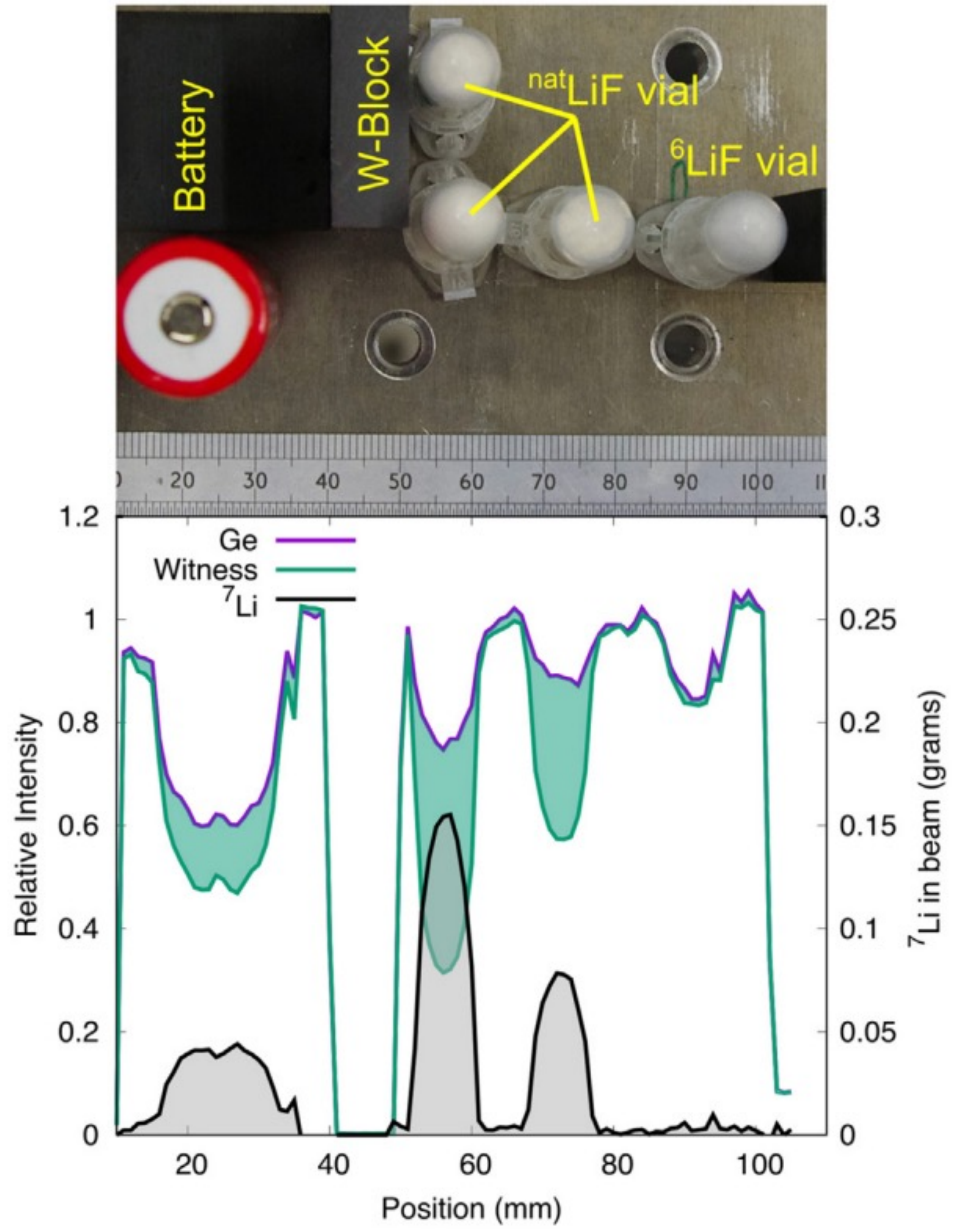

Experiment performed at ESRF with a 10^{-3} bandwidth source.

Jentschel M, Albert F, Buslaps T, Friman-Gayer U, Honkimaki V, Mertes L, Pollit AJ, Mutti P, Pietralla N, Barty CPJ. Applied Optics. Vol 61, No 6 (2022), C125-C132.

UCI

Computational Demonstration of 2D Li-7 Imaging

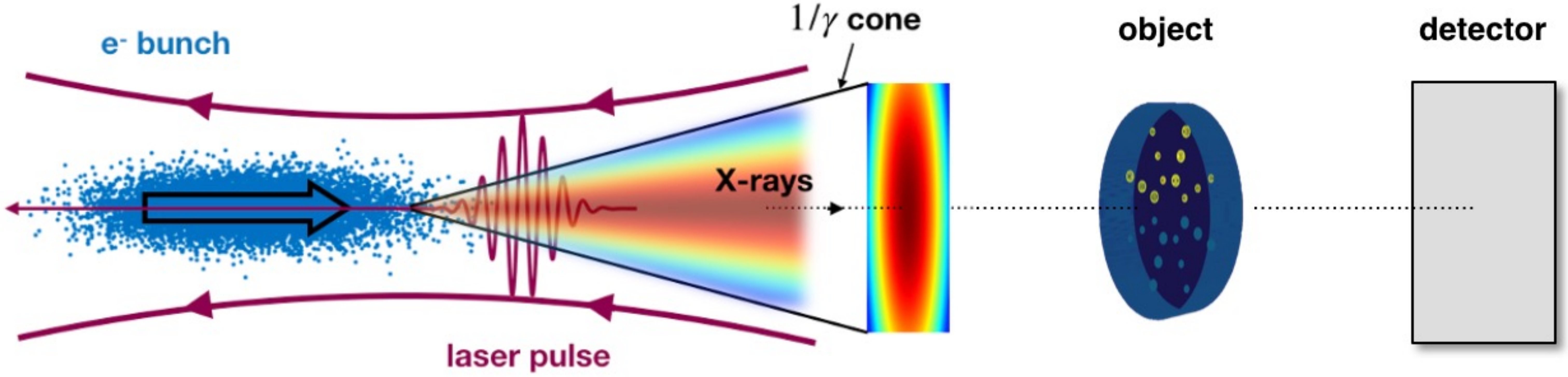

Computational Demonstration of 2D Li-7 Imaging

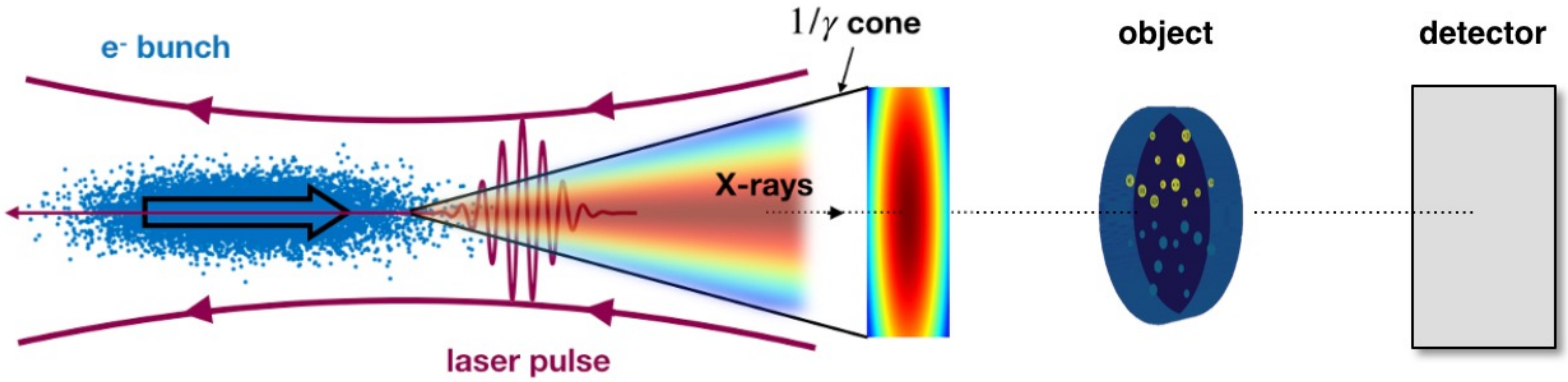

e- beam: GPT

Computational Demonstration of 2D Li-7 Imaging

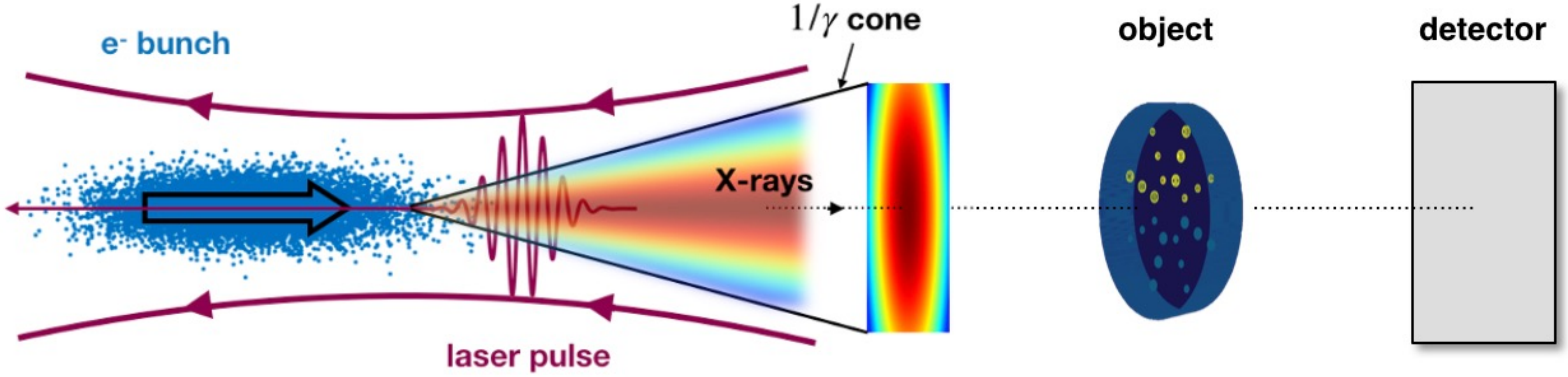

e- beam: GPT

e- bunch / laser pulse interaction: Mathematica

This method retains the spatial-energy x-ray spectrum required for accurate simulation.

Computational Demonstration of 2D Li-7 Imaging

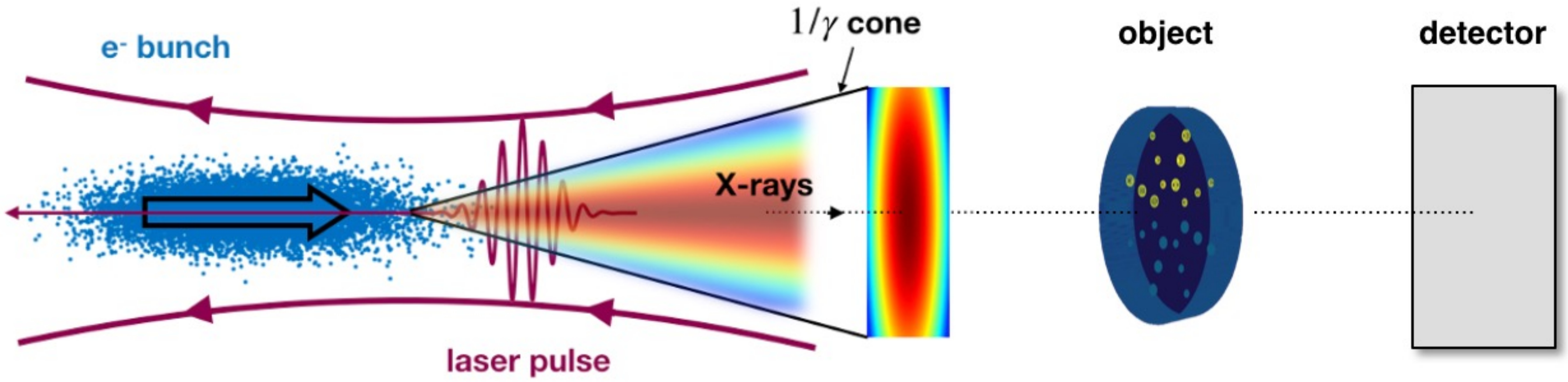

e^- beam: GPT

e^- bunch / laser pulse interaction: Mathematica

x-ray propagation through object and image generation: Matlab/Geant4 w/ G4NRF

This method retains the spatial-energy x-ray spectrum required for accurate simulation.

Computational Demonstration of 2D Li-7 Imaging

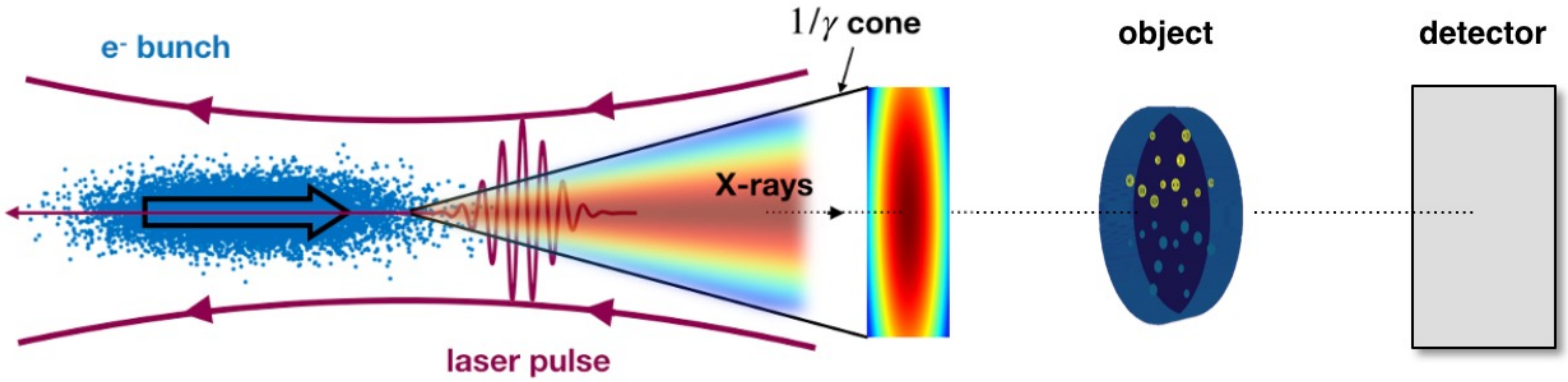

e^- beam: GPT

e^- bunch / laser pulse interaction: Mathematica

x-ray propagation through object and image generation: Matlab/Geant4 w/ G4NRF

Computational Phantom

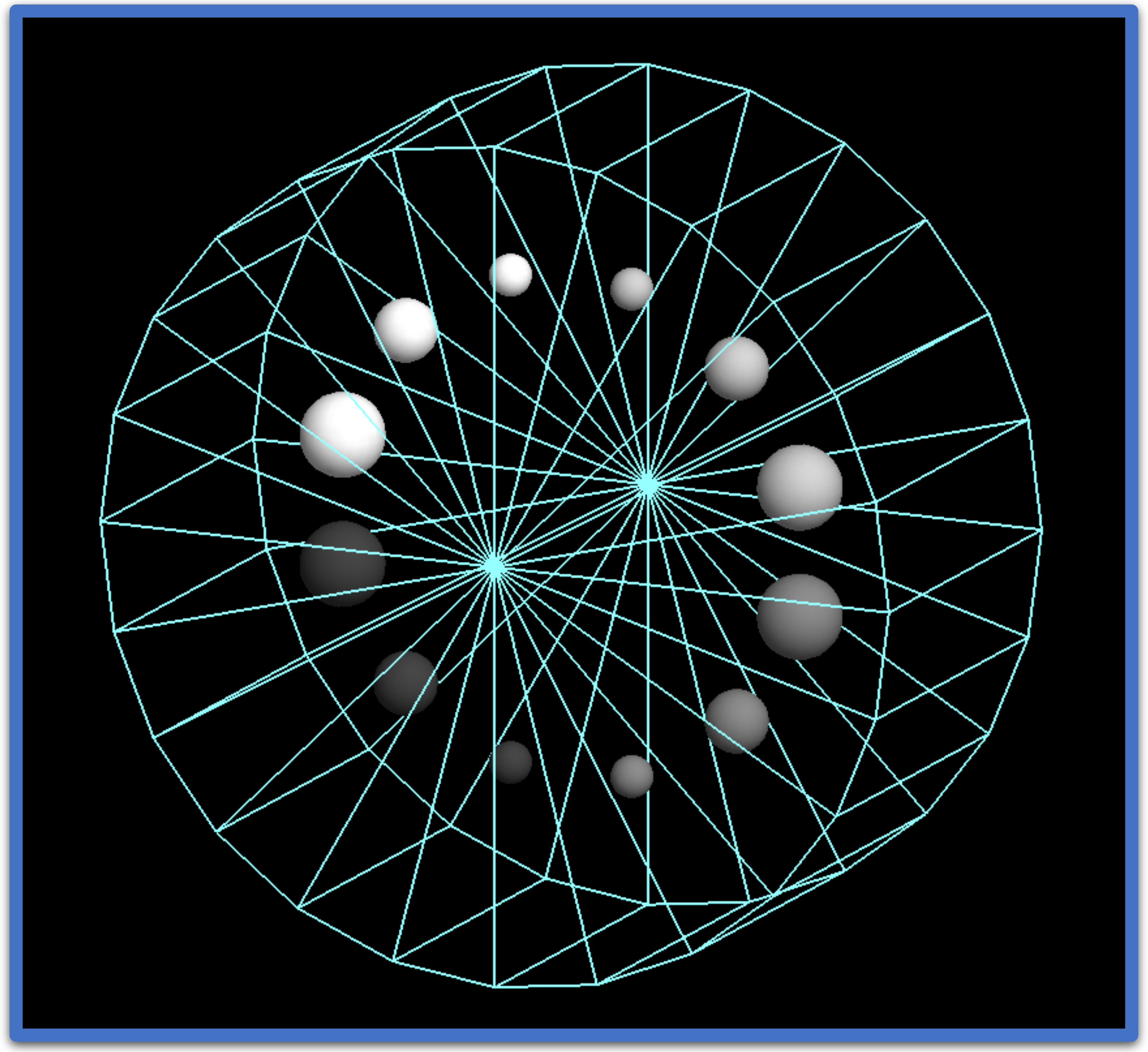

4.2 cm water cylinder with Li inserts of varying concentrations.

Bandwidth is Important

$$\frac{\Delta E}{E} = 2.3\times10^{-5} \qquad \frac{\Delta E}{E} = 1.0\times10^{-4} \qquad \frac{\Delta E}{E} = 1.1\times10^{-3}$$

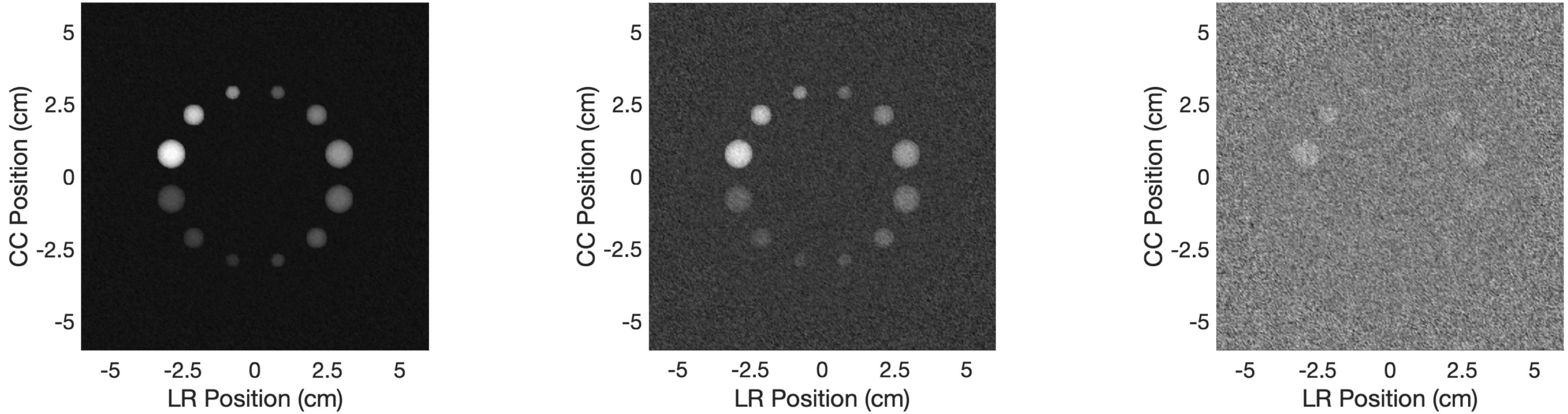

Images generated using a dual-energy approach.
Contrast increases with smaller bandwidths.

GAMS Monochromator

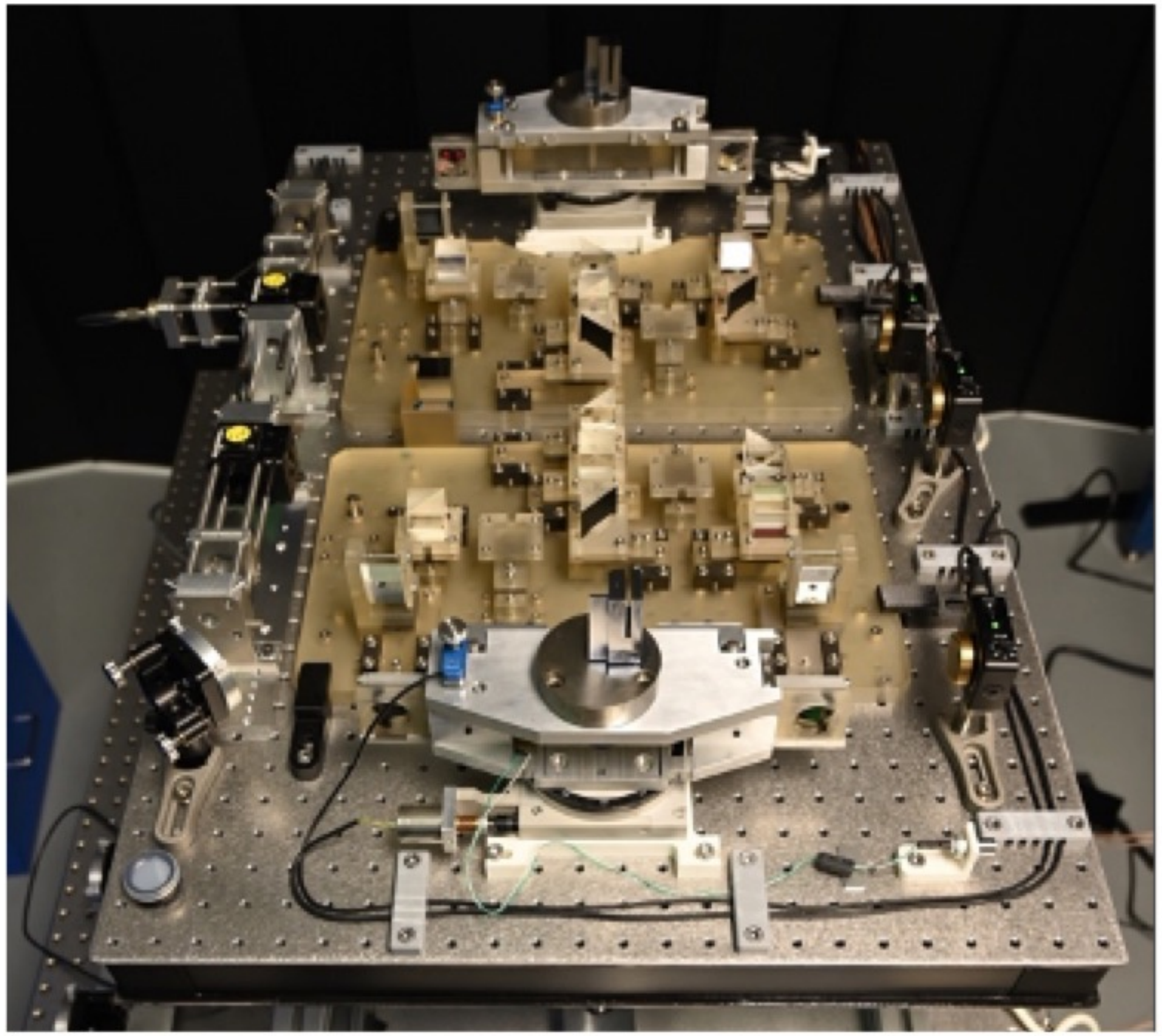

Speaker: **Michael Jentschel**
Institue Laue Langevin, Lumitron Technologies Inc.

Combination of a Diffraction Based Ultra-Narrow Band Width Filter with a Laser Compton Photon Source

Wednesday, 13 September
Junior Ballroom, 9:55 AM

Double crystal monochromator will allow further bandwidth filtering to improve contrast

Could LCS-NRF be used for Medical Imaging?

PET

SPECT

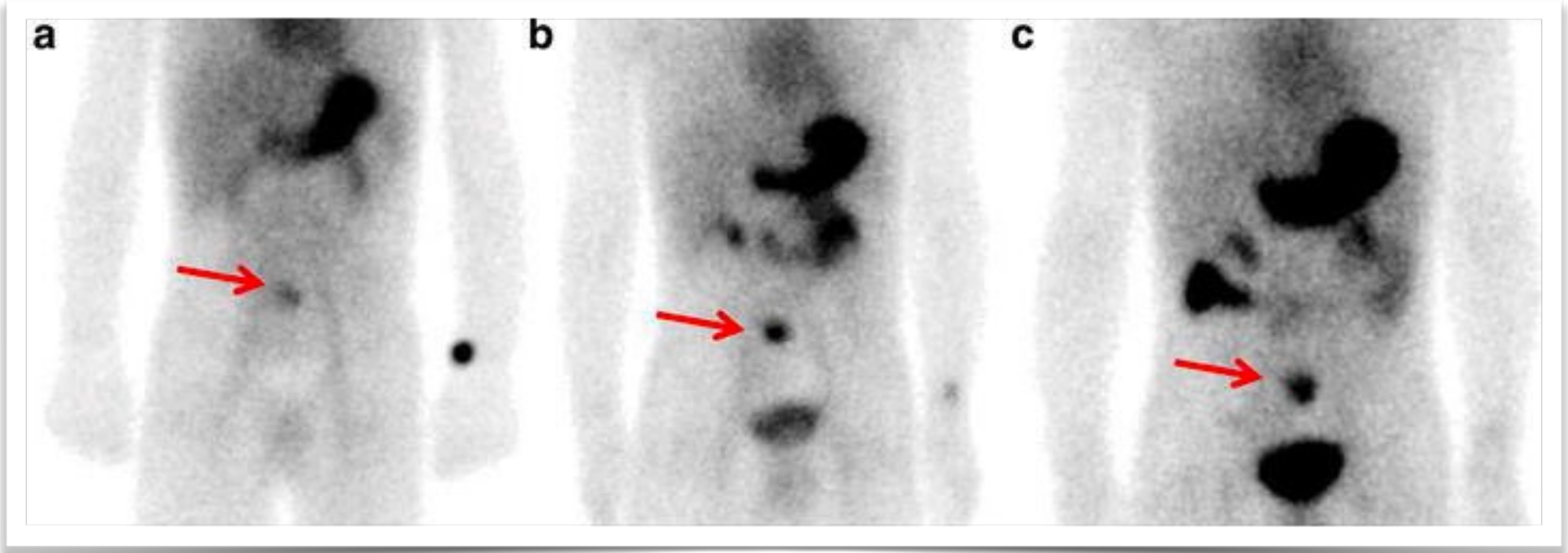

We can learn from the PET and SPECT communities.

Seam P, et al. Blood (2007) 110 (10): 3507-3516.
Xie Q, (2016); 5(1): 1270

Could We Image a Clinically Used Radiotracer?

Isotope	Abundance (%)	Energy (keV)	Integrated σ (eV b)
F-19	100	109.894	0.25
		1458.7	26.57
		1554.038	414.68
		3908.17	38.25
		4556.1	14.07
Cu-63	69.2	669.93	9.86
		962.02	4.98
		1412.16	0.78
		1547	6.31
		2012.92	13.11
Cu-65	30.9	770.64	14.33
		1115.556	7.49
		1623.43	0.62
		1725	6.40
		2107.44	3.48
		2212.84	1.63
		2329.05	12.43
Ga-69	60.1	574.22	4.69
		872.147	9.22
		1028.59	0.69
		1107.04	9.66
		1723.71	5.90
		1891.64	22.26

Isotope	Abundance (%)	Energy (keV)	Integrated σ (eV b)
Ga-71	39.9	389.94	14.41
		511.495	4.47
		910.16	8.82
		964.66	2.17
		1109.31	7.50
		1631.4	4.39
		1719.5	8.89
		1752.32	2.20
		1905.36	3.02
		2064.06	2.51
Rb-85	72.2	151.192	0.07
		731.829	0.50
		868.94	1.24
		919.73	3.00
		950.95	0.69
		1175.56	1.92
		1384.24	0.91
Rb-87	27.8	402.588	0.20
		845.44	12.14
		1389.78	4.78
		1463	1.95

Only dipole transitions considered

National Nuclear Data Center, Brookhaven National Lab, Evaluated Nuclear Structure Data File

Candidate: ^{19}F

Mass fraction of elements in human body

Element	Mass Fraction	Element	Mass Fraction
Oxygen	0.65	*Sulfur*	2.5×10^{-3}
Carbon	0.18	*Sodium*	1.5×10^{-3}
Hydrogen	0.1	*Chlorine*	1.5×10^{-3}
Nitrogen	0.03	*Magnesium*	5.0×10^{-4}
Calcium	0.014	*Iron*	6.0×10^{-5}
Phosphorus	0.011	*Fluorine*	3.7×10^{-5}
Potassium	2.0×10^{-3}	*Zinc*	3.2×10^{-5}

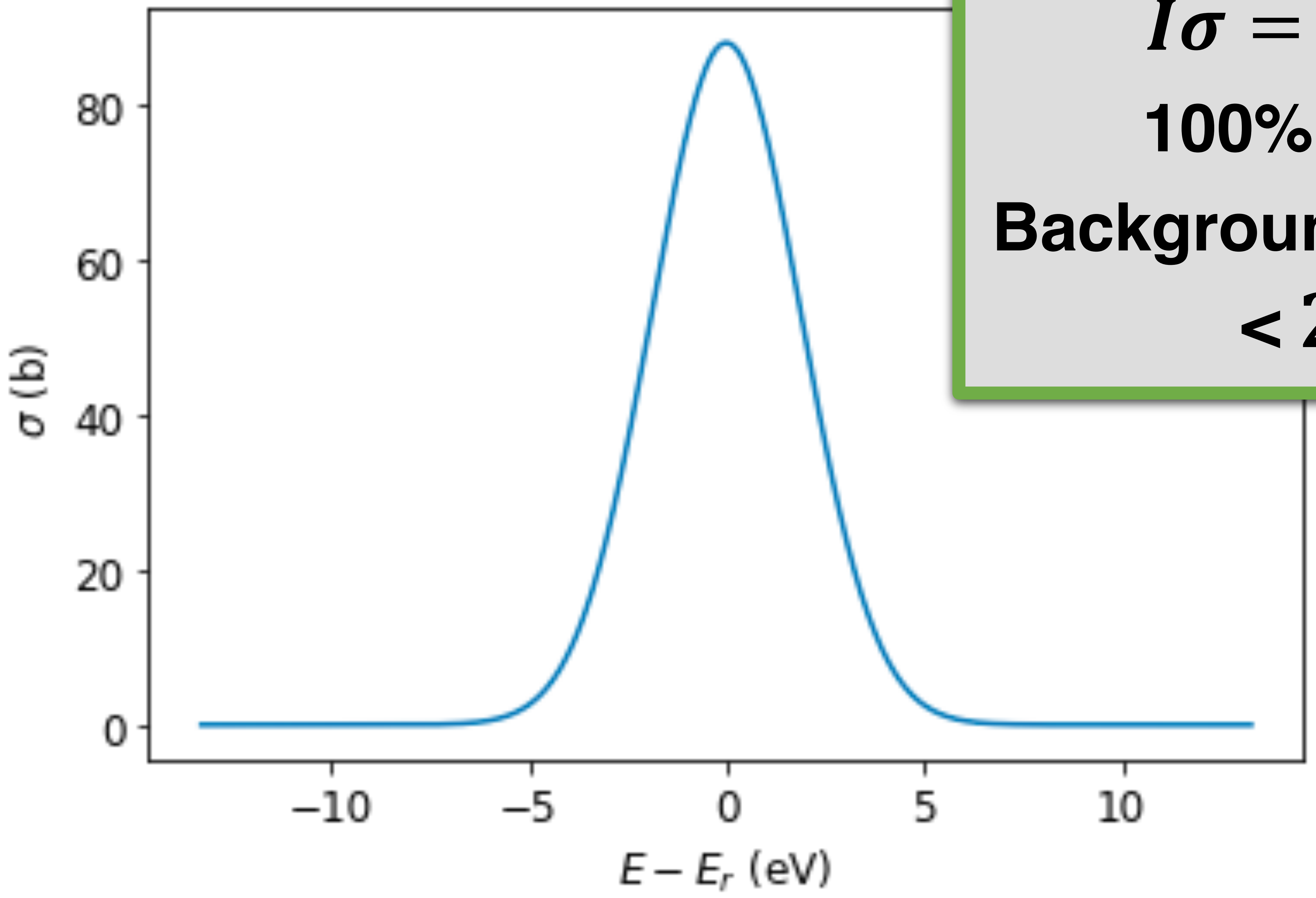

Not radioactive

$I\sigma = 414.5 eVb$

100% abundance

Background mass fraction

$< 2\times10^{-6}$

Only 5% of total fluorine is in soft tissue.

National Nuclear Data Center, Brookhaven National Lab, Evaluated Nuclear Structure Data File

Candidate ^{19}F

Glucose
(Sugar)

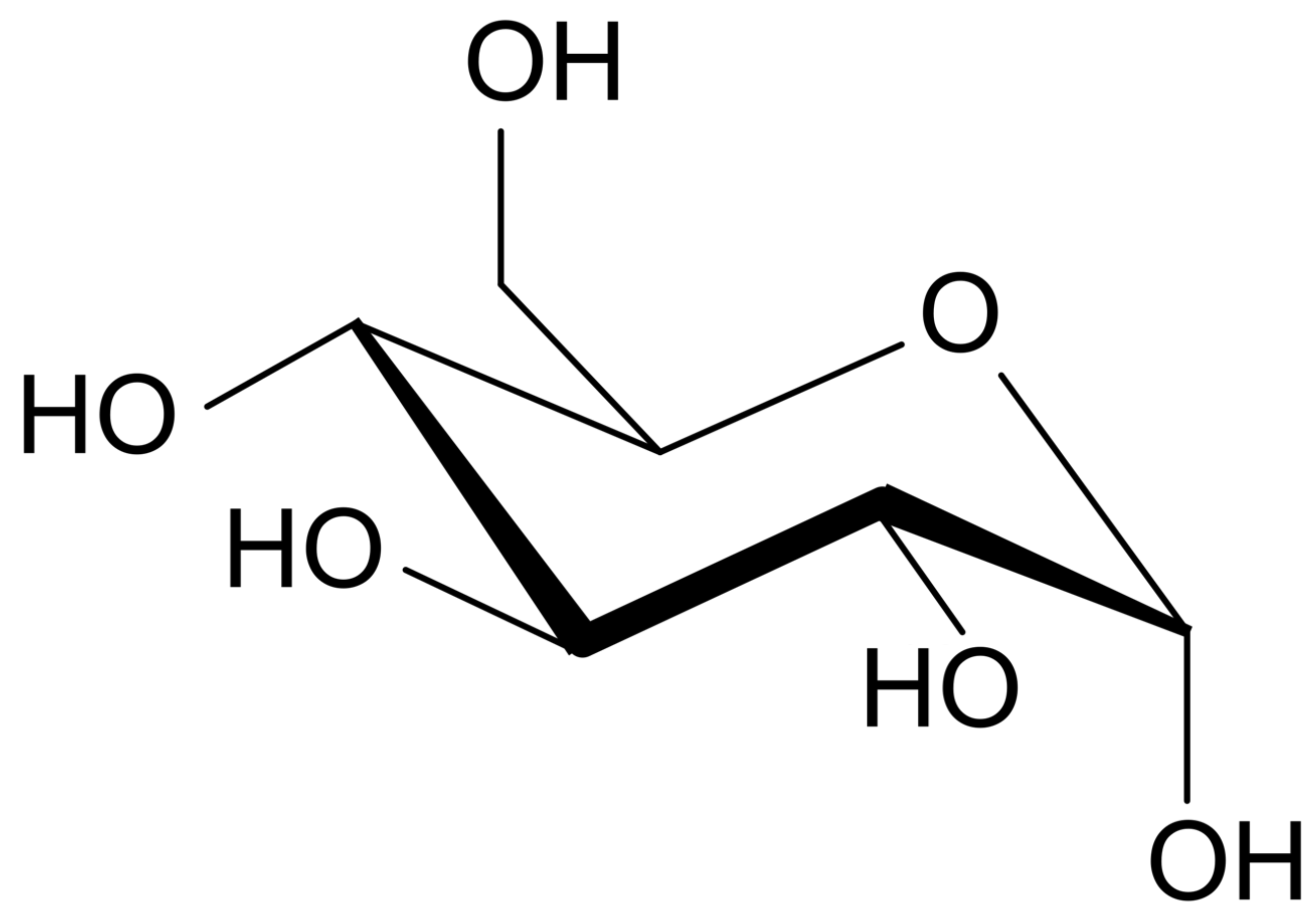

Glucose is the common molecule used for cancer PET imaging

Candidate ^{19}F

Glucose (Sugar)

18-Fluorodeoxyglucose (PET)

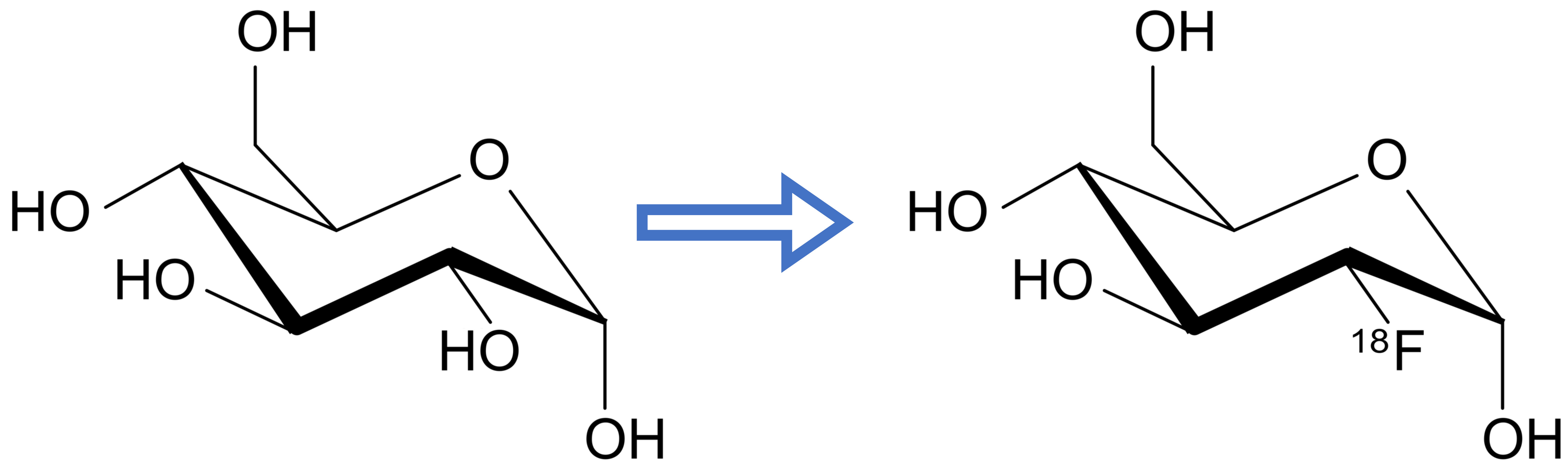

$$t_{1/2} = 110\,min$$

Substituting a hydroxyl group with a positron emitter

Candidate ^{19}F

Glucose (Sugar) | **18-Fluorodeoxyglucose (PET)** | **19-Fluorodeoxyglucose (NRF - 1.5 MeV)**

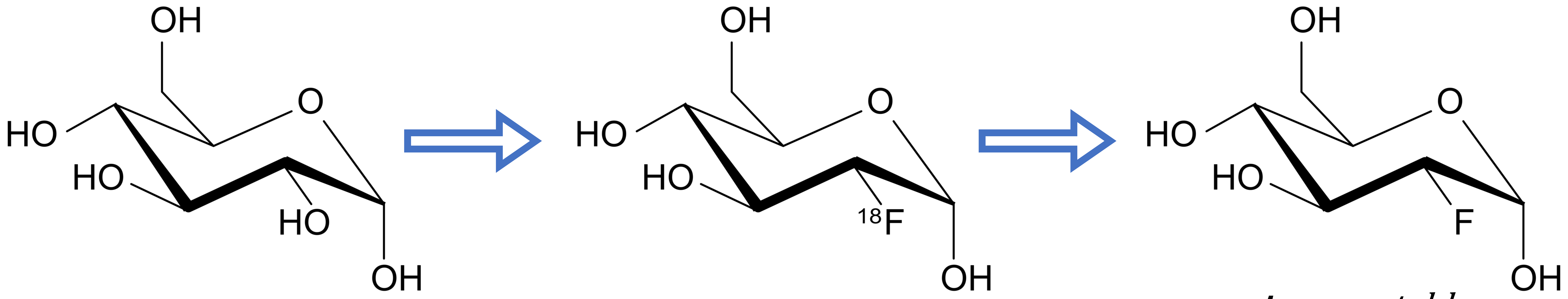

$t_{1/2} = 110\,min$

$t_{1/2} = stable$

$Abundance = 100\%$

Using NRF, we can image the same molecule, but with a stable isotope!

Transmission Nuclear Resonance Imaging

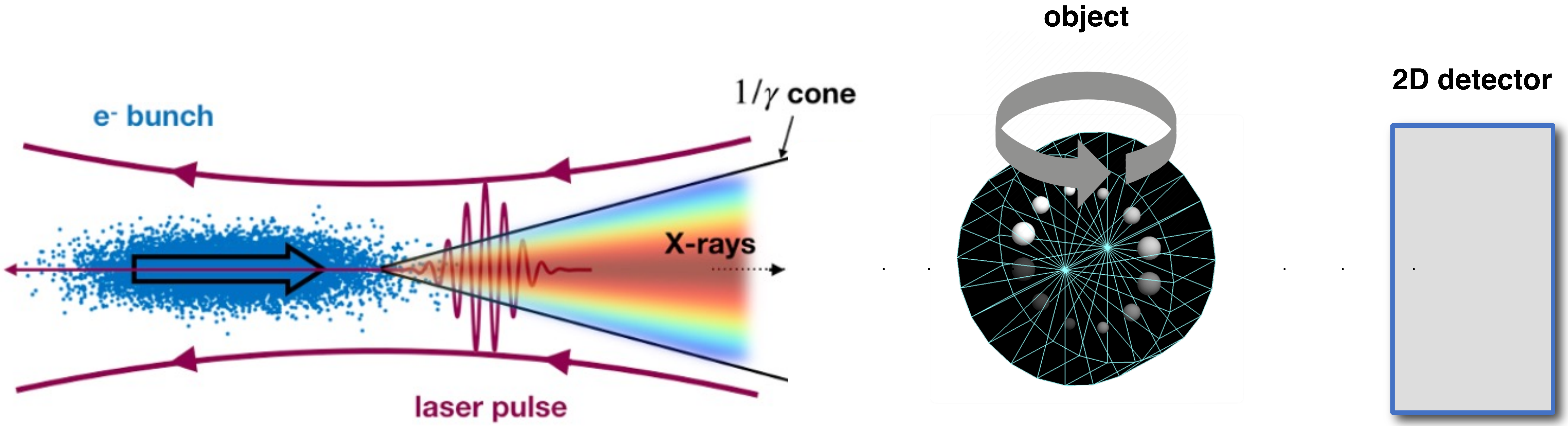

Transmission mode gives differential tomographic reconstruction capability

NR Transmission Image Reconstruction

2D Image

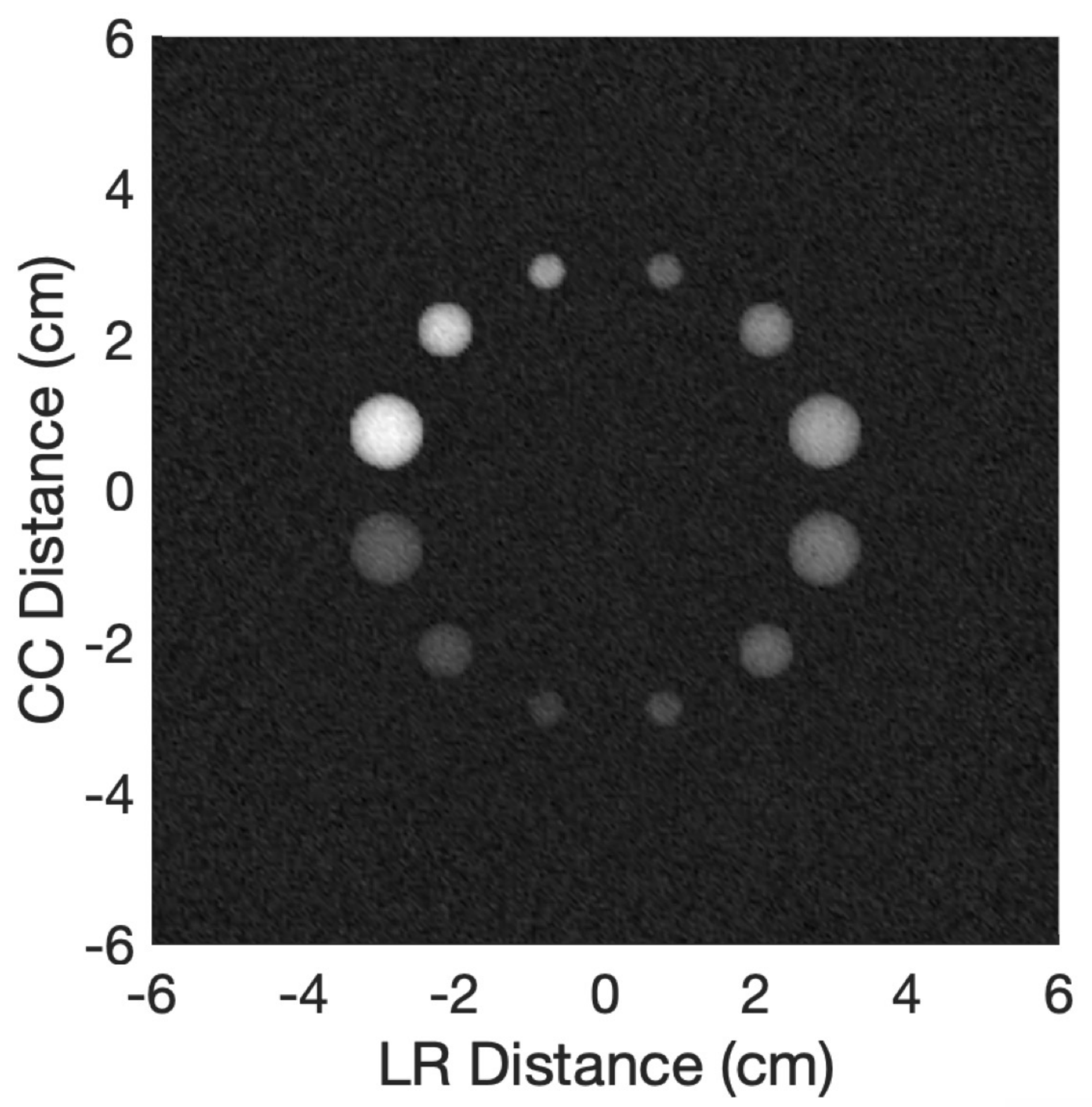

3D Reconstruction

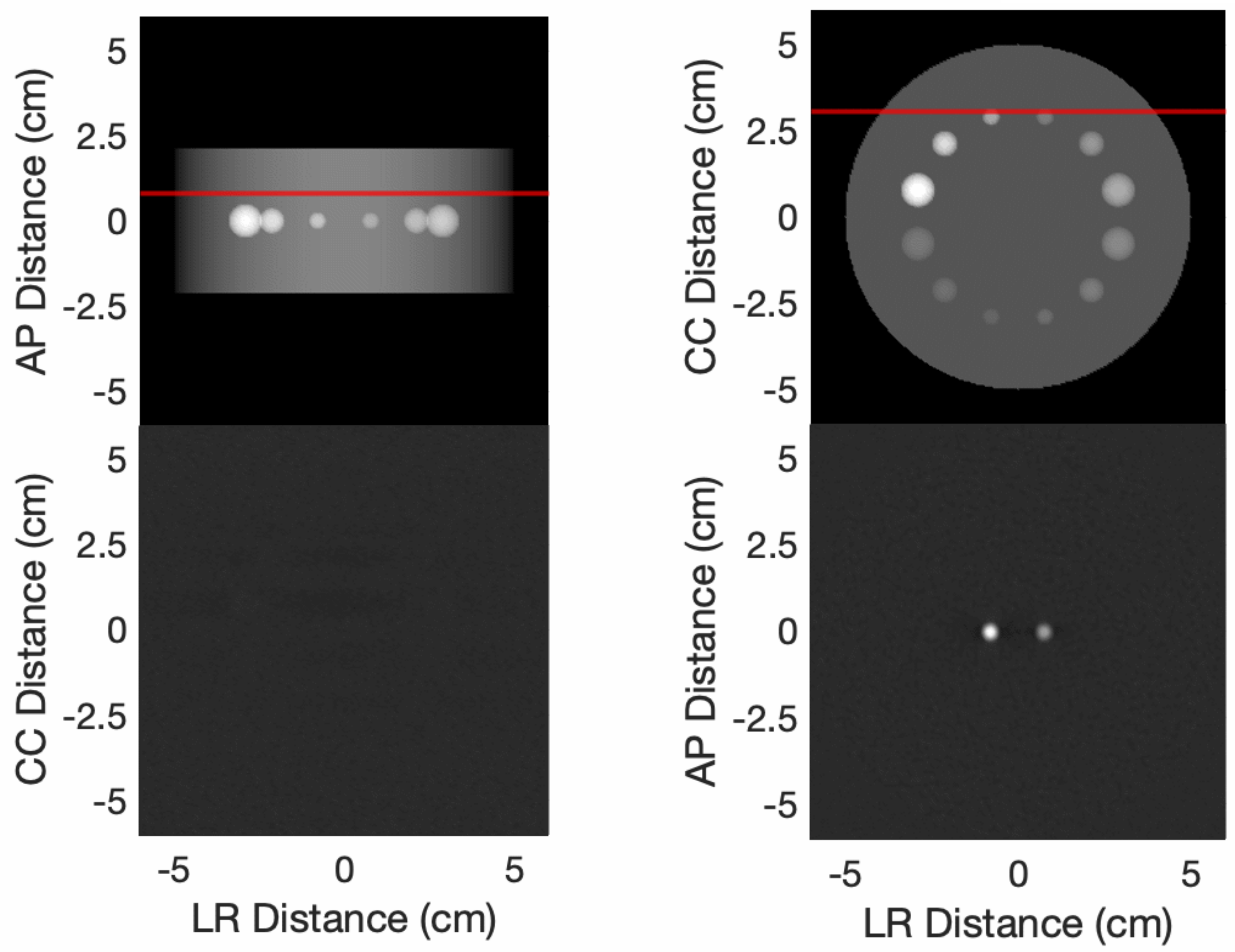

Transmission mode gives differential tomographic reconstruction capability

Fluorescence Nuclear Resonance Imaging

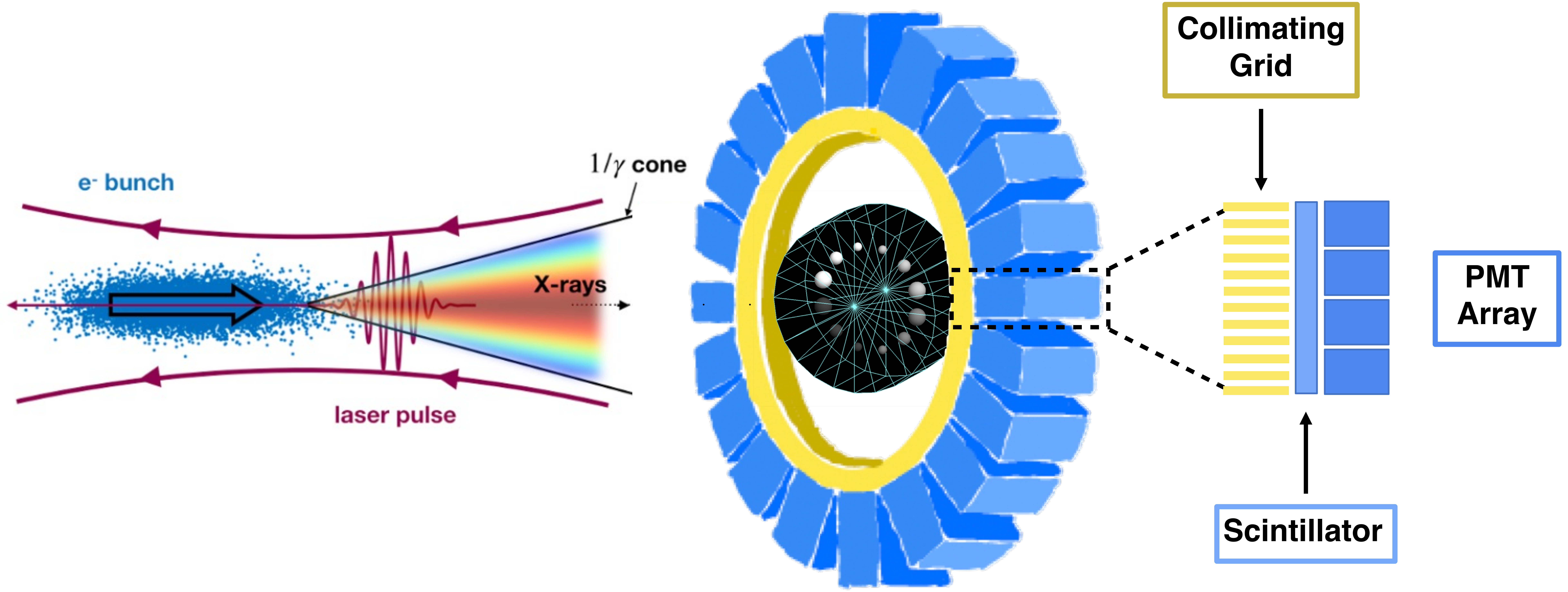

Fluorescence mode enables 3D reconstruction without rotation

NR Fluorescence Image Reconstruction

2D Images

Top-view

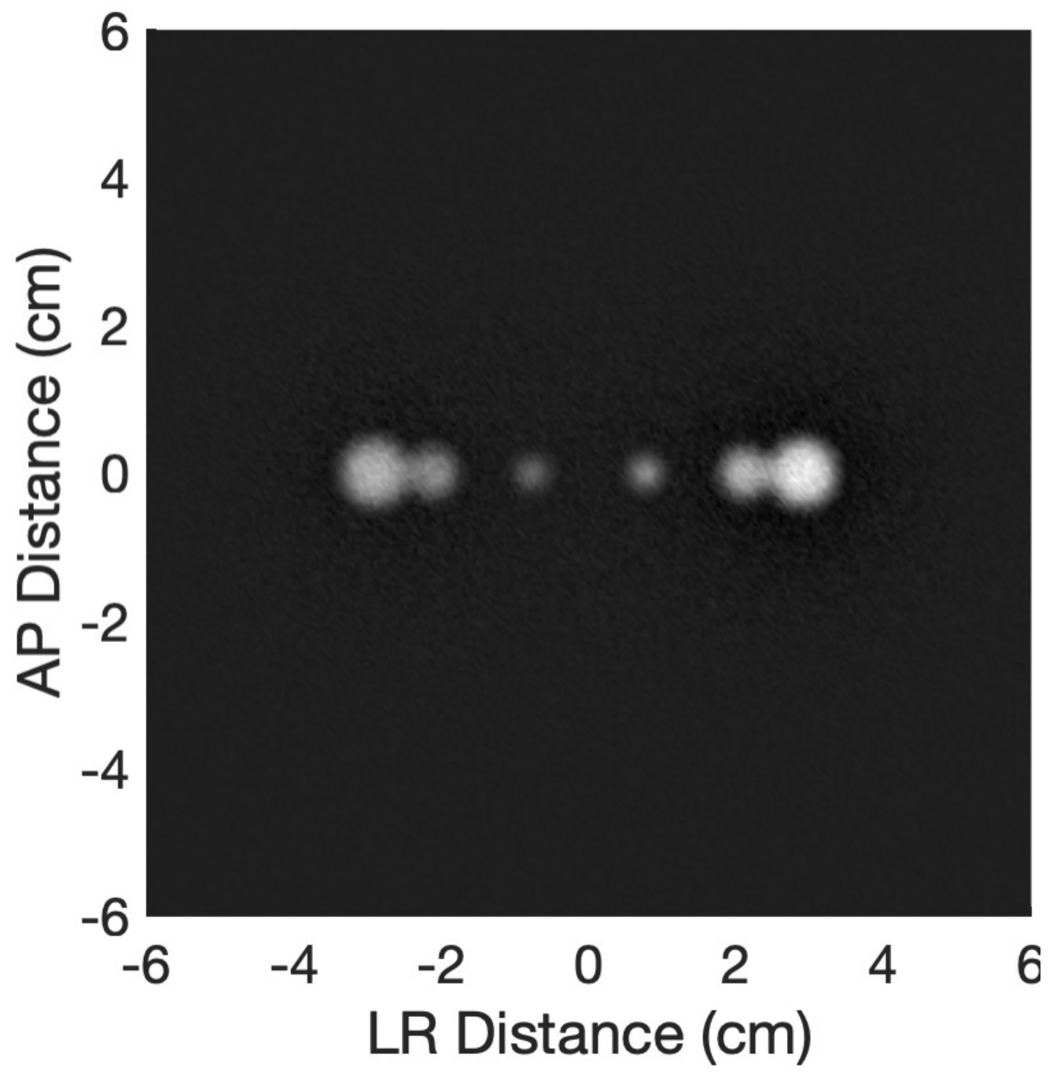

Side-view

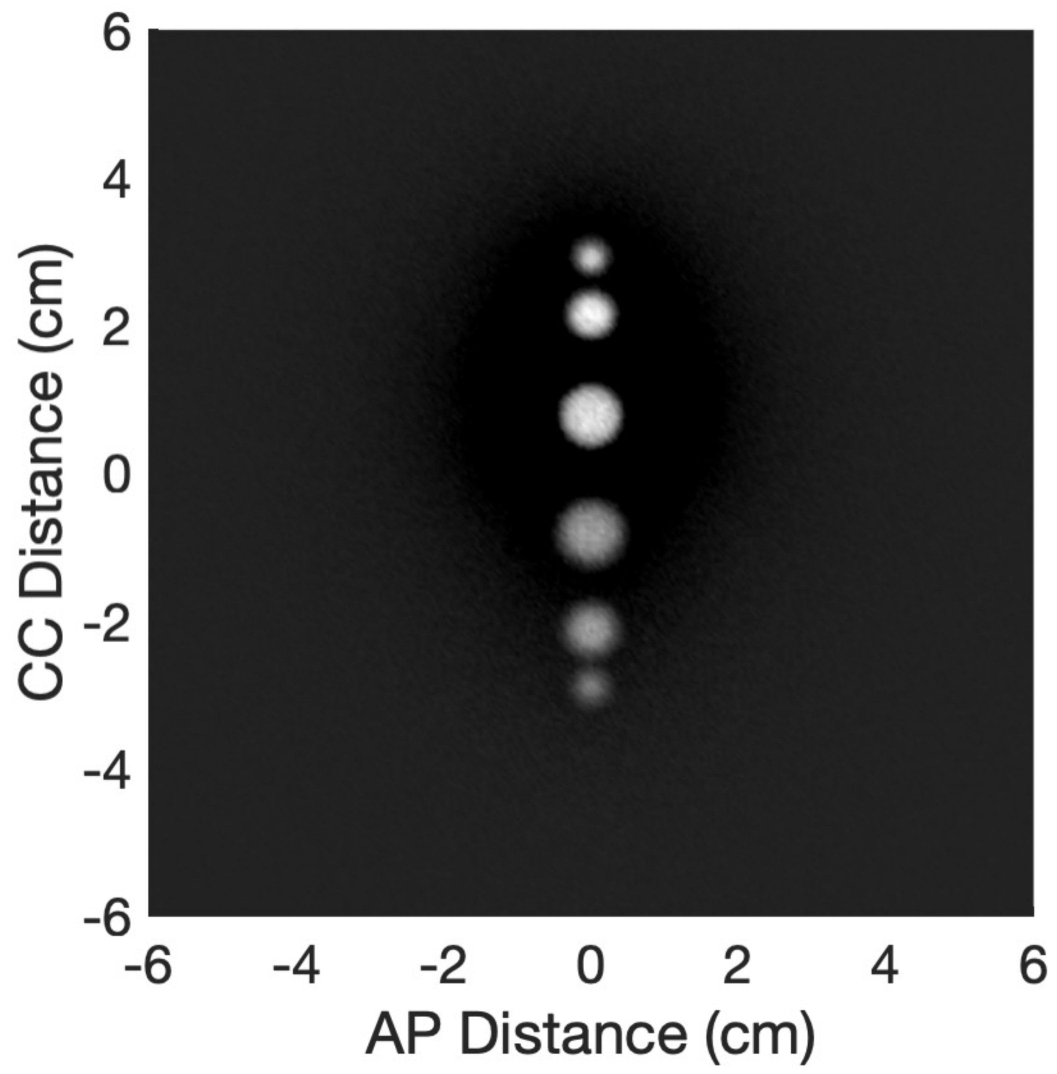

3D Reconstruction

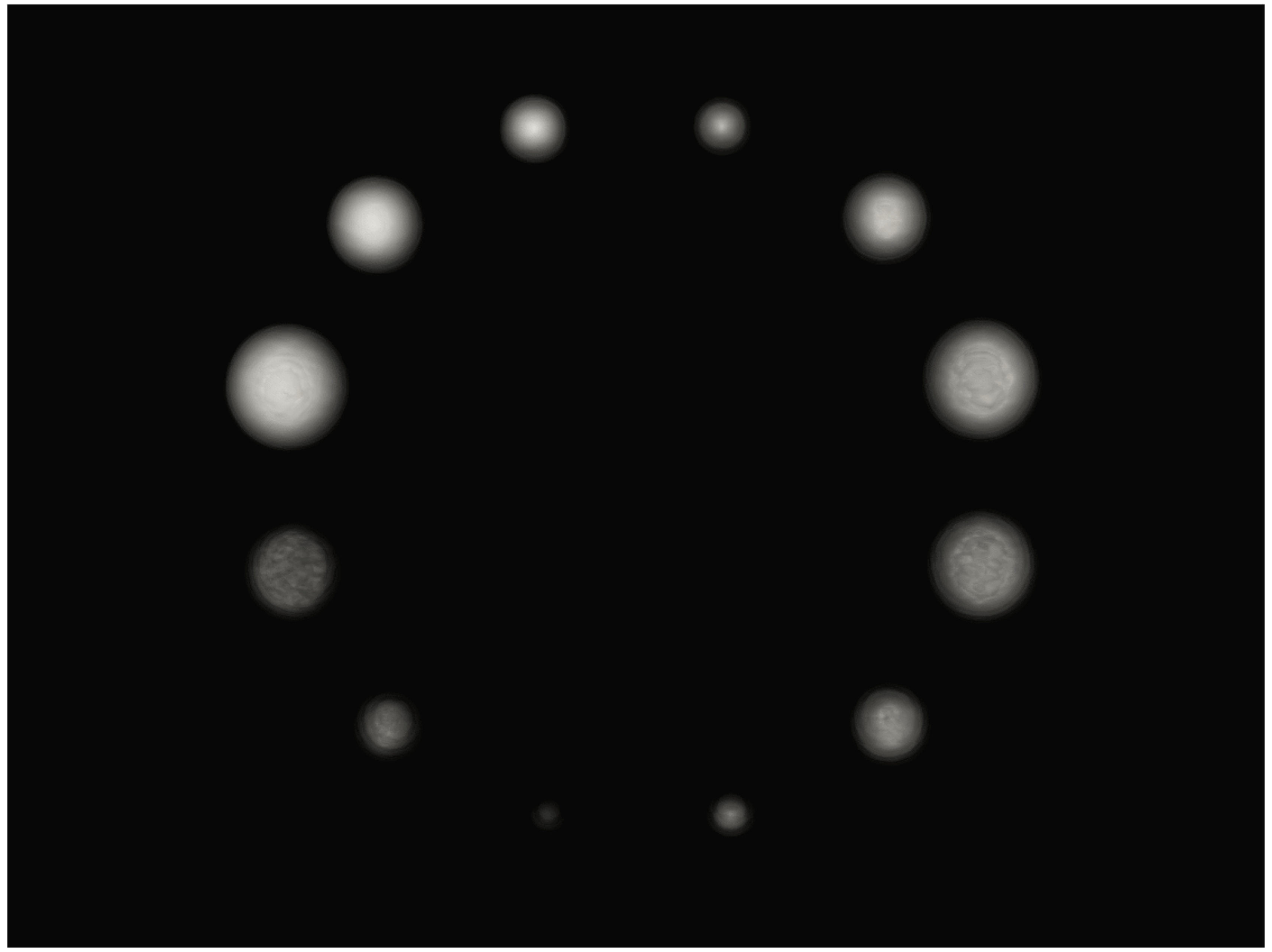

Fluorescence mode enables 3D reconstruction without rotation

NR Fluorescence Image Reconstruction

Imaging Modality	Dose (mSv)	Time
PET	7 - 9	~30 min
PET-CT	16 - 27	~30 min
SPECT	9 - 31	~30 min
LCS-NR Transmission	3.5	< 1 min
LCS-NR Fluorescence	9.7	seconds

Fluorescence mode enables 3D reconstruction without rotation

Charest M, Asselin C. Journal of Nuclear Medicine Technology. (2018) 46(2):107-113
Li Y, Jiang L, Wang H, Cai H, Xiang Y, Li L. Radiation Protection Dosimetry. (2019) 187(2):183-190

Conclusion

1) Demonstrated 2D and 3D LCS-NR medical imaging

2) Bandwidth is important for signal
LCS + monochromator can achieve this

3) Pool of isotopes to image
Isotope specific tags could be developed

4) Dose is comparable to similar imaging modalities

Acknowledgements

Research Group

Prof. CPJ Barty*
Kyle Chesnut
Michael Seggebruch
Eric Nelson
Haytham Effarah
Christine Nguyen

LUMITRON TECHNOLOGIES

Dr. Michael Jentschel
Dr. Agnese Lagzda
Dr. Yoonwoo Hwang
Dr. Fred Hartemann
Dr. Ferenc Raksi

UCI Medical Scientist Training Program

NIH

UCI

Thank You!

Extra Viewgraphs

Source Parameters

Electron Beam Parameters	
Micro-bunch charge	25 pC
Pulse structure	1000 micro-bunches/pulse
Repetition rate	400 Hz
e^- beam energy	30 – 100 MeV
e^- beam energy spread	0.03%
RF	11.424 GHz
e^- beam emittance	0.2 mm mrad
e^- beam size at the interaction point / spot size (RMS)	5 μm
e^- bunch length	2 ps
Interaction angle	π (head-on)

Laser Parameters	
Laser micro-pulse energy	10 mJ
Laser wavelength	354 nm
Repetition rate	400 Hz
Laser pulse duration	2 ps
Laser beam spot size	> 5 μm

X-ray Characteristics	
Total X-ray flux	$> 10^{12}$ ph s^{-1}
Tunable energy range	30 keV – 3 MeV
X-ray spot size (RMS)	5 μm
Minimum on-axis energy bandwidth (ΔE/E, FWHM)	10^{-3}

Reutershan T, Effarah HH, Lagzda A, Barty CPJ. Applied Optics (2022) 61(6):C162:178